2009

Performance evaluation of carbon-dioxide sensors used in building HVAC applications

Som Sagar Shrestha
Iowa State University

Performance evaluation of carbon-dioxide sensors used in building HVAC applications

by

Som Sagar Shrestha

A dissertation submitted to the graduate faculty

in partial fulfillment of the requirements for the degree of

DOCTOR OF PHILOSOPHY

Major: Mechanical Engineering

Program of Study Committee:
Gregory M. Maxwell, Major Professor
Ron M. Nelson
Steven J. Hoff
Michael B. Pate
Stephen B. Vardeman

Iowa State University
Ames, Iowa
2009

This work is dedicated to energy savvy professionals who are dedicated to energy efficiency enhancement in every engineering application.

Table of Contents

Acknowledgements

I would like to express my sincere gratitude and appreciation to my major professor Dr. Gregory M. Maxwell. I am glad to pronounce that I have had a wonderful time working under his supervision and cherished each and every moment with him. He has always been there for me in time of need for every support and guidance. I have been lucky to have been given a chance to work with Dr. Maxwell.

This research was performed for National Building Controls Information Program (NBCIP), which is sponsored by the Iowa Energy Center, NSTAR Electric & Gas Corporation and the California Commission. I am grateful for valuable advises and support from Dr. John House, Mr. Curtis J. Klaassen, and all individuals who were involved directly or indirectly in this research. I am also thankful for the cooperation and assistance from Larry Hanft and other technical staff in the Mechanical Engineering Department at Iowa State University.

Thanks to Dr. Ron M. Nelson, Dr. Steven J. Hoff, Dr. Michael B. Pate, and Dr. Stephen B. Vardeman for their valuable feedback and participation in my program of study.

I would like to gratefully acknowledge my parents Ganga Sagar Shrestha and Bikumaya Sagar Shrestha, wife Jarina Shrestha, daughter Swechha Shrestha, son Sakar Sagar Shrestha, brothers Krishna Sagar Shrestha and Dev Sagar Shrestha and all family members for their constant support and encouragement to accomplish this achievement.

Abstract

Carbon-dioxide sensors are widely used as part of a demand controlled ventilation (DCV) system for buildings requiring mechanical ventilation, and their performance can significantly impact energy use in these systems. Therefore, a study was undertaken to test and evaluate the most commonly used CO_2 sensors in HVAC applications, namely the non-dispersive infrared (NDIR) type.

Fifteen models of NDIR HVAC-grade wall-mounted CO_2 sensors were tested and evaluated to determine the accuracy, linearity, repeatability, hysteresis, humidity sensitivity, temperature sensitivity, and pressure sensitivity of each sensor as well as effect of long-term ageing on sensor performance. All tests were conducted in a chamber specifically designed and fabricated for this research. In all, 45 sensors were evaluated: three from each of the 15 models. Among the 15 models tested, eight models have a single-lamp, single-wavelength configuration, four models have a dual-lamp, single-wavelength configuration, and three models have a single-lamp, dual-wavelength configuration. All single-lamp single-wavelength sensors and one single-lamp dual-wavelength sensor incorporate an “automatic baseline adjustment” algorithm in the sensor’s electronics package.

The accuracy, linearity, repeatability, and hysteresis of the sensors were evaluated at a fixed relative humidity, temperature, and pressure, by varying CO_2 concentrations from 400 ppm to 1800 ppm. The test results showed a wide variation in sensor performance among the various manufacturers and in some cases a wide variation among sensors of the same model.

The humidity sensitivity was evaluated by varying the relative humidity from 20% to 60% while holding the CO_2 concentration, temperature, and pressure fixed. The temperature sensitivity was evaluated by varying the temperature from 66°F (18.9°C) to 80°F (26.7°C) while holding the gas composition and pressure fixed. The pressure sensitivity was evaluated by varying the pressure from 14.70 psia (101.35 kPa) to 11.80 psia (81.36 kPa) while holding the gas composition and temperature fixed.

The test results showed that while humidity sensitivity of most of the sensors is negligibly small, some sensors are strongly affected by humidity. The test results also showed that the effects of temperature and pressure variation on NDIR CO_2 sensors are unavoidable. For the range of temperature and pressure variation in

an air-conditioned space, the effect of pressure variation is more significant compared to the effect of temperature variation.

The long-term ageing effect was evaluated at four month intervals for one year. The result showed a wide variation in ageing effect among manufacturers. Some sensor models showed a nominal ageing effect of less than 30 ppm deviation in one year; whereas, all three sensors of one model showed significant ageing effects, up to -376 ppm deviation, in one year at 1100 ppm CO_2 concentration.

Chapter 1: General Introduction

INTRODUCTION

Almost 40% of total energy consumption in the U.S. is used in buildings (DOE, 2007). Typical buildings consume 20% more energy than necessary (CEC, 2002). Fortunately, the opportunities to reduce building energy consumptions are significant (Sun et al, 2006). Six-quadrillion Btu of energy that accounts for about 6% of national energy demand is consumed for space heating, cooling, and ventilation of commercial buildings. Controlling ventilation air flow rates using CO_2-based demand controlled ventilation (DCV) offers the possibility of reducing the energy penalty associated with over-ventilation during periods of low occupancy, while still ensuring adequate levels of outdoor air ventilation (Emmerich and Persily 2001). A report prepared for the U.S. Department of Energy (Roth et al. 2005) suggests that demand controlled ventilation (DCV) can reduce both heating and cooling energy of commercial buildings by about 10%.

Carbon-dioxide sensors are widely used as part of a demand controlled ventilation (DCV) system for buildings requiring mechanical ventilation to monitor indoor air CO_2 concentration and to control the outdoor air intake rate to maintain indoor air quality (IAQ). Performance of CO_2 sensors can significantly impact energy use as well as IAQ in these buildings. Overestimation of the CO_2 concentration by the sensors will lead to increased outdoor air usage causing increased energy cost. Underestimation may lead to poor IAQ and Sick Building Syndrome (SBS). The purpose of this research was to test and evaluate the most commonly used CO_2 sensors in HVAC systems, namely the non-dispersive infrared (NDIR) type.

The procedures presented here provide a methodology to test and evaluate NDIR CO_2 sensors for accuracy, linearity, repeatability, hysteresis, humidity sensitivity, temperature sensitivity, and pressure sensitivity. The test and evaluation procedures presented in this study are all inclusive in that they range from procuring the CO_2 sensor to comparing the performance of the sensors. Specifically, a procedure is presented to both procure CO_2 sensors from the manufacturers and to maintain quality control by controlling the storage and handling of the sensors. Further, it describes the apparatus and instrumentation, along with test conditions, used to test the sensors. Additionally, it outlines a detailed experimental procedure to evaluate the accuracy of the sensors. Finally, a discussion is presented on analyzing and comparing the performance of CO_2 sensors by using the test data.

DISSERTATION ORGANIZATION

There are a total of four papers included in this dissertation (Chapters 2 to 5). The first paper has been accepted for publication in ASHRAE Transactions and will be presented at the ASHRAE Summer meeting (June 2009, Louisville, KY). The remaining papers are in the final stages of editing and will be submitted to ASHRAE in the next few weeks.

The experimental procedure and the apparatus designed and fabricated for this research are discussed in Chapter 2. This procedure provides a detailed description of the methodology used to evaluate the performance of wall-mounted CO_2 sensors for accuracy, linearity, repeatability, hysteresis, humidity sensitivity, temperature sensitivity, and pressure sensitivity. Additionally, steady-state criteria for recording data from the CO_2 sensors as well as some preliminary test results are discussed.

Chapter 3 presents the performance test results, including accuracy, linearity, repeatability, and hysteresis of CO_2 sensors. The chapter describes the various configurations used by CO_2 sensor manufacturers to minimize ageing of the sensors and compares actual performance of the sensors with the manufacturer specifications.

Humidity, temperature, and pressure sensitivity of CO_2 sensors are discussed in Chapter 4. The sensitivity of the sensor reading to each of these three parameters was computed and compared to the manufacturers' specifications.

The effect of ageing on sensor drift is discussed in Chapter 5. The ageing tests are designed to assess the long-term performance of the wall-mounted NDIR CO_2 sensors that have been exposed to environmental conditions of a building application. Sensor behavior during power-up and conditioning period is also discussed in the chapter.

LITERATURE REVIEW

In the past, limited studies have been done to investigate the performance of HVAC-grade CO_2 sensors using a controlled environment. Fahlen et al. (1992) evaluated the performance of two CO_2 sensors, one photo-acoustic type and one infrared spectroscopy type, in lab tests and long term field tests. The lab tests included performance and environmental tests. The authors conclude that the deviation between actual concentration and the sensors' reading are normally well within ± 50 ppm at a concentration level of 1000 ppm. However, at a concentration of 2000 ppm the test results showed a deviation of up to -300 ppm. The output of one sensor increased dramatically during environmental testing. This sensor failed to return to its normal value.

Fisk et al. (2006) conducted a pilot study that evaluated the in-situ accuracy of 44 NDIR CO_2 sensors located in nine commercial buildings. The evaluation was performed either by multi-point calibration using CO_2 calibration gas or by a single-point calibration check using a co-located and calibrated reference CO_2 sensor. Their results indicated that the accuracy of CO_2 sensors is frequently less than what is needed to measure peak indoor-outdoor CO_2 concentration differences with an error that is less than 20%. Thus, the authors conclude that there is a need for more accurate CO_2 sensors and/or better maintenance and calibration. The effects of humidity, temperature, and pressure on the sensor readings were not considered in the study.

Pandey et al. (2007) evaluated the accuracy of two NDIR CO_2 sensor models. They tested three sensors of each model. The tests were performed in an enclosure designed for the experiment, where all six sensors were simultaneously exposed to CO_2 concentration of 0 ppm, 500 ppm, and 1000 ppm (other environmental conditions, such as humidity, temperature, and pressure were not specified.) The maximum deviation was observed as -73 ppm at a CO_2 concentration of 500 ppm. The research focused on the sensor accuracy but did not include effects of humidity, temperature, and pressure variation on the sensor output.

A study conducted at the Iowa Energy Center showed that, among the three new, co-located sensors, one sensor read about 105 ppm higher, compared to the two other sensors, at about 400 ppm (House 2006). Nine months later, the sensor that read 105 ppm higher at the beginning, read 265 ppm higher compared to the two other sensors.

Further review of the literature reveled that there is no present standard method of test available by which CO_2 sensors are evaluated. Therefore, an experimental procedure for testing and evaluating the sensors was developed for this research.

Chapter 2: An Experimental Evaluation of HVAC-Grade Carbon-Dioxide Sensors: Part 1, Test and Evaluation Procedure

A paper accepted by the ASHRAE Transactions, 2009, 115 (2)

Som S. Shrestha
Student Member ASHRAE

Gregory M. Maxwell, PhD
Member ASHRAE

ABSTRACT

Carbon-dioxide sensors are widely used as part of a demand controlled ventilation (DCV) system for buildings requiring mechanical ventilation, and their performance can significantly impact energy use in these systems. Therefore, a study was undertaken to test and evaluate the most commonly used CO_2 sensors in HVAC systems, namely the non-dispersive infrared (NDIR) type. The procedures presented here provide a methodology to test and evaluate NDIR CO_2 sensors for accuracy, linearity, repeatability, hysteresis, humidity sensitivity, temperature sensitivity, and pressure sensitivity.

The test and evaluation procedures presented in this paper are all inclusive in that they range from procuring the CO_2 sensor to comparing the performance of the sensors. Specifically, a procedure is presented to both procure CO_2 sensors from the manufacturers and to maintain quality control by controlling the storage and handling of the sensors. Further, it describes the apparatus and instrumentation, along with test conditions, used to test the sensors. Additionally, it outlines a detailed experimental procedure to evaluate the accuracy of the sensors. Finally, a discussion is presented on analyzing and comparing the performance of CO_2 sensors by using the test data. Partial results of the accuracy test and evaluation of the CO_2 sensors and the results of the linearity, repeatability, hysteresis, humidity sensitivity, temperature sensitivity, and pressure sensitivity evaluation are included in this paper. The full test results will be presented in a later publication.

INTRODUCTION

Controlling ventilation air flow rates using CO_2-based demand controlled ventilation (DCV) offers the possibility of reducing the energy penalty associated with over-ventilation during periods of low occupancy, while still ensuring adequate levels of outdoor air ventilation (Emmerich and Persily 2001). A report prepared for DOE (Roth et al. 2005) suggests that DCV can reduce both heating and cooling energy by about 10% or about 0.3 quadrillion Btu (316 quadrillion Joules) annually.

Carbon-dioxide (CO_2) sensors are gaining popularity in building HVAC systems to monitor indoor air CO_2 concentration and to control outdoor air intake rate. The sensing technology most commonly used for HVAC applications is the optical method of non-dispersive infrared (NDIR). The performance of these sensors is crucial not only to ensure energy savings but also to assure indoor air quality. In CO_2-based DCV systems, the CO_2 level of indoor air is monitored and the outdoor air flow rate is adjusted based on the sensor output to maintain acceptable CO_2 concentration in the occupied space. Sensors which read high will call for more outdoor air leading to an energy penalty. Sensors which read low will cause poor indoor air quality.

CO_2 sensors are reported to have technology-specific sensitivities, and unresolved issues including drift, overall accuracy, temperature effect, water vapor, dust buildup, and aging of the light sources, etc. (Dougan and Damiano 2004). Fahlen et al. (1992) evaluated the performance of two CO_2 sensors, one photo-acoustic type and one IR spectroscopy type, in lab tests and long term field tests. The lab tests included performance and environmental tests. The authors conclude that the error of measurement is normally well within ± 50 ppm at a measured level of 1,000 ppm. However, the test results show the deviation up to -300 ppm at 2,000 ppm. The output of one sensor increased dramatically during environmental testing and never recovered back to its normal value.

A pilot study that evaluated in-situ accuracy of 44 NDIR CO_2 sensors located in nine commercial buildings indicated that the accuracy of CO_2 sensors is frequently less than is needed to measure peak indoor-outdoor CO_2 concentration differences with less than 20% error (Fisk et al. 2006). Thus, the authors conclude that there is a need for more accurate CO_2 sensors and/or better maintenance or calibration. The evaluation was performed either by multi-point calibration using CO_2 calibration gas or by a single-point calibration check using a co-located and calibrated reference CO_2 sensor. The test was not conducted in a controlled environment hence the effect or humidity, temperature and pressure variation on the sensor output was not considered in the study.

Further review of the literature reveled that there is no present standard method of test available by which CO_2 sensors are evaluated. Therefore, an experimental procedure for testing and evaluating the sensors was developed and is presented here. This procedure provides a detailed description of the methodology to evaluate the performance of wall-mounted CO_2 sensors for accuracy, linearity, repeatability, hysteresis, humidity sensitivity, temperature sensitivity, and pressure sensitivity.

Further, this paper presents the details of the experimental test apparatus and instrumentation being used for the test. Additionally, steady-state criteria for recording data from the CO_2 sensors are also discussed, along with some preliminary test results.

HVAC-GRADE CO_2 SENSORS

For HVAC applications, two CO_2 sensor technologies are available: photoacoustic and NDIR. Of these the NDIR is the most commonly used technology for DCV application. As shown in Figure 1, the essential components of a NDIR CO_2 sensor include an IR (infrared) radiation source, detector, optical bandpass filter, and an optical path between the source and the detector which is open to the air sample. The bandpass filter limits the IR intensity that is measured in a specific wavelength region. The detector measures this intensity which is proportional to the CO_2 concentration. The main configurations used for HVAC grade CO_2 sensors are: (1) single-beam, single-wavelength, (2) dual-beam, single-wavelength, and (3) single-beam, dual-wavelength.

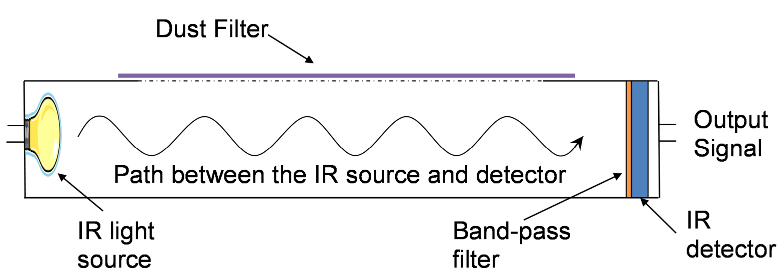

Figure 1. Schematic of a NDIR CO_2 sensor.

IR light interacts with most molecules by exciting molecular vibrations and rotations. When the IR frequency matches a natural frequency of the molecule, some of the IR energy is absorbed.

While carbon dioxide has several absorption bands, the 4.26 μm band is the strongest. At this wavelength, absorption by other common components of air is negligible. Hence, CO_2 sensors use the 4.26 μm band. Quantitative analysis of a gas sample is based on the Beer-Lambert law (Equation 1), which relates the amount of light absorbed to the sample's concentration and path length.

$$A = [\log_{10} (I_0 / I)] = \varepsilon cl \qquad (1)$$

where,

A = decadic absorbance

I_0 = light intensity reaching detector with no absorbing media in beam path

I = light intensity reaching detector with absorbing media in beam path

ε = molar absorption coefficient (absorption coefficient of pure components of interest at analytical wavelength)

c = molar concentration of the sample component

l = beam path length

From Equation 1 it is evident that the attenuation of an IR beam at 4.26 μm is proportional to the number density of CO_2 molecules in the optical path. For gases, the molecular density is directly proportional to the pressure and inversely proportional to the temperature. Thus temperature and pressure corrections must be applied when using IR absorption to determine CO_2 concentrations.

Operational and environmental conditions affect the performance of all CO_2 sensors. An unavoidable operational effect is a result of the degradation of the IR light source over time. Since the principle of operation is based on measured attenuation of the IR beam, a decrease in lamp intensity affects the sensor output. Environmental conditions such as dust, aerosols and chemical vapors may also affect the sensor performance by altering the optical properties of the sensor components due to long-term exposure to these contaminants. To minimize the effects of air-born particulates, sensor manufacturers use a filter media across the opening of the sensor's optical cavity where the air sample is analyzed.

Various techniques are used by CO_2 sensor manufacturers to compensate for the long-term effects of operational and environmental conditions. Some sensors automatically reset the baseline value (normally 400 ppm) according to a minimum CO_2 concentration observed over a time period. However, the logic used to reset the baseline and frequency of correction varies with manufacturer, and often it is not well documented. This technique relies on the fact that many buildings experience an unoccupied period during which CO_2 levels drop to outdoor levels. Other compensation techniques include dual-beam, single-wavelength and single-beam, dual-wavelength designs. The working principles, physical construction, advantages and disadvantages of NDIR CO_2

sensors are well documented in the literature (Raatschen (1990), Emmerich and Persily (2001), Schell and Int-House (2001), Fahlen et al. (1992)).

PROCUREMENT AND HANDLING OF THE SENSORS

HVAC CO_2 sensors are available with various options such as digital display, selectable output signal (voltage or current), output relay and selectable CO_2 operating ranges (with 0 to 2000 ppm being the most common). For this research, preference was given to the sensor models that meet Title 24 criteria of the California Energy Commission (CEC 2006) for CO_2 sensors that can be used for DCV. Among the acceptance criteria are requirements that the CO_2 sensor(s) have an accuracy of ±75 ppm, and a calibration interval of at least five years. Similarly, preference was given to the sensor models with 0 to 10 V output, and with an operating range of 0 to 2000 ppm.

Carbon dioxide sensors used for HVAC controls application are either duct mounted or wall mounted; however, only wall-mounted sensors meet the Title 24 acceptance criteria. Wall mounted sensors package the sensing element and electronics in a single unit that is mounted to a base plate secured to the wall. Most wall-mounted sensors provide a port where calibration gas can flow across the sensing element for “field calibration”.

Sensors are available from numerous suppliers. In some cases sensors are sold directly through the manufacturer while in other cases manufacturers produce products which are sold under a variety of product names. Due to the competitive nature of the sensor business and the various after markets, it is difficult to know how many “unique” sensor products there are. In this study, fifteen models of sensors with three of each model were purchased for the tests. The sensors are divided into three groups: A, B, and C, where each group contains one sensor of each model.

The sensors were ordered in two separate batches over a period of several weeks to increase the probability that they would come from different manufacturing lots. Manufacturer provided guidelines for installation and operation of the sensors were adhered to.

After receiving all sensors, an “as received” test was conducted for each sensor to check its functionality. This check is not a part of the formal testing of the sensors. The “as received” test consists of connecting the sensor to the proper power supply, waiting for the appropriate warm-up time, and measuring the output signal from the sensor. Handling of the sensors is always noted on log sheets.

All sensors used for testing are mounted on one of three fixtures specifically designed for this research (referred to hereafter as “trays” and described more fully in Experimental Apparatus and Instrumentation section). Each tray holds one of the three groups (A, B or C) of sensors. Prior to testing, all trays were placed in the lab station and the sensors were powered up for a three week period before commencing the first formal test. This time period provided assurance that all sensors acclimate to the conditions (temperature, humidity and CO_2 concentration) in the laboratory and that sensors which “self-calibrate” over a period of several weeks are given adequate time to complete the calibration process. Ambient conditions in the laboratory (temperature, relative humidity, and CO_2 concentration) are continuously recorded to provide a record of the environmental conditions.

EXPERIMENTAL APPARATUS AND INSTRUMENTATION

A test chamber (hereafter, chamber) was designed and fabricated for this study. Figure 2 is a schematic diagram of the test system used. The sealed chamber is constructed of 8 in. (20.3 cm) square 0.25 in. (6.35 mm) wall steel tubing. An external water jacket is used to maintain the desired temperature inside the chamber. Flanges are welded to each end of the chamber to enable removable end plates with gaskets to be attached. The front endplate is made of Lexan® while the rear endplate is 0.25 in. (6.35 mm) steel. The chamber was sized to accommodate one tray of test sensors at a time.

Air cylinders are connected through one end plate and are used to control the pressure inside the chamber during the pressure sensitivity tests. The chamber vent valve (valve #8) is partially closed to pressurize the test chamber to sea-level pressure while allowing continuous flow of the gas mixture through the test chamber during accuracy, linearity, repeatability, hysteresis, humidity sensitivity, and temperature sensitivity tests.

A gas mixture of CO_2 and N_2 is supplied to the test chamber from a commercially-available gas-mixing system[1]. The gas-mixing system uses mass-flow controllers calibrated using a primary flow standard traceable to the United States’ National Institute of Science and Technology (NIST). The system is capable of producing gas mixtures from 334 to 3333 ppm CO_2 (1% accuracy) at a flow rate of 3 liters/min. The gas mixing system is

[1] Environics® S-4000

annually calibrated as recommended by the manufacturer. The technical specification of the gas mixing system is provided in Table 1.

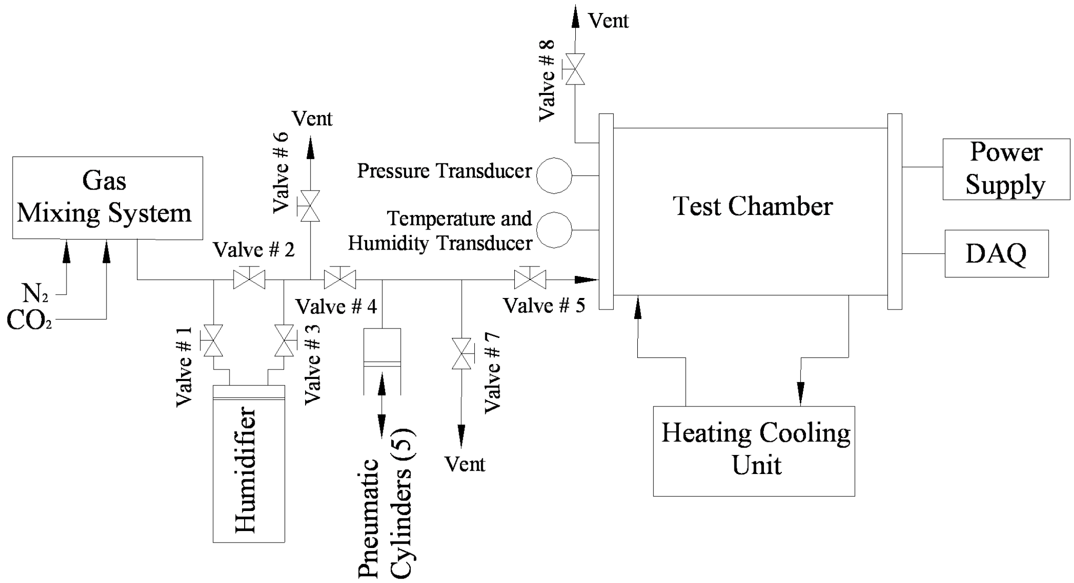

Figure 2. Schematic of the test system.

Table 1. Technical Specifications of the Gas Mixing System

Accuracy	
Concentration	± 1.0% Setpoint
Flow	± 1.0% Setpoint
Repeatability	± 0.05% Setpoint
Full scale flow of mass flow controller 1 (N_2)	3 SLPM*
Full scale flow of mass flow controller 2 (CO_2)	0.01 SLPM

* Based on a reference temperature of 0°C (32°F) and a reference Pressure of 760 mm Hg (29.92 in. Hg)

The dry-gas mixture from the gas mixing system is "bubbled" through a deionized water column to add water vapor (humidity). The bubbler is capable of producing relative humidity ranging from dry gas (no humidification) to approximately 80% relative humidity.

Adding water vapor to a dry gas mixture changes the mole fraction of the gases in the mixture; therefore, the concentration of CO_2 in a mixture will decrease as water vapor content increases. To achieve a desired CO_2 concentration under humid conditions, it is necessary to adjust the CO_2 concentration in the dry-gas mixture. The ideal gas model is used to calculate this adjustment. The procedure is discussed in Appendix A.

Figure 3 illustrates the inside of the chamber which contains a tray for holding one group of sensors, a test-chamber CO_2 sensor[2], and a fan. Figure 4 is a photograph of a group of sensors mounted on a tray. The overall length of the chamber is adequate to accommodate one tray and the necessary connectors.

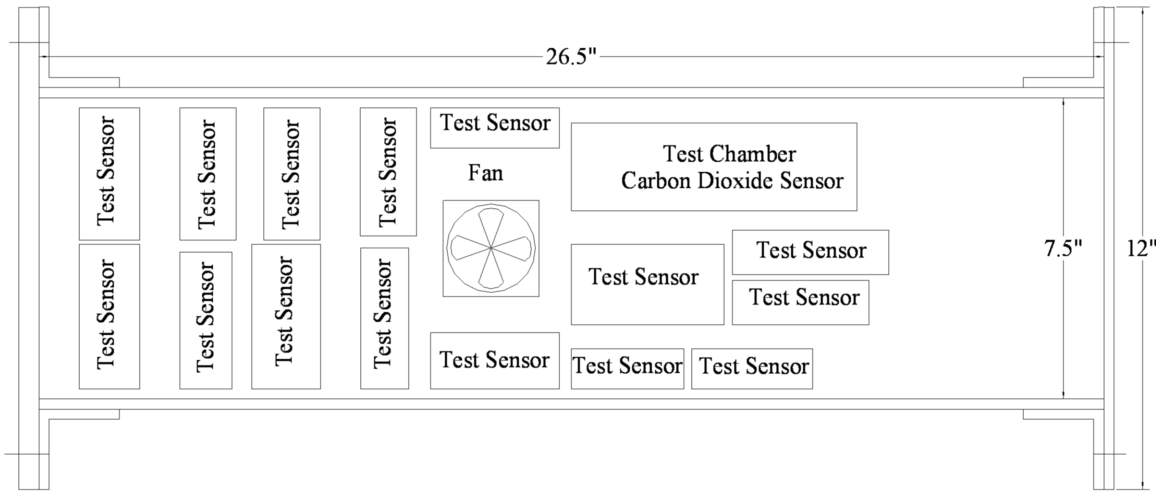

Figure 3. Test chamber interior.

Input power for the sensors and sensor output signals pass through the Lexan® endplate using steel machine screws and nuts as connectors. The machine screws are threaded through the Lexan® to provide a hermetic seal while at the same time providing electrical conductivity. Figure 5 is a photograph of the Lexan® endplate with connectors attached to the chamber. Several tests (using a separate set of sensors not used for the formal testing) were conducted to evaluate possible electronic noise on the sensor output signals due to the sensors being mounted in close proximity to one another or from the unshielded machine screw terminals. The output signal from each sensor was examined using an oscilloscope to see the waveform of the output signal. Measurements were made when a single sensor was powered and when all of the sensors were powered. Comparison between the output signals showed there was no detectable interaction effect as a result of the close proximity of the sensors to one another, nor was there any effect of electrical noise due to the connectors.

[2] Vaisala GMP343

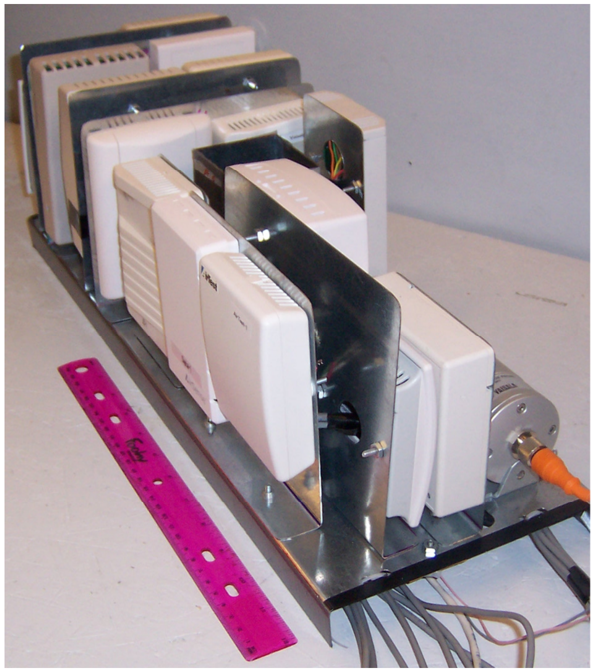

Figure 4. CO_2 sensors mounted on tray.

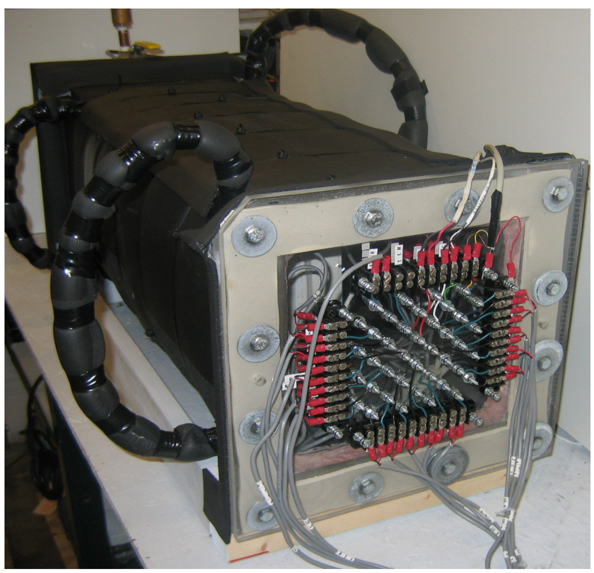

Figure 5. Photograph of the Lexan® end plate with connectors mounted on the test chamber.

An absolute pressure sensor[3] (hereafter, test chamber pressure sensor) is mounted on the steel end plate to measure absolute pressure in the chamber. The technical specification of the test chamber pressure sensor is

[3] Omega PX209

provided in Table 2. A humidity and temperature sensor[4] (hereafter, test-chamber humidity sensor or test-chamber temperature sensor) is also mounted on this end plate to measure relative humidity and temperature in the chamber. The technical specification of the test chamber humidity and temperature sensor is provided in Table 3.

Table 2. Technical Specifications of the Test Chamber Pressure Sensor

Description	Value
Measurement range	0 to 15 psia (0 to 130.4 kPa)
Accuracy	0.25% FS
Response time	2 ms

The temperature inside the chamber is maintained at a prescribed value by controlling the temperature of the water circulating through the water jacket. The water jacket temperature is controlled using a water bath[5].

The DC axial fan installed inside the chamber provides a means of maintaining uniform temperature conditions throughout the chamber's interior. The circulating fan draws air from the top of the chamber and blows air beneath the tray on which the sensors are mounted. The mounting tray has holes located below each sensor to allow air to flow up and around each sensor. Tests were performed (using a separate set of sensors not used for the formal testing) to check for uniformity of temperature in the chamber. RTD's were used to measure the temperature of the air being supplied to the sensors at various locations throughout the chamber. The maximum variation in temperature between the RTD's was 0.29°F (0.16°C).

A multimeter[6] and a switch/control unit[7] are used to measure output from the CO_2 sensors, the temperature sensor, the humidity sensor, and the pressure sensor. National Instruments LabView software is used in conjunction with the multimeter and switch/control unit as a data acquisition system to record the output from each sensor.

[4] Vaisala HMT334
[5] Haake A81
[6] Hewlett Packard 3457A
[7] Hewlett Packard 3488A

Table 3. Technical Specifications of the Test Chamber Humidity and Temperature Sensor

Description	Value
Relative humidity	
Measurement range	0 to 100%
Accuracy at 59 to 77 °F (15 to 25 °C)	± 1% RH (0 to 90%), ± 1.7% RH (90 to100%)
Accuracy at -4 to 104 °F (-20 to 40 °C)	± (1.0 + 0.008 x reading) %RH
Temperature	
Measurement range	-94 to 356°F (-70 to 180°C)
Accuracy at 68°F (20°C)	± 0.36°F (± 0.2°C)
Accuracy over temperature range	

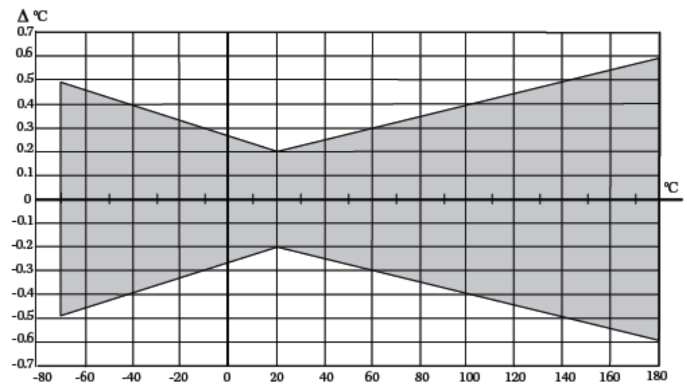

Initially the gas mixture at the desired CO_2 concentration flows continuously through the test chamber until the concentration of the gas in the chamber has stabilized. As a way of monitoring the gas mixture in the chamber, a test-chamber CO_2 sensor is installed in the chamber to provide an independent measurement of CO_2 concentration. Technical specifications of the test-chamber CO_2 sensor are provided in Table 4.

Table 4. Technical Specifications of the Test Chamber CO_2 Sensor

Description	Value
Measurement range	0 to 2000 ppm
Accuracy	± 2.5% of reading
Accuracy at calibration points (at 370 ppm, 1000 ppm and 4000 ppm)	± 1.5% of reading
Accuracy below 300 ppm CO_2	± 5 ppm
Long-term stability (for easy operating conditions)	< ± 2% reading / year
Operating temperature	-40 to + 140°F (- 40 to + 60°C)
Operating pressure	0 to 72.5 psia (0 to 500 kPa)

EXPERIMENTAL METHODOLOGY

The range of temperature, pressure, humidity, and CO_2 concentration used for testing the CO_2 sensor performance is extended over the conditions encountered in a typical building HVAC application and for building locations at various altitudes above sea level. The test includes evaluation of accuracy, linearity, repeatability, hysteresis, humidity sensitivity, temperature sensitivity, and pressure sensitivity of the CO_2 sensors.

Accuracy, Linearity, Repeatability, and Hysteresis Test

The accuracy, linearity, repeatability, and hysteresis of the sensors is evaluated by varying the CO_2 concentration while maintaining the chamber relative humidity, temperature and pressure at 40%, 73ºF (22.8ºC) and 14.70 psia (101.35 kPa), respectively. Vent valves #6 and #7 are closed and vent valve #8 is partially closed to pressurize the test chamber to sea-level pressure while allowing continuous flow of the gas mixture through the test chamber. Pressurization is necessary given that the testing location (Ames, Iowa) is 960 feet (293 meters) above sea level with an atmospheric pressure of 14.2 psia (97.9 kPa). The tests are performed in the following sequence:

1. Initially the CO_2 concentration in the test chamber is set at 400 ppm. The-gas mixing system runs continuously providing continuous purge. Data collection at this condition and at all other conditions follow a protocol described below.

2. Holding the chamber humidity, temperature, and pressure steady, the CO_2 concentration is increased up to 1800 ppm in 350 ppm increments. These measurements, including the initial measurement at 400 ppm (data points 1-5 in Figure 6), are referred to as the forward measurements.
3. After reaching 1800 ppm, the test is reversed, i.e., the CO_2 concentration is decreased from 1800 ppm to 400 ppm in 350 ppm increments while maintaining the chamber humidity, temperature, and pressure steady. These measurements (data points 6-9 in Figure 6) are referred to as the reverse measurements.
4. Once the 400 ppm level is attained, the CO_2 concentration is increased to 1450 ppm in 350 ppm increments while maintaining the chamber humidity, temperature, and pressure steady. These measurements (data points 10-12 in Figure 6) are also referred to as the forward measurements.

Test data recording from all test sensors begins once steady-state conditions are established. Requirements for steady-state conditions are detailed in the Test Procedure section. At each test condition, 10 samples of sensor output collected at 1-minute intervals are averaged and used to report the "Measured CO_2 Concentration" for the sensor.

Accuracy and linearity are evaluated using the first forward and the reverse measurements (points 1-9 in Figure 6). Repeatability is evaluated using the two forward measurements at 750, 1100 and 1450 ppm (data points 2 and 10, 3 and 11, and 4 and 12 in Figure 6). Hysteresis is evaluated using the first forward measurement and the reverse measurement at 750, 1100 and 1450 ppm (data points 2 and 8, 3 and 7, and 4 and 6 in Figure 6).

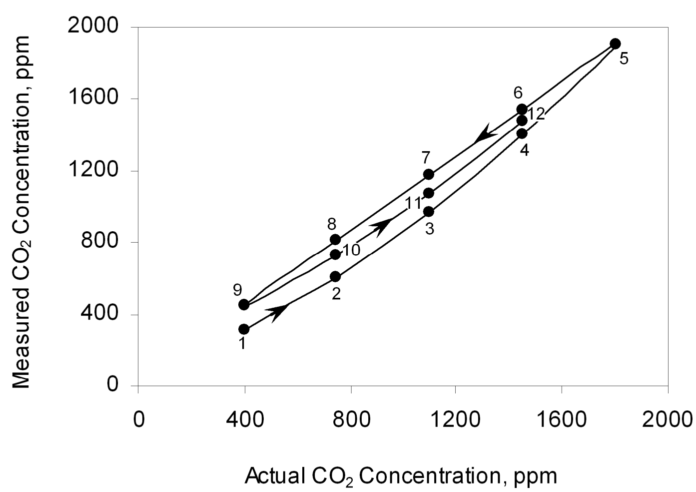

Figure 6. Example data set to illustrate numbering scheme used to identify data points.

Test Procedure. Output from the sensors is recorded while the test environment settles to the steady-state conditions defined in Table 5. For clarity, this data is referred to as “settling data” and data collected at steady-state conditions for quantifying the performance of the test sensors is referred to as “test data”. Interpreting Table 5, to attain and maintain a steady-state condition in the test chamber, the following conditions must be maintained for 10 minutes prior to the collection of the test data as well as throughout the collection of the test data: the CO_2 concentration reading from the test chamber CO_2 sensor must not vary more than ± 20 ppm from its mean output, the test chamber humidity sensor output must not vary more than ± 2.5% from the desired relative humidity, the test chamber temperature sensor output must not vary more than ± 1.8ºF (1ºC) from the desired temperature, and the test chamber pressure sensor output must not vary more than ± 0.14 psia (0.965 kPa) from the desired pressure.

Table 5. Steady-State Conditions for the Accuracy, Linearity, Repeatability and Hysteresis Tests

Parameter	Steady-state condition
CO_2 concentration	Within ± 20 ppm of mean output from the test chamber CO_2 sensor for 10 minutes prior to and during the collection of the test data
Temperature	Within ± 1.8ºF (1ºC) of the desired temperature condition measured by the test chamber temperature sensor for 10 minutes prior to and during the collection of the test data
Pressure	Within ± 0.14 psi (0.965 kPa) of the desired pressure condition measured by the test chamber pressure sensor for 10 minutes prior to and during the collection of the test data
Relative humidity	Within ± 2.5% of the desired relative humidity measured by the test chamber humidity sensor for 10 minutes prior to and during the collection of the test data

Effect of Humidity on CO_2 Sensors

The effect of humidity on the CO_2 sensors is evaluated by varying the relative humidity in the test chamber while maintaining the chamber CO_2 concentration, temperature, and pressure at 1100 ppm, 73ºF (22.8ºC) and 14.7 psia (101.35 kPa), respectively. The tests are performed in the following sequence:

1. Initially the relative humidity in the test chamber is set at 20%. The gas-mixing system runs continuously allowing continuous purge (the vent valves #6 and #7 are closed and vent valve #8 is partially closed). Data collection at this condition and at all other conditions follow a protocol described below.

2. Holding the CO_2 concentration, temperature, and pressure steady, the test chamber relative humidity is increased first to 40% and then to 60%.

Test data recording from all test sensors begins once steady-state conditions are established. Requirements for steady-state conditions are defined in Table 5. At each test condition, 10 samples of sensor output collected at 1-minute intervals are averaged and used to report the "Measured CO_2 Concentration" for the sensor. The test procedure is the same as the test procedure used for accuracy, linearity, repeatability, and hysteresis tests.

Effect of Temperature on CO_2 Sensors

The effect of temperature on the CO_2 sensors is evaluated by varying the temperature in the test chamber while maintaining the chamber CO_2 concentration and pressure at 1100 ppm, and 14.70 psia (101.35 kPa), respectively. The relative humidity in the test chamber is maintained at 40% at 73°F (22.8°C) temperature. The test chamber temperature is varied while maintaining the composition of the gas mixture steady. Hence, the relative humidity varies at temperatures other than 73°F (22.8°C).

The tests are performed in the following sequence:

1. Initially the temperature in the test chamber is set at 73°F (22.8°C). The gas-mixing system runs continuously allowing continuous purge (the vent valves #6 and #7 are closed and vent valve #8 is partially closed). Data collection at this condition and at all other conditions follow a protocol described below.
2. Holding the CO_2 concentration, gas mixture composition, and pressure steady, the test chamber temperature is decreased first to 66°F (18.9°C) and then increased to 80°F (26.7°C).

Test data recording from all test sensors begins once steady-state conditions are established. Requirements for steady-state conditions are detailed below in the Test Procedure section. At each test condition, 10 samples of sensor output collected at 1-minute intervals are averaged and used to report the "Measured CO_2 Concentration" for the sensor.

Test Procedure. Output from the sensors is recorded while the test environment settles to the steady-state conditions defined in Table 6. For clarity, this data is referred to as "settling data" and data collected at steady-state conditions for quantifying the performance of the test sensors is referred to as "test data". Interpreting Table 6, to attain and maintain a steady-state condition in the test chamber, the following conditions must be maintained for 10 minutes prior to the collection of the test data as well as throughout the collection of the test data: the CO_2 concentration reading from the test chamber CO_2 sensor must not vary more than ± 20 ppm from its mean output, the test chamber temperature sensor output must not vary more than ± 1.8ºF (1ºC) from the desired temperature, the test chamber pressure sensor output must not vary more than ± 0.14 psia (0.965 kPa) from the desired pressure, and the test chamber relative humidity sensor output must not vary more than 2.5% from the desired relative humidity at 73°F (22.8°C) temperature.

Table 6. Steady-State Conditions for the Temperature Sensitivity Test

Parameter	Steady-state condition
CO_2 concentration	Within ± 20 ppm of mean output from the test chamber CO_2 sensor for 10 minutes prior to and during the collection of the test data
Temperature	Within ± 1.8ºF (1ºC) of the desired temperature condition measured by the test chamber temperature sensor for 10 minutes prior to and during the collection of the test data
Pressure	Within ± 0.14 psia (0.965 kPa) of the desired pressure condition measured by the test chamber pressure sensor for 10 minutes prior to and during the collection of the test data
Relative humidity	Within ±2.5% of the desired relative humidity at 73ºF (22.8°C) temperature, measured by the test chamber humidity sensor for 10 minutes prior to and during the collection of the test data

Effect of Pressure on CO_2 Sensors

The effect of pressure on the CO_2 sensors is evaluated by varying the pressure in the test chamber while maintaining the chamber CO_2 concentration and temperature at 1100 ppm and 73°F (22.8°C), respectively. Relative humidity in the test chamber is maintained at 40% at 14.70 psia (101.35 kPa) pressure. The test chamber pressure is varied while maintaining the composition of the gas mixture steady. Hence, the relative humidity varies at pressures other than 14.70 psia (101.35 kPa). The test is conducted at three pressures: 14.70 psia (101.35 kPa), 13.25 psia (91.36 kPa), and 11.80 psia (81.36 kPa). The pressure levels correspond to standard atmospheric pressures for altitudes corresponding to sea level, 2838 feet (865 meters) and 5948 feet (1813 meters) above sea level.

The gas mixture at the desired CO_2 concentration and relative humidity (at 73°F (22.8°C) temperature and 14.70 psia (101.35 kPa) pressure), flows continuously through the test chamber until the CO_2 concentration, relative humidity, temperature, and pressure of the gas in the chamber has stabilized. The tests are performed in the following sequence:

1. Initially the pressure in the test chamber is set at 14.70 psia (101.35 kPa). At steady-state conditions, the test chamber is isolated by closing valves # 4, #5, #7, and #8. Data collection at this condition and at all other conditions follow a protocol described below.
2. Holding the CO_2 concentration, gas-mixture composition, and temperature steady, the test chamber pressure is changed first to 13.25 psia (91.36 kPa) and then to 11.80 psia (81.36 kPa). To adjust the chamber pressure, keeping valves #4, #7, and #8 closed, valve #5 is opened thus connecting the chamber to the five pneumatic cylinders. The pneumatic cylinders (purged with the same gas concentration that is in the chamber) are positioned to change the gas pressure in the chamber.

Test data recording from all test sensors begins once steady-state conditions are established. Requirements for steady-state conditions are detailed below in the Test Procedure section. At each test condition, 10 samples of sensor output collected at 1-minute intervals are averaged and used to report the "Measured CO_2 Concentration" for the sensor.

Test Procedure. Output from the sensors is recorded while the test environment settles to the steady-state conditions defined in Table 7. For clarity, this data is referred to as "settling data" and data collected at steady-state conditions for quantifying the performance of the test sensors is referred to as "test data". Interpreting Table 7, to attain and maintain a steady-state condition in the test chamber, the following conditions must be maintained for 10 minutes prior to the collection of the test data as well as throughout the collection of the test data: the CO_2 concentration reading from the test chamber CO_2 sensor must not vary more than ± 20 ppm from its mean output, the test chamber temperature sensor output must not vary more than ± 1.8ºF (1ºC) from the desired temperature, the test chamber pressure sensor output must not vary more than ± 0.14 psia (0.965 kPa) from the desired pressure, and the test chamber relative humidity sensor output must not vary more than 2.5% from the desired relative humidity at 14.70 psia (101.35 kPa) pressure.

Table 7. Steady-State Conditions for the Pressure Sensitivity Test

Parameter	Steady-state condition
CO_2 concentration	Within ± 20 ppm of mean output from the test chamber CO_2 sensor for 10 minutes prior to and during the collection of the test data
Temperature	Within ± 1.8ºF (1ºC) of the desired temperature condition measured by the test chamber temperature sensor for 10 minutes prior to and during the collection of the test data
Pressure	Within ± 0.14 psia (0.965 kPa) of the desired pressure condition measured by the test chamber pressure sensor for 10 minutes prior to and during the collection of the test data
Relative humidity	Within ±2.5% of the desired relative humidity at 14.70 psia (101.35 kPa) pressure, measured by the test chamber humidity sensor for 10 minutes prior to and during the collection of the test data

Long-term test

This section describes the test procedure pertaining to the evaluation of long-term performance of CO_2 sensors. The test will be conducted in four months interval for one year.

The sensors are located in the "lab station" apparatus (hereafter referred to as lab station) when they are not undergoing performance testing in the chamber. The lab station allows for continuous monitoring of the sensors while they are exposed to ambient conditions that exist in the laboratory space where the research project is taking place. Since the laboratory space is large and well ventilated, CO_2 levels are normally near outdoor CO_2 concentrations. The lab station provides the capability to periodically expose the sensors to higher levels of CO_2 concentrations as they would experience in an office or classroom environment.

A photograph of the lab station is provided in Figure 7 while Figure 8 provides a schematic of the station. The lab station consists of a wooden base with Plexiglas walls. The three trays on which the test sensors are mounted are placed within the Plexiglas walls. During time periods when the sensors are only exposed to ambient conditions in the lab, the top Plexiglas panel is removed allowing room air to freely interact with the sensors. To produce conditions of higher CO_2 concentrations (such as in an occupied space), the top panel is put in place and a gas mixture is supplied into the plenum section below the trays. The gas mixture passes through holes and flows past each CO_2 sensor. The Plexiglas enclosure and fans (one mounted on each tray) provide a near uniform CO_2 concentration to all sensors.

During the four months in between performance testing, the sensors will be periodically exposed to higher levels of CO_2. For three days per week, the CO_2 concentration will be increased to approximately 1100 ppm for a period of 8 to 12 hours. The specific days of the week and number of hours per day are chosen at random. At all other times, the sensors will experience ambient laboratory conditions. Sensor output and laboratory conditions will be continuously recorded during the four months. At the end of the four-month time period, the sensors will be tested following the same procedures as the performance tests (accuracy, linearity, repeatability, hysteresis, humidity sensitivity, temperature sensitivity and pressure sensitivity).

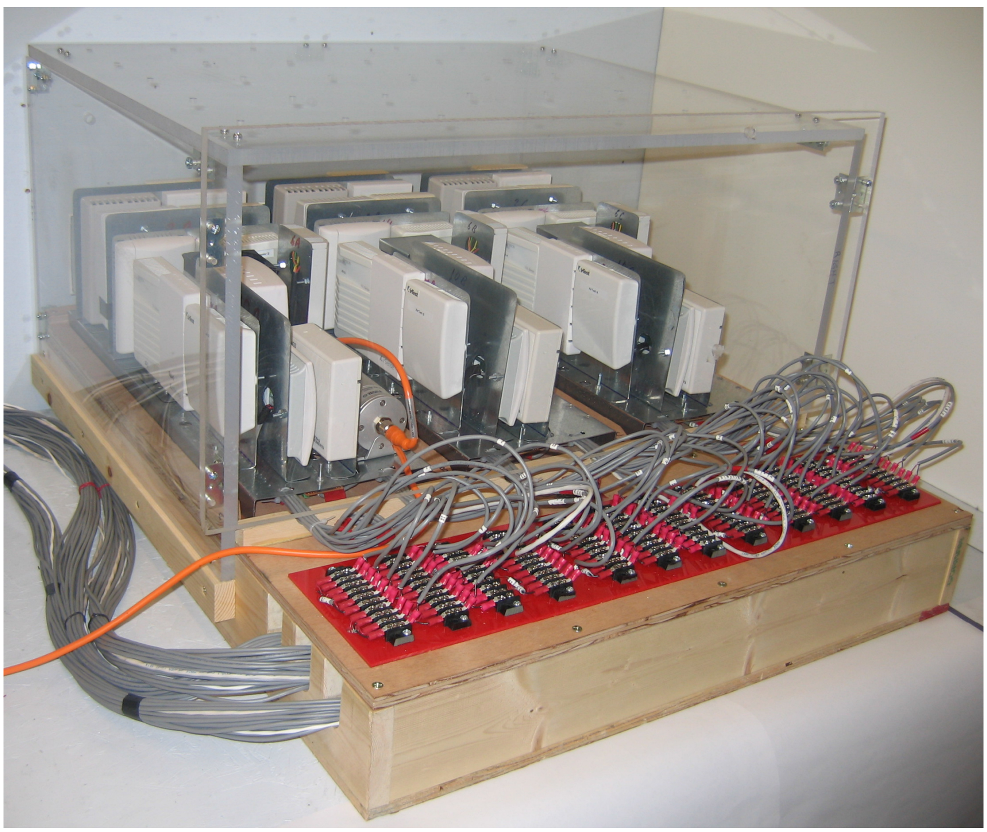

Figure 7. Lab station.

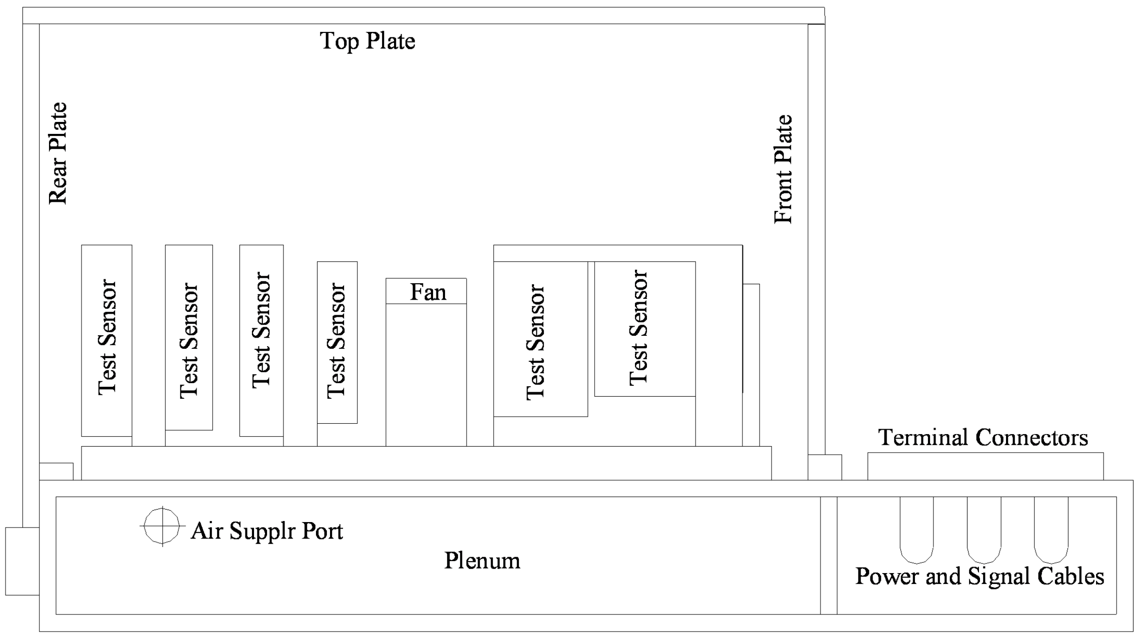

Figure 8. Schematic of the lab station.

DATA ANALYSIS

The accuracy test results are presented in terms of the deviation of the measured CO_2 concentration by a sensor from the actual CO_2 concentration in the test chamber (i.e., deviation = measured CO_2 concentration – actual CO_2 concentration). Deviation is calculated for each sensor at each test condition. Mean deviation for a given sensor at a given condition is the average deviation of the first forward measurement and the reverse measurement.

The data plots are used to investigate and analyze the accuracy of the CO_2 sensors. Specifically, a plot that compares the mean deviation and actual CO_2 concentration for a single sensor model at 40% relative humidity, 73ºF (22.8ºC) temperature, and 14.70 psia (101.35 kPa) pressure is created. Separate figures are created for each sensor model. In addition, these plots are used to compare the manufacturer specified accuracy with the measured sensor accuracy. A sample plot that shows the mean deviation of the measured CO_2 concentration from the actual CO_2 concentration for three sensors of a single sensor model is shown in Figure 9. The dotted lines in the figure illustrate the manufacturer's specified accuracy.

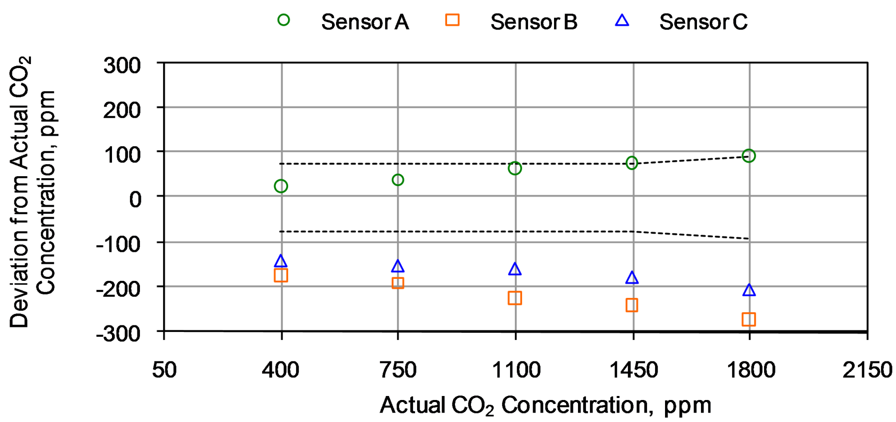

Figure 9. Comparison of mean deviation from actual CO_2 for three sensors of the same model.

The humidity sensitivity test results are presented in terms of the deviation from reading at 40% RH (i.e., deviation from reading at 40% RH = measured CO_2 concentration at a particular RH – measured CO_2 concentration at 40% RH). Humidity sensitivity is calculated for each sensor at each test condition.

The data plots are used to investigate and analyze the humidity sensitivity of the CO_2 sensors. Specifically, a plot that compares the deviation from reading at 40% RH for a single sensor model at 1100 ppm CO_2 concentration, 73ºF (22.8ºC) temperature, and 14.70 psia (101.35 kPa) pressure is created. Separate figures are created for each sensor model. Due to figure limitation in this paper, a sample plot that shows the humidity sensitivity of three different sensor models is shown in Figure 10. Although no humidity dependence on sensor performance is reported by the manufacturers, clearly some sensors are affected by humidity.

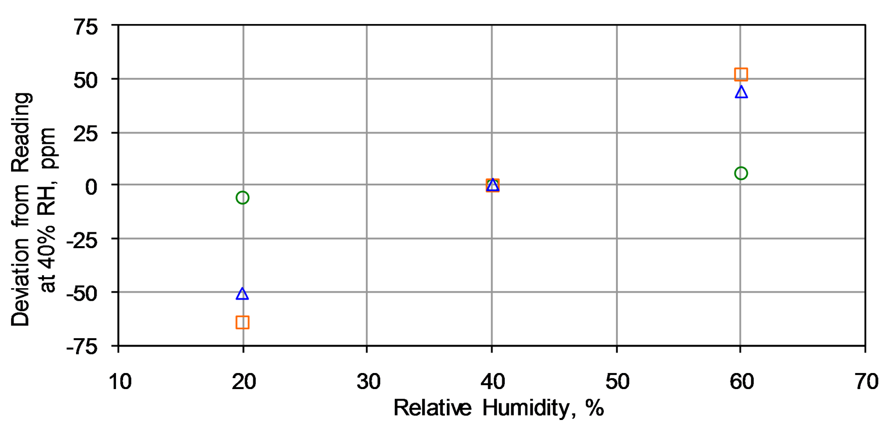

Figure 10. Humidity sensitivity of three different sensor models.

The temperature sensitivity test results are presented in terms of the deviation from reading at 73ºF (22.8ºC) temperature (i.e., deviation from reading at 73ºF (22.8ºC) = measured CO_2 concentration at a particular temperature – measured CO_2 concentration at 73ºF (22.8ºC) temperature). Temperature sensitivity is calculated for each sensor at each test condition.

The data plots are used to investigate and analyze the temperature sensitivity of the CO_2 sensors. Specifically, a plot that compares the deviation from reading at 73ºF (22.8ºC) temperature for a single sensor model at 1100 ppm CO_2 concentration, 40% RH, and 14.70 psia (101.35 kPa) pressure is created. Separate figures are created for each sensor model. A sample plot that shows the temperature sensitivity of three different sensor models is shown in Figure 11.

The pressure sensitivity test results are presented in terms of the deviation from reading at 14.70 psia (101.35 kPa) pressure (i.e., deviation from reading at 14.70 psia (101.35 kPa) pressure = measured CO_2 concentration at a particular pressure – measured CO_2 concentration at 14.70 psia (101.35 kPa) pressure). Pressure sensitivity is calculated for each sensor at each test condition.

The data plots are used to investigate and analyze the pressure sensitivity of the CO_2 sensors. Specifically, a plot that compares the deviation from reading at 14.70 psia (101.35 kPa) pressure for a single sensor model at 1100 ppm CO_2 concentration, 40% RH, and 73ºF (22.8ºC) temperature is created. Separate figures are created for each sensor model. A sample plot that shows the pressure sensitivity of three different sensor models is shown in Figure 12.

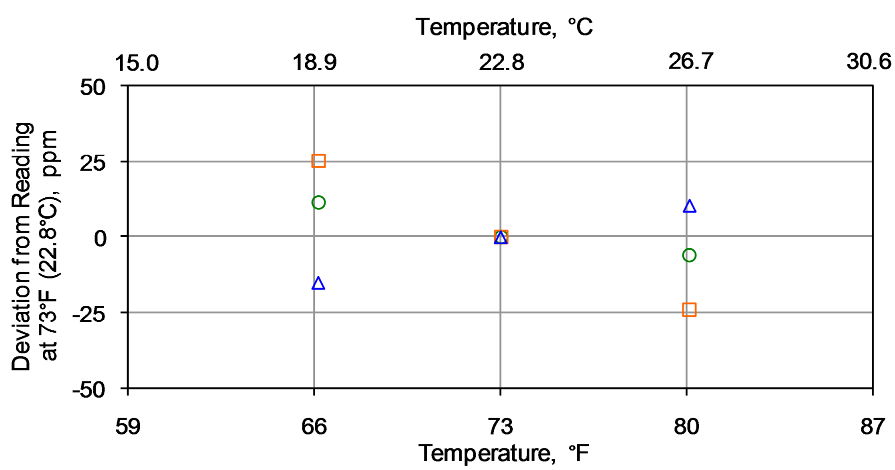

Figure 11. Temperature sensitivity of three different sensor models.

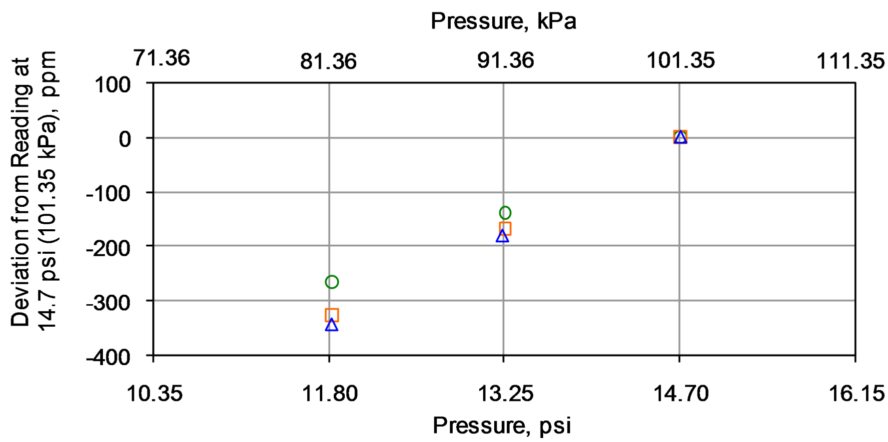

Figure 12. Pressure sensitivity of three different sensor models.

CONCLUSIONS

The effectiveness of CO_2-based DCV relies upon the performance of CO_2 sensors. However, studies on performance of CO_2 sensors and the effects of humidity, temperature, and pressure on sensor output are limited, despite the importance of sensor performance. Moreover, the findings of some studies are contradictory.

This paper presents systematic procedures to test and evaluate the accuracy, linearity, repeatability, hysteresis, humidity sensitivity, temperature sensitivity, and pressure sensitivity of NDIR CO_2 sensors used in HVAC applications. Further, it describes the experimental apparatus, instrumentation, and data acquisition system that are needed to conduct the experimental performance evaluation. Additionally, a procedure for procurement and handling of sensors is also described.

The results from testing forty-five HVAC-grade NDIR CO_2 sensors from fifteen models under accurate and repeatable conditions have shown a wider variation in sensor performance among manufacturers. In some cases, significant variations in sensor performance exist between sensors of the same model. The complete set of test results will be published in part 2 of this paper.

ACKNOWLEDGEMENTS

This work is performed for National Building Controls Information Program (NBCIP), which is sponsored by the Iowa Energy Center, NSTAR Electric & Gas Corporation and the California Energy Commission.

REFERENCES

CEC. 2006. *2005 Building Energy Efficiency Standards for Residential and Nonresidential Buildings*. CALIFORNIA ENERGY COMMISSION Title 24, Part 6, of the California Code of Regulations.

DOE. 2007. 2007 Building Energy Databook. http://buildingsdatabook.eere.energy.gov/ Washington, DC: U.S. Department of Energy, Energy Efficiency and Renewable Energy.

Dougan, D.S., and L. Damiano. 2004. CO_2-based demand control ventilation: do risk outweigh potential rewards?. *ASHRAE Journal* Vol. 46, No. 10: 47-53.

Emmerich, S.J., and A.K. Persily. 1997. Literature review on CO_2-based demand-controlled ventilation. *ASHRAE Transactions* 103 (2): 229-43.

Emmerich, S.J., and A.K. Persily. 2001. *State-of-the-art review of CO_2 demand controlled ventilation technology and application, Report NISTIR 6729, National Institute of Science and Technology (NIST), USA.*

Fahlen, P., H. Andersson, and S. Ruud. 1992. Demand Controlled Ventilating Systems - Sensor Tests. Swedish National Testing and Research Institute, Boras, Sweden, SP Report 1992:13.

Fisk, W.J., D. Faulkner, and D.P. Sullivan. 2006. Accuracy of CO_2 sensors in commercial buildings: a pilot study. LBNL-61962, Lawrence Berkeley National Laboratory, Berkeley, CA.

Hyland, R.W., and A. Wexler. 1983. Formulations for the thermodynamic properties of the saturated phases of H_2O from 173.15 K to 473.15 K. *ASHRAE Transactions* 89(2A):500-519.

Raatschen, W., ed. 1990. Demand Controlled Ventilating System. State of the Art Review. Stockholm, Sweden: Swedish Council for Building Research, Stockholm, Sweden, D9:1990.

Roth, K.W., D. Westphalen, M.Y. Pheng, P. Llana, and L. Quartararo. 2005. Energy impact of commercial building controls and performance diagnostics: Market characterization, energy impact of building faults and energy saving potential. http://www.tiaxllc.com/aboutus/pdfs/energy_imp_comm_bldg_cntrls_perf_diag_110105.pdf

Schell, M., and D. Int-Hout. 2001. Demand control ventilation using CO_2. *ASHRAE Journal* Vol. 43, No. 2: 18-24.

APPENDIX

For a dry-gas mixture of nitrogen and carbon dioxide, the concentration of $CO_{2,d}$ (The subscript, *d*, is used to emphasize the dry-gas mixture) is achieved by accurately controlling the mass flow rate of each gas during the mixing process. This process is controlled by the gas-mixing system. The concentration of the $CO_{2,d}$ in units of parts per million (ppm) is the volume fraction of the $CO_{2,d}$ expressed as the volume units of $CO_{2,d}$ per 10^6 volume units of mixture. When water vapor is subsequently added to the mixture, (as a result of bubbling the dry gas through a water column), the total number of moles in the mixture increases and the concentration of $CO_{2,d}$ is reduced. Thus, in order to achieve a particular value of CO_2 concentration in the moist gas mixture, a higher value of $CO_{2,d}$ concentration must be produced by the gas-mixing system.

Determination of the CO_2 concentration in the new mixture requires knowledge of the concentration of water vapor in the moist-gas mixture. The concentration of water vapor present in a mixture of gases can be calculated based on psychometric relations for ideal-gas mixtures and values of three independent thermodynamic properties such as pressure, temperature and relative humidity. The concentration of water vapor is directly related to the partial pressure of water vapor (P_w) in the mixture as given by Equation (A-1)

$$ppm_w = \frac{P_w\left(10^6\right)}{P} \qquad \text{(A-1)}$$

The partial pressure of the water vapor is related to the relative humidity and saturation pressure (P_{ws}) of water through the definition of relative humidity (ϕ) as given by Equation (A-2)

$$\phi(\%) = \frac{P_w}{P_{ws}} * 100 \qquad \text{(A-2)}$$

The saturation pressure of the water vapor (P_{ws}) is only a function of temperature and is computed using the formula by Hyland and Wexler (Hyland and Wexler 1983) as given by Equation (A-3).

$$\ln P_{ws} = \frac{C_8}{T} + C_9 + C_{10}T + C_{11}T^2 + C_{12}T^3 + C_{13}\ln T \qquad \text{(A-3)}$$

where

$C_8 = -1.044\ 039\ 7\ \text{E+04}$

$C_9 = -1.129\ 465\ 0$ E+01
$C_{10} = -2.702\ 235\ 5$ E−02
$C_{11} = 1.289\ 036\ 0$ E−05
$C_{12} = -2.478\ 068\ 1$ E−09
$C_{13} = 6.545\ 967\ 3$ E+00
T = gas temperature (°R)
P_{ws} = saturation pressure (psia)

The mole fraction of water molecules (y_w) in a gas mixture is computed from the ratio of the partial pressure of the water vapor (P_w) to the mixture pressure (P) as given in Equation (A-4).

$$y_w = \frac{P_w}{P} = \frac{n_w}{n} \qquad \text{(A-4)}$$

In Equation (A-4), n_w is the number of moles of water vapor and n is the total number of moles in the mixture.

Multiplying the number of moles by Avogadro's number (N_A) gives the number of molecules (N) in a given moles of gas, hence:

$$\frac{n_w}{n} = \frac{n_w(N_A)}{n(N_A)} = \frac{N_w}{N} \qquad \text{(A-5)}$$

In Equation (A-5), N_w is the number of H_2O molecules and N is the total number of molecules in the mixture.

Applying Avogadro's hypothesis, the concentration of H_2O molecules in the mixture (ppm_w) by volume yields:

$$ppm_w = \frac{N_w(10^6)}{N} = \frac{P_w(10^6)}{P} \qquad \text{(A-6)}$$

Then the required CO_2 concentration of the dry gas $(ppm_{CO_2,d})$ from the gas-mixing system to get the desired CO_2 concentration after adding water vapor (ppm_{CO_2}) can be calculated as:

$$ppm_{CO_2,d} = ppm_{CO_2}\left(1 + \frac{ppm_w}{10^6 - ppm_w}\right) \qquad \text{(A-7)}$$

Table A1 shows the required $CO_{2,d}$ concentration of the dry-gas mixture from the gas-mixing system to obtain the desired CO_2 concentration of the moist-gas mixture in the test chamber for various CO_2 concentrations and relative humidity at 73°F (22.8°C) temperature and 14.70 psia (101.35 kPa) pressure.

Table A1. CO_2 Concentration Correction Values

Desired CO_2 Concentration of the moist gas mixture $\left(ppm_{CO_2}\right)$, ppm	Relative Humidity of the gas mixture (ϕ), %	Required CO_2 Concentration of the Dry Gas Mixture from the Gas Mixing System $\left(ppm_{CO_2,d}\right)$, ppm
400	40	404.4
750	40	758.3
1100	40	1112.1
1450	40	1466.0
1800	40	1819.9
1100	20	1106.0
1100	60	1118.3

Chapter 3: An Experimental Evaluation of HVAC-Grade Carbon-Dioxide Sensors: Part 2, Performance Test Results

A paper to be submitted to the ASHRAE Transactions

Som S. Shrestha
Student Member ASHRAE

Gregory M. Maxwell, PhD
Member ASHRAE

ABSTRACT

This is the second paper in a four-part series reporting on the test and evaluation of typical carbon-dioxide sensors used in building HVAC applications. Fifteen models of NDIR HVAC-grade CO_2 sensors were tested and evaluated to determine the accuracy, linearity, repeatability, and hysteresis of each sensor. This paper describes the performance of the sensors and provides a comparison with the manufacturers' specifications. The sensors were tested at 40% relative humidity, 73°F (22.8°C) temperature, 14.70 psia (101.35 kPa) pressure, and at five different CO_2 concentrations (400 ppm, 750 ppm, 1100 ppm, 1450 ppm, and 1800 ppm). The test results showed a wide variation in sensor performance among the various manufacturers and in some cases a wide variation among sensors of the same model.

In all, 45 sensors were evaluated: three from each of the 15 models. Among the 15 models tested, eight models have a single-lamp, single-wavelength configuration, four models have a dual-lamp, single-wavelength configuration, and three models have a single-lamp, dual-wavelength configuration.

INTRODUCTION

This is part two of a four-part series of papers reporting on the test and evaluation of typical CO_2 sensors used in building HVAC systems. In this study, fifteen models of NDIR (non-dispersive infrared) HVAC-grade CO_2 sensors were tested and evaluated. In all, 45 sensors (three from each model) were evaluated to determine the sensor accuracy, linearity, repeatability, and hysteresis. The results are compared with the manufacturers' specifications. The experimental procedure used to test and evaluate the sensors was described in Part 1 (Shrestha and Maxwell 2009) of this paper. Among the 15 models tested, eight models have a single-lamp, single-wavelength configuration, four models have a dual-lamp, single-wavelength configuration, and three models have a single-lamp, dual-wavelength configuration. All single-lamp, single-wavelength sensors and one single-lamp, dual-wavelength sensor incorporate an “automatic baseline adjustment” algorithm in the sensor’s electronics package.

This paper presents an overview of the past studies performed by researchers to evaluate the performance of CO_2 sensors used in HVAC application. Further, a brief discussion on CO_2 sensor specifications and experimental test procedures (detailed in Part 1 of this paper) is provided. In addition, the paper presents test and evaluation results, including a comparison of the performance of various CO_2 sensors.

PREVIOUS STUDIES

In the past, limited studies have been done to investigate the performance of HVAC-grade CO_2 sensors using a controlled environment. Fahlen et al. (1992) evaluated the performance of two CO_2 sensors, one photo-acoustic type and one infrared spectroscopy type, in lab tests and long term field tests. The lab tests included performance and environmental tests. The authors conclude that the deviation between actual concentration and the sensors’ reading are normally well within ± 50 ppm at a concentration level of 1000 ppm. However, at a concentration of 2000 ppm the test results showed a deviation of up to -300 ppm. The output of one sensor increased dramatically during environmental testing. This sensor failed to return to its normal value.

Fisk et al. (2006) conducted a pilot study that evaluated the in-situ accuracy of 44 NDIR CO_2 sensors located in nine commercial buildings. The evaluation was performed either by multi-point calibration using CO_2 calibration gas or by a single-point calibration check using a co-located and calibrated reference CO_2 sensor. Their results indicated that the accuracy of CO_2 sensors is frequently less than what is needed to measure peak indoor-outdoor CO_2 concentration differences with an error that is less than 20%. Thus, the authors conclude that there is a need for more accurate CO_2 sensors and/or better maintenance and calibration.

Pandey et al. (2007) evaluated the accuracy of two NDIR CO_2 sensor models. They tested three sensors of each model. The tests were performed in an enclosure where all six sensors were simultaneously exposed to CO_2 concentration of 0 ppm, 500 ppm, and 1000 ppm (other environmental conditions, such as humidity, temperature, and pressure were not specified.) The maximum deviation was observed as -73 ppm at a CO_2 concentration of 500 ppm.

CONFIGURATIONS OF NDIR CO_2 SENSORS

Various techniques are used by CO_2 sensor manufacturers to compensate for the long-term effects of operational and environmental conditions. These techniques have lead to the three basic configurations currently used in NDIR CO_2 sensors: (1) single-lamp,[8] single-wavelength, (2) dual-lamp, single-wavelength, and (3) single-lamp, dual-wavelength. Figure 1 illustrates these configurations.

All single-lamp, single-wavelength sensors (illustrated in Figure 1a) incorporate an "automatic baseline adjustment" algorithm in the sensor's electronics package. The algorithm "adjusts" the sensor's output according to the minimum CO_2 concentration observed over a time period. It is assumed that the minimum CO_2 concentration observed corresponds to the outdoor CO_2 concentration. A value of 400 ppm is commonly used as the value for the outdoor CO_2 concentration level to which the sensor output is set when the automatic baseline adjustment is made. The programming logic used in the algorithm varies among sensor manufacturers. Some algorithms adjust the baseline value as frequently as every hour. Other algorithms perform adjustments based on several weeks of sampling and only make incremental step adjustments to the baseline value. It is important to note that sensors which use any algorithm to adjust the sensor output based upon minimum CO_2 concentration observed must only be used in applications where they will be periodically exposed to levels of CO_2 in the outdoor air.

The dual-lamp, single-wavelength configuration (illustrated in Figure 1b) uses two IR (infrared) sources (lamps). One lamp pulses several times per minute while the second lamp pulses much less frequently (on the order of one or two pulse every 24 hours). Due to the relatively infrequent pulsing of the second lamp, the ageing of the second lamp is much less than the ageing of the first lamp, thus the second lamp is used as a reference for sensor compensation.

Figures 1c and 1d illustrate two configurations which are both referred to as single-lamp, dual-wavelength sensors. The principle behind either configuration is understood by examining the spectral properties of the filters used. Filter 1 (Figure 1c) passes IR radiation in a portion of the IR spectrum that contains no absorption bands for any of the gases commonly found in air. For this wavelength, the output from the IR detector is

---

[8] The term "beam" is used by sensor manufacturers; however, this leads to confusion on the technology employed in the sensor configuration. A single lamp can produce multiple "beams", so when the term "dual beam" is used, it is not clear if one or two lamps are employed.

independent of the mixture of gases in the air sample; therefore, this output provides a reference signal used for sensor compensation. Filter 2 (Figure 1c) passes 4.26 μm IR radiation which is used for the CO_2 concentration measurement.

The configuration shown in Figure 1d uses a silicone-based electronically-tunable Fabry-Perot interferometer in front of the detector. This solid-state device provides an electronic method of switching between the band pass filters, thus allowing for sensor compensation using a single filter-detector package.

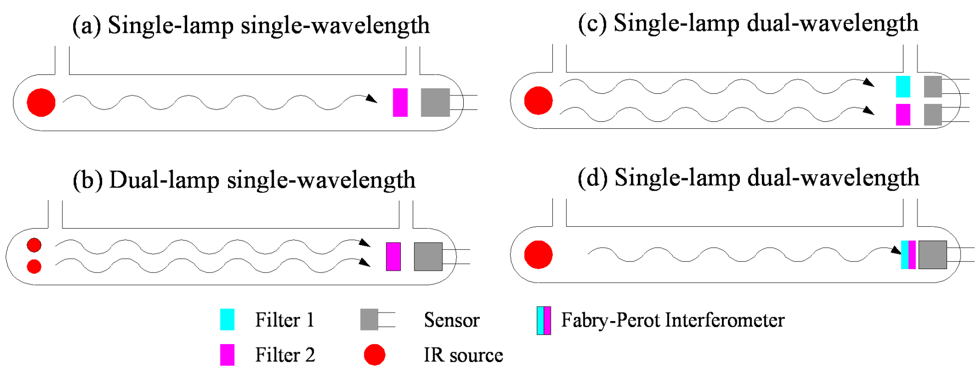

Figure 1. NDIR sensor configurations.

CO_2 SENSOR SPECIFICATIONS

CO_2 sensor manufacturers provide detailed specifications for their products. This information is available from the company's website and/or literature packaged with the product. Table 1 summarizes some of the product information for the models evaluated in this study. (Specific product names are not used in this paper, rather the sensors are referred to as S1 through S15.) The table indicates the sensor configuration, the manufacturer-specified accuracy, linearity, and repeatability. The accuracy statements for some sensor models include the pressure and temperature conditions for which the accuracy statement applies. For other sensor models, these conditions are not explicitly stated. Three manufacturers state the nonlinearity of their sensors, and five manufacturers state the repeatability of their sensors. None of the manufacturers specify humidity levels as part of the accuracy statement nor explicitly state the hysteresis of their sensors.

Sensors S1 through S8 are single-lamp, single-wavelength sensor, sensors S9 through S12 are dual-lamp, single-wavelength sensors, and sensors S13 through S15 are single-lamp, dual-wavelength sensors. Of the three single-lamp, dual-wavelength sensors, sensor model S14 incorporates an "automatic baseline adjustment"

Table 1. Manufacturer-Specified Accuracy, Nonlinearity, and Repeatability for CO_2 Sensors

Sensor Model	Configuration	Accuracy	Manufacturer-Specified Nonlinearity	Manufacturer-Specified Repeatability
S1	Single-lamp, single-wavelength	± 1% of measurement range + 5% of measured value	NA	NA
S2	Single-lamp, single-wavelength	± 100 ppm or 7% whichever is greater	NA	NA
S3	Single-lamp, single-wavelength	± 50 ppm or + 3% of reading (at 25°C (77°F)at standard pressure)	< 1% FS	NA
S4	Single-lamp, single-wavelength	± 5% of reading or 75 ppm, whichever is greater	NA	± 20 ppm
S5	Single-lamp, single-wavelength	± 75 ppm or 3% of reading, whichever is greater (15°C to 32°C (59°F to 90°F))	NA	± 20 ppm
S6	Single-lamp, single-wavelength	± (30 ppm + 2% of reading)	NA	NA
S7	Single-lamp, single-wavelength	± 5% of reading or ± 75 ppm, whichever is greater	NA	± 20 ppm
S8	Single-lamp, single-wavelength	± 30 ppm ± 5% of measured value	NA	± 20 ppm ± 1% measured value
S9	Dual-lamp, single-wavelength	± 75 ppm if 0 to 1500 ppm: ± 5% if > 1500ppm (readings at standard pressure 760 mm Hg & 25°C (77°F))	NA	± 8 ppm
S10	Dual-lamp, single-wavelength	≤ ± 50 ppm + 2% of measured value	NA	NA
S11	Dual-lamp, single-wavelength	± 100 ppm + 3% of reading	NA	NA
S12	Dual-lamp, single-wavelength	< ± (50 ppm + 2% of measure value) at 20°C (68°F)	NA	NA
S13	Single-lamp, dual-wavelength	< ± (30 ppm + 2.0% of reading) at 68°F (20°C)	< 1% FS	NA
S14	Single-lamp, dual-wavelength	± 50 ppm or 5% whichever is greater (7% for levels over 1500 ppm) at 60°F to 90°F (15°C to 32°C)	NA	NA
S15	Single-lamp, dual-wavelength	< ± (30ppm + 2% of reading) at 25°C (77°F)	< ± 1% FS	NA

Notes: NA indicates that the information was not available in the manufacturer's product literature. Full scale (FS) is 2000 ppm for all sensors. The nominal operating temperature range is 32°F to 122° (0°C to 50°C) with 0% to 95% RH.

algorithm. Many sensor models provide options for the output signal produced. In this study, all sensors were tested using an output signal of 0 to 10 VDC. Sensor model S11 only provides an output signal of 4 to 20 mA. For this sensor, a precision resistor was used to convert the signal into VDC. Measurement range of all sensors is 0 to 2000 ppm.

EXPERIMENTAL TEST PROCEDURE

The CO_2 sensors were tested using a test chamber specifically designed and fabricated for the performance evaluation. Technical details of the test chamber and instrumentation are described in Part 1 (Shrestha and Maxwell 2009) of this paper. All tests were conducted while maintaining the chamber relative humidity, temperature, and pressure at 40%, 73ºF (22.8ºC) and 14.70 psia (101.35 kPa), respectively. Established testing procedures, including requirements for steady-state conditions, are described in Part 1 (Shrestha and Maxwell 2009). The accuracy and linearity of the sensors were evaluated using the first forward and reverse measurements at CO_2 concentrations of 400, 750, 1100, 1450, and 1800 ppm (corresponding to data points 1 to 9 in Figure 2). Repeatability was evaluated using the two forward measurements at CO_2 concentrations of 750, 1100 and 1450 ppm (corresponding to data points 2 to 4 and 10 to 12 in Figure 2). Hysteresis was evaluated using the first forward measurement and the reverse measurement at CO_2 concentrations of 750, 1100 and 1450 ppm (corresponding to data points 2 to 4 and 6 to 8 in Figure 2).

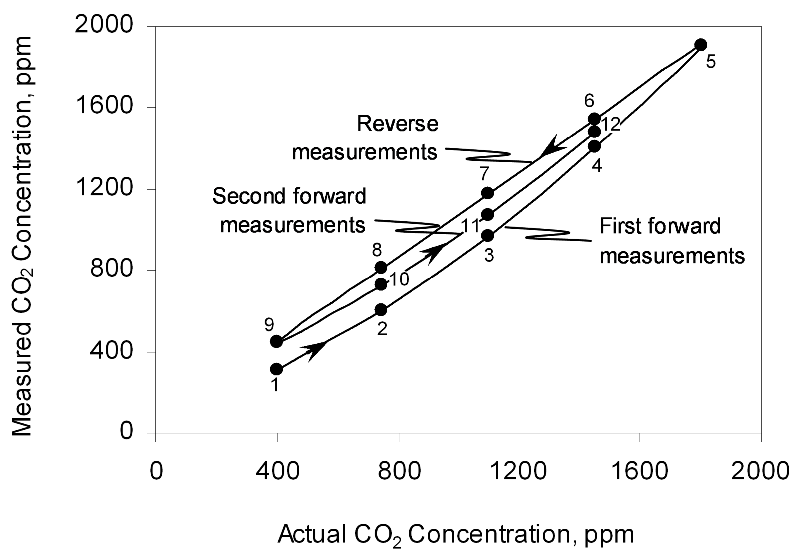

Figure 2. Example data set to illustrate numbering scheme used to identify data points.

ACCURACY TEST RESULTS

The accuracy test results are presented in terms of the deviation of the measured CO_2 concentration by a sensor from the actual CO_2 concentration in the test chamber (i.e., deviation = measured CO_2 concentration – actual CO_2 concentration). Deviation is calculated for each sensor at each test condition. The mean deviation for a given sensor at a given condition is the average deviation of the first forward measurement and the reverse measurement. As mentioned above, three sensors from each of fifteen models were tested. The letters A, B and C are used to distinguish between each sensor of a given model.

Data plots are used to illustrate the accuracy of the CO_2 sensors while numerical results are provided in tables. Specifically, a plot that compares the mean deviation and actual CO_2 concentration for a single sensor model was created. Each accuracy plot also illustrates the manufacturer-specified accuracy. The accuracy statement appears as a set of dotted lines on the plot. For most sensor models, the accuracy band increases at higher CO_2 levels; therefore, the dotted lines are seen to diverge as the CO_2 level increases.

Before discussing the results for each sensor, it should be pointed out that for some sensors the maximum output voltage (nominally 10 VDC) was reached when the sensors were exposed to the higher level CO_2 concentration test conditions. This is seen in Figure 3 which shows the output voltage from sensor S2B (model S2, sensor group B) as the CO_2 concentration in the test chamber increases. As seen in the figure, when the CO_2 concentration reaches approximately 1700 ppm, the output voltage of the sensor is 10 VDC. Since this is the maximum voltage produced by the sensor, further increases in CO_2 concentration do not produce any change in the output voltage. For sensor S2B, the output reading would indicate 2000 ppm for any CO_2 concentration in excess of 1700 ppm. The sensor is said to be saturated. For all sensor models tested, the operating range of each sensor is 0 to 2000 ppm. Saturated data points were not considered for analysis.

Analysis of Deviations for each Sensor Model

Analysis of deviations for each sensor model is presented in this section. All sensors were tested under "as received" conditions from the suppliers. No calibration was performed on the sensors prior to testing. Sensors were powered up and allowed to stabilize in the laboratory environment before they were tested.

Single-lamp, single-wavelength sensors: Figure 4 shows the accuracy test results for the sensors that use the single-lamp, single-wavelength configuration. These sensors use a manufacturer-specific proprietary algorithm to periodically adjust the baseline CO_2 concentration according to the minimum CO_2 concentration observed over a time period. It is assumed that the minimum CO_2 concentration observed corresponds to the outdoor CO_2 concentration. A value of 400 ppm is commonly used as the value for the outdoor CO_2 concentration level to which the sensor output is set when the automatic baseline adjustment is made.

Prior to placing the sensors in the test chamber for performance testing, all sensors were operating in the laboratory environment where the average environmental conditions (relative humidity, temperature, and barometric pressure) were, 14.7% , 76°F (24.2°C), and 14.3 psia (98.6 KPa), respectively. The minimum CO_2 concentration in the laboratory varies on a daily basis according to the variation in the ambient CO_2 concentration. Figure 5 shows the CO_2 concentration in the laboratory for two weeks prior to the performance test.

Operating in the laboratory environment for an extended period of time allowed the sensors with automatic baseline adjustment algorithm to "adjust" their baseline; therefore, when these sensors are placed under test conditions and compared to "actual" CO_2 concentration levels, there is some bias in the measured value reported by the sensor. Because this bias is unknown, no compensation was made when showing the test results. It is therefore up to the reader to interpret the meaningfulness of the comparison of the sensor accuracy to the accuracy statement for each sensor that uses an "automatic baseline adjustment" algorithm.

Table 2 shows the numerical values of the deviations for each sensor at each CO_2 level. Data points corresponding to saturated sensor output are highlighted in the table.

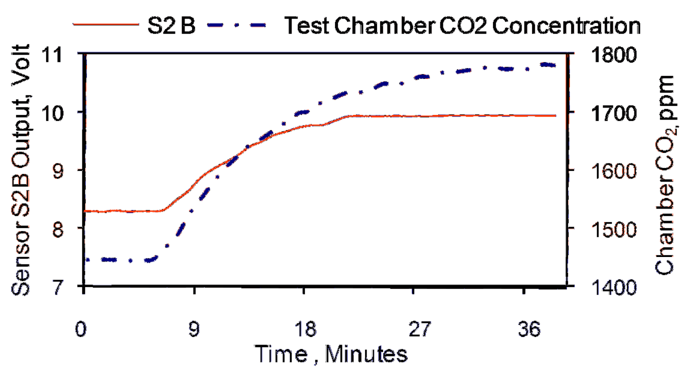

Figure 3. Saturated reading of S2B sensor at 1800 ppm.

Sensor S1

The deviations of the measured CO_2 concentration from the actual CO_2 concentration for Model S1 sensors are presented graphically in Figure 4(a). The manufacturer-stated accuracy for this sensor model is ± 1% of measurement range + 5% of measured value. The deviation of all three sensors shifts upward when the actual CO_2 concentration was increased. However, the slope of sensors A and C are a little higher than the slope of sensor B. The reference relative humidity, temperature, and pressure for the stated accuracy were not specified by the manufacturer.

The deviation of sensor B is within the manufacturer-stated accuracy at all CO_2 levels. The deviations of sensors A and C are also within the manufacturer-stated accuracy at 1800 ppm CO_2. The maximum discrepancy between the actual deviation and the manufacturer-stated accuracy is 22 ppm (sensor A at 750 ppm).

Sensor S2

The deviations of the measured CO_2 concentration from the actual CO_2 concentration for Model S2 sensors are presented graphically in Figure 4(b). The manufacturer-stated accuracy for this sensor model is ± 100 ppm or 7%, whichever is greater. The reference relative humidity, temperature, and pressure for the stated accuracy were not specified by the manufacturer. The deviation of all three sensors shifts upward when the actual CO_2 concentration was increased. The reading of sensor B is saturated at 1800 ppm reading.

The deviation of sensor C is within the manufacturer-stated accuracy at all CO_2 levels. The deviation of sensor A at 400 and 750 ppm CO_2 and that of sensor B at 400 ppm CO_2 are also within the manufacturer-stated accuracy. The maximum discrepancy between the actual deviation and the manufacturer-stated accuracy is 109 ppm (sensor B at 1450 ppm).

Sensor S3

The deviations of the measured CO_2 concentration from the actual CO_2 concentration for Model S3 sensors are presented graphically in Figure 4(c). The manufacturer-stated accuracy for this sensor model is ± 50 ppm or 3% of reading. The reference temperature and pressure for the stated accuracy are 77°F (25°C) and standard pressure, respectively. When the actual CO_2 concentration was increased, the deviation of sensors A and B shifts upward, whereas the deviation of sensor C shifts downward. The reading of sensor A is saturated at 1800 ppm reading.

The deviation of sensor B and C are within the manufacturer-stated accuracy at all CO_2 levels. The deviation of sensor A at 400 ppm CO_2 is also within the manufacturer-stated accuracy. The maximum discrepancy between the actual deviation and the manufacturer-stated accuracy is 118 ppm (sensor A at 1450 ppm).

Sensor S4

The deviations of the measured CO_2 concentration from the actual CO_2 concentration for Model S4 sensors are presented graphically in Figure 4(d). The manufacturer-stated accuracy for this sensor model is ± 5% of reading or 75 ppm, whichever is greater. The reference temperature and pressure for the stated accuracy are not specified by the manufacturer. The deviation of all three sensors shifted upward when the actual CO_2 concentration was increased. The readings for all three sensors are saturated at 1800 ppm.

None of the sensors read within the manufacturer-stated accuracy. The maximum discrepancy between the actual deviation and the manufacturer-stated accuracy is 302 ppm (sensor C at 1450 ppm).

Sensor S5

The deviations of the measured CO_2 concentration from the actual CO_2 concentration for Model S5 sensors are presented graphically in Figure 4(e). The manufacturer-stated accuracy for this sensor model is ± 75 ppm or 3% of reading, whichever is greater. The reference temperature for the stated accuracy is 59°F to 90°F (15°C to 32°C). The reference pressure for the stated accuracy is not specified. When the actual CO_2 concentration was increased, the deviations of all three sensors shift upward. The reading of sensor A is saturated at 1800 ppm.

The deviation of all three sensors is within the manufacturer-stated accuracy at 400 ppm CO_2, whereas none of the sensors read within manufacturer-stated accuracy at other CO_2 levels. The maximum discrepancy between the actual deviation and the manufacturer-stated accuracy is 184 ppm (sensor A at 1450 ppm).

Sensor S6

The deviations of the measured CO_2 concentration from the actual CO_2 concentration for Model S6 sensors are presented graphically in Figure 4(f). The manufacturer-stated accuracy for this sensor model is ± 30 ppm + 2% of reading. The reference temperature and pressure for the stated accuracy are not specified by the manufacturer. The deviation of all three sensors shifts upward when the actual CO_2 concentration was increased. The reading of sensor C is saturated at 1800 ppm.

None of the sensors read within the manufacturer-stated accuracy at any CO_2 levels. The maximum discrepancy between the actual deviation and the manufacturer-stated accuracy is 129 ppm (sensor C at 1450 ppm).

Sensor S7

The deviations of the measured CO_2 concentration from the actual CO_2 concentration for Model S7 sensors are presented graphically in Figure 4(g). The manufacturer-stated accuracy for this sensor model is ± 5% of reading or 75 ppm, whichever is greater. The reference temperature and pressure for the stated accuracy are not specified by the manufacturer. The deviation of all three sensors shifts upward when the actual CO_2 concentration was increased. The reading of all three sensors is saturated at 1800 ppm.

None of the sensors read within the manufacturer-stated accuracy. The maximum discrepancy between the actual deviation and the manufacturer-stated accuracy is 407 ppm (sensor A at 1450 ppm).

Sensor S8

The deviations of the measured CO_2 concentration from the actual CO_2 concentration for Model S8 sensors are presented graphically in Figure 4(h). The manufacturer-stated accuracy for this sensor model is ± 30 ppm ± 5% of measured value. The reference temperature and pressure for the stated accuracy are not specified by the manufacturer. The deviation of all sensors shifts upward when the actual CO_2 concentration was increased. The reading of sensor A is saturated at 1800 ppm reading.

The deviation of sensor B is within the manufacturer-stated accuracy at all CO_2 levels. The deviations of sensor C at 400 and 1800 ppm CO_2 are also within the manufacturer-stated accuracy. The maximum discrepancy between the actual deviation and the manufacturer-stated accuracy is 113 ppm (sensor A at 1450 ppm).

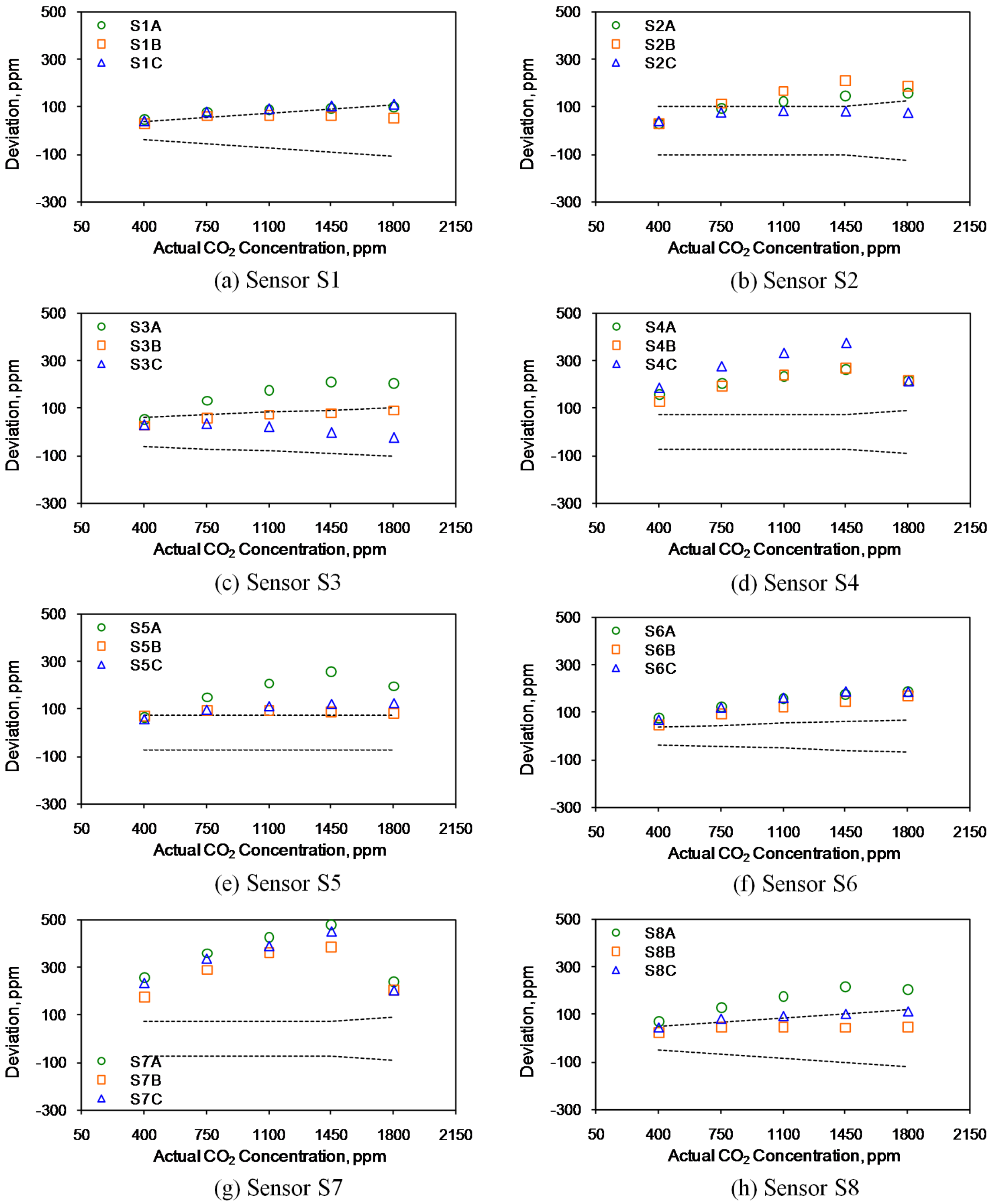

(a) Sensor S1
(b) Sensor S2
(c) Sensor S3
(d) Sensor S4
(e) Sensor S5
(f) Sensor S6
(g) Sensor S7
(h) Sensor S8

Figure 4. Comparison of deviation from actual CO_2 concentration of single-lamp, single-wavelength sensors.

Table 2. Deviation from Actual CO_2 Concentration (ppm), Single-Lamp, Single-Wavelength Sensors

Sensor Model	Sensor	Deviation at, ppm				
		400	750	1100	1450	1800
S1	A	47	79	86	96	99
	B	26	59	62	58	49
	C	42	78	91	102	109
S2	A	28	94	125	147	161
	B	30	115	167	211	188
	C	37	74	80	79	73
S3	A	49	129	174	212	206
	B	26	57	73	80	90
	C	29	34	21	-2	-22
S4	A	156	202	233	262	214
	B	126	192	239	270	216
	C	188	279	335	377	216
S5	A	64	151	208	259	197
	B	71	96	95	91	85
	C	56	97	113	123	126
S6	A	73	120	156	171	185
	B	47	94	124	149	171
	C	69	121	161	188	187
S7	A	257	361	428	482	240
	B	171	288	359	385	201
	C	233	337	390	452	202
S8	A	66	125	172	216	201
	B	23	48	50	45	48
	C	44	82	94	103	114

Note: The highlighted numbers indicate that the sensor reading was saturated.

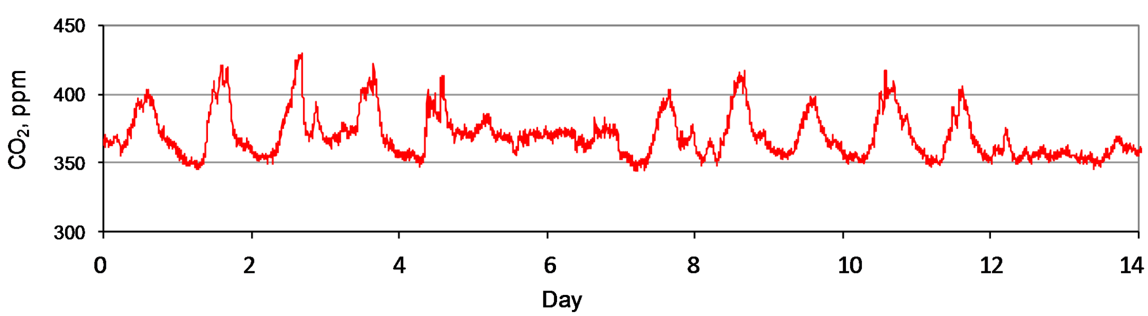

Figure 5. CO_2 concentration in the laboratory for two weeks prior to commencing the performance test.

Dual-lamp, single-wavelength sensors: Figure 6 shows the accuracy test results of the sensors that use the dual-lamp, single-wavelength configuration. Table 3 shows the numerical values of the deviation for each sensor. In some cases, the sensors' outputs corresponding to a concentration of 1,800 ppm are saturated. These data points are highlighted in the table.

Sensor S9

The deviations of the measured CO_2 concentration from the actual CO_2 concentration for Model S9 sensors are presented graphically in Figure 6(a). The manufacturer-stated accuracy for this sensor model is ± 75 ppm for 0 to 1500 ppm and 5% of reading for greater than 1500 ppm. The reference temperature and pressure for the stated accuracy are 77°F (25°C) and 14.70 psia (101.35 kPa), respectively. The deviation of sensor A shifts upward when the actual CO_2 concentration was increased, whereas the deviation of the sensors B and C shifts downward when the actual CO_2 concentration was increased.

The deviation of sensor A at 400, 750, and 1100 ppm are within the manufacturer-stated accuracy at all CO_2 levels. The maximum discrepancy between the actual deviation and the manufacturer-stated accuracy is -184 ppm (sensor B at 1800 ppm).

Sensor S10

The deviations of the measured CO_2 concentration from the actual CO_2 concentration for Model S10 sensors are presented graphically in Figure 6(b). The manufacturer-stated accuracy for this sensor model is ± 50 ppm + 2% of measured value. The reference temperature and pressure for the stated accuracy are not specified by the manufacturer. The deviation of all three sensors shifts upward when the actual CO_2 concentration was increased. The reading of sensor C is saturated at 1800 ppm. None of the sensors read within the manufacturer-stated accuracy. The maximum discrepancy between the actual deviation and the manufacturer-stated accuracy is 141 ppm (sensor C at 1450 ppm).

Sensor S11

The deviations of the measured CO_2 concentration from the actual CO_2 concentration for Model S11 sensors are presented graphically in Figure 6(c). The manufacturer-stated accuracy for this sensor model is ± 100 ppm + 3% of reading. The reference temperature and pressure for the stated accuracy were not specified by the manufacturer. The deviation of sensors B and C shifts upward when the actual CO_2 concentration was increased, whereas, the deviation of sensor A shifts downward when the actual CO_2 concentration was increased.

The deviations of sensors A and C are within the manufacturer-stated accuracy at all CO_2 levels. The deviation of sensor B is also within the manufactured stated accuracy at 400 ppm CO_2. The maximum discrepancy between the actual deviation and the manufacturer-stated accuracy is 46 ppm (sensor B at 1800 ppm).

Sensor S12

The deviations of the measured CO_2 concentration from the actual CO_2 concentration for Model S12 sensors are presented graphically in Figure 6(d). The manufacturer-stated accuracy for this sensor model is ± 50 ppm + 2% of measured value. The reference temperature for the stated accuracy is 68°F (20°C). The reference pressure for the stated accuracy is not specified. Deviations of all three sensors shift upward when the actual CO_2 concentration was increased. The reading of sensors A and B are saturated at 1800 ppm. None of the sensors read within the manufacturer-stated accuracy. The maximum discrepancy between the actual deviation and the manufacturer-stated accuracy is 116 ppm (sensor B at 1450 ppm).

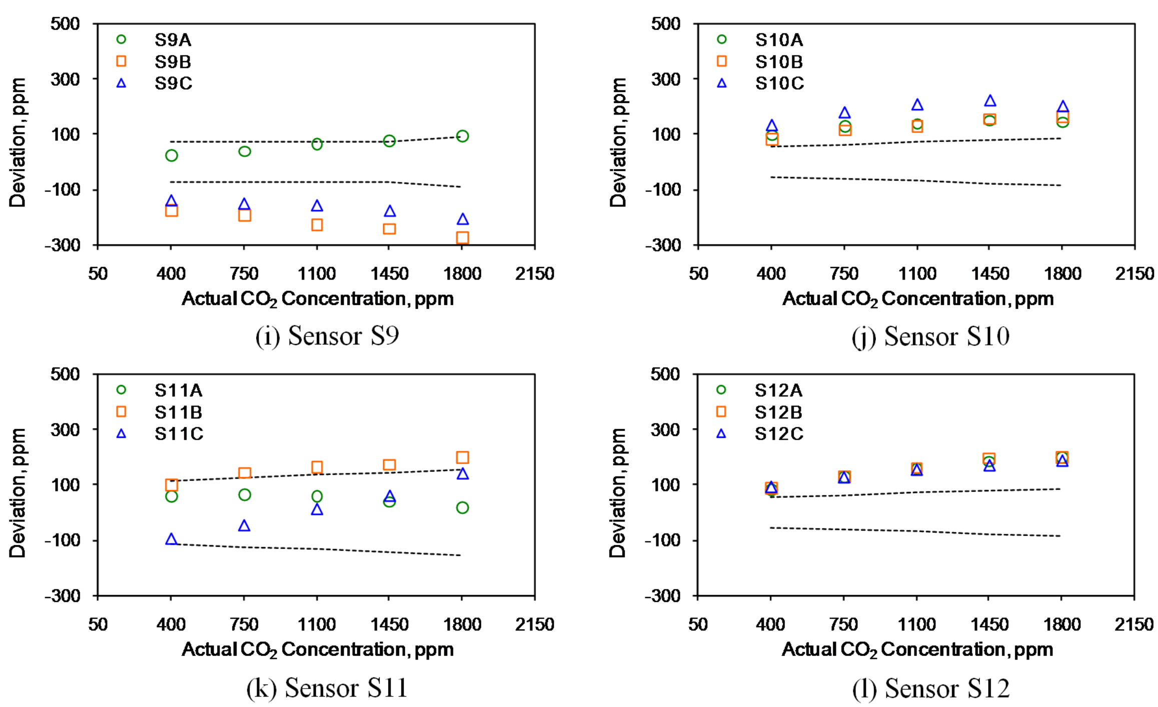

Figure 6. Comparison of deviation from actual CO_2 concentration of dual-lamp, single-wavelength sensors.

Table 3. Deviation from Actual CO_2 Concentration (ppm), Dual-Lamp, Single-Wavelength Sensors

Sensor Model	Sensor	Deviation at, ppm				
		400	750	1100	1450	1800
S9	A	23	39	64	77	94
	B	-172	-191	-226	-242	-274
	C	-140	-152	-158	-178	-207
S10	A	96	127	138	148	144
	B	83	115	130	155	163
	C	131	177	206	220	199
S11	A	57	64	55	38	17
	B	97	143	164	171	200
	C	-93	-45	14	62	143
S12	A	79	127	158	183	199
	B	85	129	159	195	200
	C	92	126	153	169	185

Note: The highlighted numbers indicate that the sensor reading was saturated.

Single-lamp, dual-wavelength sensors: Figure 7 shows the accuracy test results of the sensors that use the single-lamp, dual-wavelength configuration. Table 4 shows the numerical values of the deviation for each sensor. In some cases the sensor outputs at 1,800 ppm are saturated. These data points are highlighted in the table.

Sensor S13

The deviations of the measured CO_2 concentration from the actual CO_2 concentration for Model S13 sensors are presented graphically in Figure 7(a). The manufacturer-stated accuracy for this sensor model is ± 30 ppm + 2% of reading. The reference temperature for the stated accuracy is 68°F (20°C). The reference pressure for the stated accuracy is not specified. Deviations of all three sensors shift upward when the actual CO_2 concentration was increased. The reading of sensors B and C are saturated at 1800 ppm. The deviation of sensor A is within the manufacturer-stated accuracy at 400 ppm. The maximum discrepancy between the actual deviation and the manufacturer-stated accuracy is 284 ppm (sensor B at 1450 ppm).

Sensor S14

The deviations of the measured CO_2 concentration from the actual CO_2 concentration for Model S14 sensors are presented graphically in Figure 7(b). The manufacturer-stated accuracy for this sensor model is ± 50 ppm or 5% of reading whichever is greater (7% for levels over 1500 ppm). The reference temperature for the stated accuracy is 60°F to 90°F (15°C to 32°C). The reference pressure for the stated accuracy is not specified. The deviations of sensor B at all CO_2 levels, the deviation of sensor A at 400 ppm, and the deviation of sensor C at 1800 ppm are within the manufacturer-stated accuracy. The maximum discrepancy between the actual deviation and the manufacturer-stated accuracy is 92 ppm (sensor A at 1450 ppm). This sensor incorporates an "automatic baseline adjustment" algorithm in the sensor's electronics package.

Sensor S15

The deviations of the measured CO_2 concentration from the actual CO_2 concentration for Model S15 sensors are presented graphically in Figure 7(c). The manufacturer-stated accuracy for this sensor model is ± 30 ppm + 2% of reading. The reference temperature for the stated accuracy is 77°F (25°C). The reference pressure for the stated accuracy is not specified. Deviations of all three sensors shift upward when the actual CO_2 concentration was increased. The deviations of sensor A at all CO_2 levels except at 400 ppm and the deviation of sensor B at 1800 ppm are within the manufacturer-stated accuracy. The maximum discrepancy between the actual deviation and the manufacturer-stated accuracy is 65 ppm (sensor C at 1100 and 1800 ppm).

Table 4. Deviation from Actual CO_2 Concentration (ppm), Single-Lamp, Dual-Wavelength Sensors

Sensor Model	Sensor	Deviation at, ppm				
		400	750	1100	1450	1800
S13	A	16	55	83	105	137
	B	159	233	288	343	206
	C	111	175	217	256	208
S14	A	-25	70	126	165	196
	B	10	49	53	45	22
	C	78	107	103	85	56
S15	A	-44	-22	-18	-14	-13
	B	54	74	75	70	65
	C	67	101	117	122	131

Note: The highlighted numbers indicate that the sensor reading was saturated.

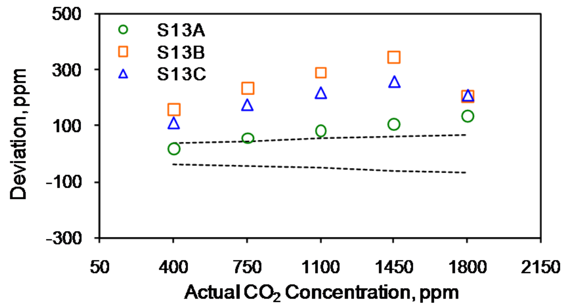

(m) Sensor S13

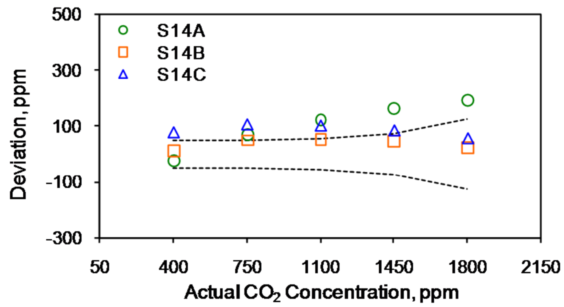

(n) Sensor S14

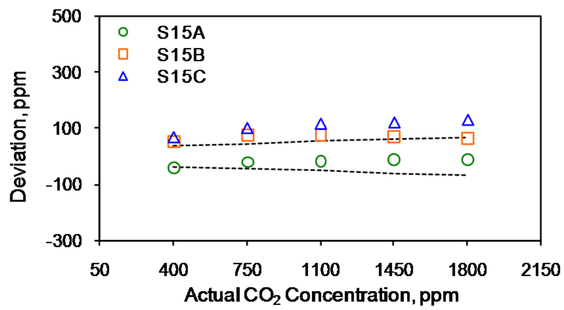

(o) Sensor S15

Figure 7. Comparison of deviation from actual CO_2 concentration of single-lamp, dual-wavelength sensors.

LINEARITY TEST RESULTS

The term linearity denotes the extent to which a sensor input and output can be approximated by a linear function. A sensor that is highly linear will be accurate over its operating range based on a two-point calibration. A two-point calibration often includes two operating conditions that span the normal operating range of the sensor. CO_2 sensors are often calibrated using a zero (0 ppm CO_2) gas and a span gas. Span gases are available in any CO_2 concentration with 500 ppm, 1000 ppm, 1500 ppm, and 2000 ppm being common. Span gases most often use nitrogen as the base gas. Sensors that are non-linear will require a multi-point calibration in order to establish the functional relationship of input/output.

Knowledge of a sensor's linearity characteristics can be embedded in a controller to best represent and compensate for the sensor's true behavior. The nonlinearity is assessed as the difference between the measured CO_2 concentrations and a linear least-squares regression of the measured values. For the sensors that exhibited saturation (as discussed previously), the data points at 1800 ppm were omitted from the regression calculation.

Nonlinearity for each sensor at 400, 750, 1100, 1450, and 1800 ppm is calculated using mean value of the first forward measurement and the reverse measurement, at 40% relative humidity, 73ºF (22.8ºC) temperature, and 14.7 psia (101.35 kPa) pressure as discussed in Part 1 (Shrestha and Maxwell 2009) of this paper. Only three sensors models (S3, S13, and S15) specified their nonlinearity as less than 1% of full scale (20 ppm). All three sensor models meet their linearity specification. Figure 8 shows the linearity plot of the sensor model with largest nonlinearity (27 ppm). The maximum nonlinearity of each sensor is summarized in Table 5. Sensor manufacturers may define and report linearity differently; therefore, the results in Table 5 should be used to compare performance among sensor models, rather than comparing individual results with manufacturer reported data.

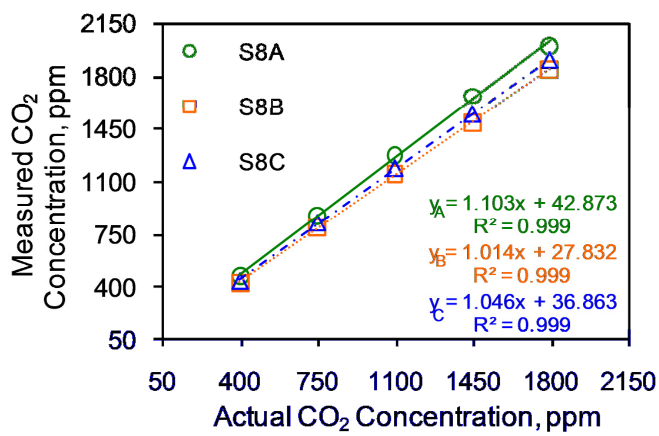

Figure 8. Example of a linearity plot.

REPEATABILITY TEST RESULTS

Repeatability is the degree to which a CO_2 sensor produces the same measurement when subjected repeatedly to the same conditions as they are approached from the same direction. The repeatability error was calculated as the difference between the two forward measurements at CO_2 concentrations of 750 ppm, 1100 ppm, and 1450 ppm at 40% relative humidity, 73ºF (22.8ºC) temperature, and 14.7 psia (101.35 kPa) pressure as discussed in Part 1 (Shrestha and Maxwell 2009) of this paper. Repeatability information was available from five sensor models. Sensors S4, S5, and S7 specified their repeatability as ± 20 ppm, sensor S9 specified its repeatability as ± 8 ppm, and sensor S8 specified its repeatability as ± 20 ppm ± 1% of measured value. All five sensor models meet their repeatability specification. The maximum repeatability error of each sensor is summarized in Table 5. Sensor S10 showed a maximum repeatability error of 25 ppm. All other sensors have repeatability within 14 ppm.

HYSTERESIS TEST RESULTS

Hysteresis is the degree to which a CO_2 sensor produces the same measurement when subjected repeatedly to the same conditions as they are approached from a lower and then a higher concentration condition. Hysteresis was calculated as the difference between the first forward measurement and the reverse measurement at CO_2 concentrations of 750 ppm, 1100 ppm, and 1450 ppm at 40% relative humidity, 73ºF (22.8ºC) temperature, and 14.70 psia (101.35 kPa) pressure as discussed in Part 1 (Shrestha and Maxwell 2009) of this paper. The maximum hysteresis of each sensor is summarized in Table 5. Sensor S10 showed a hysteresis value of 31 ppm and sensor S11 showed a value of 18 ppm. All other sensors have values within 13 ppm.

CONCLUSIONS

The result from the tests conducted under accurate and repeatable conditions showed a wide variation in sensor performance among the fifteen NDIR CO_2 sensor models. In some cases, significant variations in sensor performance exist between sensors of the same model while in other cases, all sensors of the same model showed almost identical behavior. None of the sensor models meet their manufacturer specified accuracy statement for all three sensors of a given model over the full range of test conditions. For some models, none of the three sensors of the model meet the accuracy specifications over the range. Table 6 summarizes the sensor models and the number of sensors of the given model that meet the accuracy statement for the model.

Table 5. Linearity, Repeatability, and Hysteresis of Each Sensor

Sensor Model	Sensor	Linearity, ppm	Repeatability, ppm	Hysteresis, ppm
Single lamp, single wavelength sensors				
S1	A	10	1	3
	B	16	7	3
	C	11	6	3
S2	A	19	5	6
	B	14	4	6
	C	16	4	5
S3	A	15	5	4
	B	9	4	9
	C	11	4	3
S4	A	6	7	1
	B	9	6	7
	C	15	4	5
S5	A	12	7	4
	B	12	10	6
	C	14	5	4
S6	A	15	11	6
	B	9	7	5
	C	19	7	6
S7	A	16	14	11
	B	25	9	9
	C	18	6	7
S8	A	27	6	7
	B	10	7	3
	C	11	5	3
Dual-lamp, single-wavelength sensors				
S9	A	5	4	4
	B	5	6	6
	C	9	1	4
S10	A	11	2	5
	B	6	25	31
	C	8	14	15
S11	A	11	5	6
	B	11	6	8
	C	12	10	18
S12	A	11	3	12
	B	13	7	12
	C	8	12	13
Single-lamp, dual-wavelength sensors				
S13	A	5	11	12
	B	8	8	7
	C	9	5	7
S14	A	24	4	6
	B	22	2	3
	C	21	2	6
S15	A	8	7	6
	B	10	3	3
	C	11	8	10

Given the test results and that the sensors were tested under "as received" conditions, it appears that sensor calibration should be performed before putting sensors into service. However, for sensors with automatic baseline adjustment algorithm, it is impossible to predict the sensor's performance over a prolonged time period during which the sensor baseline might make multiple adjustments. In fact, the literatures for several sensor models that incorporate automatic baseline adjustment algorithm claim that the sensors do not require calibration. Given the sensor is "self adjusting" using an arbitrary background reading of 400 ppm, it is unclear how the sensor manufacturer can claim an absolute accuracy for their sensor. However, some of the models that utilize automatic baseline adjustment algorithm do appear to be "accurate" if one accounts for the bias created by the baseline adjustment. For example, all three sensors of model S1 (see Figure 4A) would perform as specified if the sensors readings were adjusted downward by approximately 50 ppm. The same is true for several other sensors that show a relatively constant value of deviation as the CO_2 concentration is increased. For sensors that show increasingly larger values of deviation as the CO_2 concentration increases (see Figure 4g), a simple bias adjustment would not make the sensors reading accurate over the full range of CO_2 concentrations.

The test results for sensors that use dual-lamp, single-wavelength or single-lamp, dual-wavelength configuration generally show a constant value of deviation as the CO_2 concentration increases.

Table 6. Sensor Accuracy Summary

Sensor Model	All 3 sensors meet the manufacturer's accuracy statement	Two sensors meet the manufacturer's accuracy statement	One sensor meets the manufacturer's accuracy statement	None on the sensors meet the manufacturer's accuracy statement
S1			X	
S2			X	
S3		X		
S4				X
S5				X
S6				X
S7				X
S8			X	
S9				X
S10				X
S11		X		
S12				X
S13				X
S14			X	
S15				X

Nonlinearity, repeatability and hysteresis do not appear to be significant for most of the sensors tested. Only three sensors models specified their nonlinearity as less than 1% full scale (20 ppm), and all three sensor models meet their linearity specification. The S8A sensor has the largest nonlinearity of 27 ppm, while many sensors' nonlinearity is less than 5 ppm.

Five sensor models specified their repeatability and all five sensor models meet their repeatability specification. Sensor S10 showed maximum repeatability error of 25 ppm. All other sensors have repeatability within 14 ppm.

None of the sensor manufacturers specified hysteresis for their sensors. Sensor S10 showed maximum hysteresis of 31 ppm and sensor S11 showed maximum hysteresis of 18 ppm. All other sensors have hysteresis within 13 ppm.

ACKNOWLEDGEMENTS

This work is performed for National Building Controls Information Program (NBCIP), which is sponsored by the Iowa Energy Center, NSTAR Electric & Gas Corporation and the California Energy Commission.

REFERENCES

Fahlen, P., H. Andersson, and S. Ruud. 1992. Demand Controlled Ventilating Systems - Sensor Tests. Swedish National Testing and Research Institute, Boras, Sweden, SP Report 1992:13.

Fisk, W.J., D. Faulkner, and D.P. Sullivan. 2006. Accuracy of CO_2 sensors in commercial buildings: a pilot study. LBNL-61962, Lawrence Berkeley National Laboratory, Berkeley, CA.

Pandey, S.K., K. Kim, and S. Lee. 2007. Use of a dynamic enclosure approach to test the accuracy of the NDIR sensor: evaluation based on the CO_2 equilibration pattern. Molecular Diversity Preservation International, Matthaeusstrasse, Switzerland, ISSN: 1424-8220.

Shrestha, S.S., and G.M. Maxwell. 2009. An experimental evaluation of HVAC-grade carbon-dioxide sensors: part 1, test and evaluation procedure. *ASHRAE Transactions* 115(2).

Chapter 4: An Experimental Evaluation of HVAC-Grade Carbon-Dioxide Sensors: Part 3, Humidity, Temperature, and Pressure Sensitivity Test Results

A paper to be submitted to the ASHRAE Transactions

Som S. Shrestha
Student Member ASHRAE

Gregory M. Maxwell, PhD
Member ASHRAE

ABSTRACT

This is the third paper in a four-part series reporting on the test and evaluation of typical wall-mounted carbon-dioxide sensors used in building HVAC applications. Fifteen models of NDIR HVAC-grade wall-mounted CO_2 sensors were tested and evaluated to determine the humidity, temperature, and pressure sensitivity of the sensors. This paper reports the performance of the sensors at various relative humidity, temperature, and pressure levels common to building HVAC applications and provides a comparison with manufacturer specifications. Among the 15 models tested, eight models have a single-lamp, single-wavelength configuration, four models have a dual-lamp, single-wavelength configuration, and three models have a single-lamp, dual-wavelength configuration.

The sensors were tested in a chamber specifically fabricated for this research. A description of the apparatus and the method of test are described in Part 1 (Shrestha and Maxwell 2009). The humidity sensitivity was evaluated by varying the relative humidity while holding the CO_2 concentration, temperature, and pressure fixed. The temperature sensitivity was evaluated by varying the temperature while holding the gas composition and pressure fixed. The pressure sensitivity was evaluated by varying the pressure while holding the gas composition and temperature fixed.

The test result showed a wide variation in humidity, temperature, and pressure sensitivity of CO_2 sensors among manufacturers. In some cases, significant variations in sensor performance exist between sensors of the same model. Even the natural variation in relative humidity could significantly vary readings of some CO_2 sensor readings. The effects of temperature and pressure variation on NDIR CO_2 sensors are unavoidable without an algorithm to compensate for the changes. For the range of temperature and pressure variation in an

air-conditioned space, the effect of pressure variation is more significant compared to the effect of temperature variation.

INTRODUCTION

This is the third part of a four-part series of papers reporting on the test and evaluation of typical wall-mounted CO_2 sensors used in building HVAC systems. In this study, fifteen models of NDIR (non-dispersive infrared) HVAC-grade wall-mounted CO_2 sensors were tested and evaluated. In all, 45 sensors (three from each model) were tested in order to determine the effects of humidity, temperature, and pressure on the CO_2 sensors' readings. The sensitivity of the sensor reading to each of these three parameters was computed and compared to the manufacturers' specifications. The experimental procedure used to test and evaluate the sensors is described in Part 1 (Shrestha and Maxwell 2009) of this paper. Among the fifteen models tested, eight models have a single-lamp, single-wavelength configuration, four models have a dual-lamp, single-wavelength configuration, and three models have a single-lamp, dual-wavelength configuration. All single-lamp, single-wavelength sensors and one single-lamp, dual-wavelength sensor incorporate an "automatic baseline adjustment" algorithm in the sensor's electronics package. The working principles of NDIR CO_2 sensors are described in Part 1 (Shrestha and Maxwell 2009) of this paper.

PREVIOUS STUDIES

In the past, limited studies have been done to investigate the effects of humidity, temperature, and pressure variations on HVAC-grade CO_2 sensors. Fahlen et al. (1992) evaluated the performance of two CO_2 sensors, one photo-acoustic type and one infrared spectroscopy type, in lab tests and long term field tests. The lab tests included performance and environmental tests. The authors found that the CO_2 sensors tested were sensitive to humidity below a threshold value, however the threshold humidity level was not determined and the effect of humidity on the sensors' readings was not evaluated. During the low-temperature test at 5°C (which was within the stated operating range of the sensors), the output of both sensors dropped to an unrealistic value. The authors conclude that the deviation between actual concentration and the sensors' reading are normally well within ± 50 ppm at a concentration level of 1000 ppm. However, at a concentration of 2000 ppm the test results showed a deviation of up to -300 ppm.

A pilot study that evaluated in-situ accuracy of 44 NDIR CO_2 sensors located in nine commercial buildings indicated that the accuracy of CO_2 sensors is frequently less than is needed to measure peak indoor-outdoor CO_2 concentration differences with less than 20% error (Fisk et al. 2006). The evaluation was performed either by multi-point calibration using CO_2 calibration gas or by a single-point calibration check using a co-located and calibrated reference CO_2 sensor. The effects of humidity, temperature, and pressure on the sensor readings were not considered in the study.

Pandey et al. tested three NDIR CO_2 sensors each from two sensor models. The tests were conducted in an enclosure fabricated for the research. The sensors were tested with CO_2 concentrations of 0 ppm, 500 ppm, and 1000 ppm. The research focused on the sensor accuracy but did not include effects of humidity, temperature, and pressure variation on the sensor output.

CO_2 SENSOR SPECIFICATIONS

CO_2 sensor manufacturers provide detailed specifications for their products. This information is available from the company's website and/or literature packaged with the product. Table 1 summarizes some of the product information for the models evaluated in this study. (Specific product names are not used in this paper, rather the sensors are referred to as S1 through S15.) The table indicates the sensor configuration, the sensitivity of the sensor reading due to variations in temperature, the sensitivity of the sensor reading due to variation in pressure, and the operating range of temperature and relative humidity. None of the manufacturers specify the sensitivity of the sensor reading due to variation in humidity.

Sensors S1 through S8 are single-lamp, single-wavelength sensor, sensors S9 through S12 are dual-lamp, single-wavelength sensors, and sensors S13 through S15 are single-lamp, dual-wavelength sensors. All single-lamp, single-wavelength sensors and one single-lamp, dual-wavelength sensor (S14) incorporate an "automatic baseline adjustment" algorithm in the sensor's electronics package. The details of the "automatic baseline adjustment" algorithm are described in part 2 of this paper.

Of the fifteen sensor models considered in this study, seven do not explicitly state any sensitivity to temperature. For the seven models that do provide temperature sensitivity statements, the affect of temperature on the sensor reading is not clear. For example, model S1 states a temperature sensitivity of 5 ppm/°C. Does this mean that the CO_2 reading will increase by 5 ppm when the temperature increases by 1°C, or will the reading decrease by 5 ppm? Furthermore, no reference temperature is provided on which to evaluate the temperature change. Sensor S15 is the only model that provides a reference temperature.

Similarly, of the fifteen sensor models studied, seven do not explicitly state any sensitivity to pressure. For the eight models that do indicate pressure sensitivity, seven specify a reference pressure (or altitude) on which to base the pressure (or altitude) correction. For all sensors that show pressure dependence, a correction value must be added to the sensor reading as the pressure decreases (or altitude increases).

EXPERIMENTAL TEST PROCEDURE

The CO_2 sensors were tested using a test chamber specifically designed and fabricated for this study. Technical details of the test chamber and instrumentation are described in Part 1 (Shrestha and Maxwell 2009) of this paper. Humidity sensitivity tests were conducted at 20, 40 and 60% relative humidity while maintaining the CO_2 concentration, temperature, and pressure at 1100 ppm, 73ºF (22.8ºC) and 14.70 psia (101.35 kPa), respectively.

Temperature sensitivity tests were conducted at 66°F (18.9°C), 73ºF (22.8ºC) and 80°F (26.7°C), while maintaining the CO_2 concentration and pressure at 1100 ppm, and 14.70 psia (101.35 kPa), respectively. Pressure sensitivity tests were conducted at 14.70 psia (101.35 kPa), 13.25 psia (91.36 kPa) and 11.80 psia (81.36 kPa) while maintaining the CO_2 concentration and temperature at 1100 ppm and 73°F (22.8°C), respectively. These pressures correspond to standard atmospheric pressures for altitudes at sea level, 2838 feet (865 meters) above sea level, and 5948 feet (1813 meters) above sea level, respectively.

The temperature sensitivity and pressure sensitivity tests were conducted at a fixed gas mixture composition. The humidity ratio was maintained at 0.0069 lb moisture/lb dry air (0.0069 kg moisture/kg dry air), which corresponds to 40% RH at 73ºF (22.8ºC) temperature and 14.70 psia (101.35 kPa) pressure. Since relative humidity depends on both pressure and temperature, the relative humidity varies during the pressure and temperature sensitivity tests; however, the absolute humidity remained constant.

Established procedures, including guidelines for steady-state conditions, described in Part 1 (Shrestha and Maxwell 2009) of this paper were used to perform the testing.

Table 1. Manufacturer-Specified Temperature Sensitivity, Pressure Sensitivity, and Operating Range for their Sensors

Sensor Model	Configuration	Temperature Sensitivity	Pressure Sensitivity	Temperature and humidity Operating Range
S1	Single-lamp, single-wavelength	5 ppm/1.8°F (1°C)	NA	32°F to 122°F (0°C to 50°C) 0% to 95% RH
S2	Single-lamp, single-wavelength	NA	Add 6.7% of reading per psi (6.89 kPa) decrease from 14.70 psia (101.35 kPa)*	60°F to 90°F (15°C to 32°C) 0% to 95% RH
S3	Single-lamp, single-wavelength	3 ppm/1.8°F (°C)*	6.7% of reading per psi (6.89 kPa) from 14.70 psia (101.35 kPa)*	59°F to 90°F (15°C to 32°C) 0% to 95% RH
S4	Single-lamp, single-wavelength	NA	NA	32°F to 122°F (0°C to 50°C) 5% to 95% RH
S5	Single-lamp, single-wavelength	4 ppm/1.8°F (°C)*	6.7% of reading per psi (6.89 kPa)*	32°F to 122° (0°C to 50°C) 0% to 95% RH
S6	Single-lamp, single-wavelength	NA	9.6% of reading per psi (6.89 kPa) deviation from 14.5 psia (100 kPa)*	32°F to 122°F (0°C to 50°C) 0% to 95% RH
S7	Single-lamp, single-wavelength	NA	Add 7.2% of reading per psi (6.89 kPa) decrease from 14.70 psia (101.35 kPa)*	32°F to 122°F (0°C to 50°C) 0% to 90% RH
S8	Single-lamp, single-wavelength	NA	NA	32°F to 122°F (0°C to 50°C) 0% to 95% RH
S9	Dual-lamp, single-wavelength	5 ppm/1.8°F (°C)	9.8% of reading per psi (6.89 kPa)*	32°F to 122°F (0°C to 50°C) 5% to 95% RH
S10	Dual-lamp, single-wavelength	± 2 ppm/1.8°F (°C)	NA	23°F to 113°F (-5°C to 45°C) 0% to 85% RH
S11	Dual-lamp, single-wavelength	NA	NA	32°F to 100°F (0°C to 40°C) 0% to 95% RH
S12	Dual-lamp, single-wavelength	5 ppm/1.8°F (°C)	NA	23°F to 131°F (-5°C to 55°C) 0% to 90% RH
S13	Single-lamp, dual-wavelength	2 ppm/1.8°F (°C)*	Add 10.2% of reading per psi (6.89 kPa) decrease from 14.18 psia (97.77 kPa)*	23°F to 113°F (-5°C to 45°C) 0% to 85% RH
S14	Single-lamp, dual-wavelength	NA	Add 6.7% of reading per psi (6.89 kPa) decrease from 14.70 psia (101.35 kPa)*	32°F to 122°F (0°C to 50°C) 0% to 95% RH
S15	Single-lamp, dual-wavelength	3 ppm/1.8°F (°C)* (reference 77°F (25°C))	NA	23°F to 113°F (-5°C to 45°C) 0% to 85% RH

Notes: NA indicates that the information was not available in the manufacturer's product literature.

* indicates that the value was calculated from the manufacturer's product literature

HUMIDITY SENSITIVITY TEST RESULTS

The effect of humidity on a CO_2 sensor's output is determined by comparing the sensor readings at 20% and 60% RH to the sensor reading at 40% RH. The humidity sensitivity test results are presented graphically in terms of the deviation of the sensor readings at 20% and 60% from the readings at 40% RH (i.e., deviation from reading at 40% RH = measured CO_2 concentration at a particular RH – measured CO_2 concentration at 40% RH). Figures 1, 2, and 3 illustrate the humidity sensitivity test results for the single-lamp single-wavelength, dual-lamp single-wavelength, and single-lamp dual-wavelength configurations, respectively.

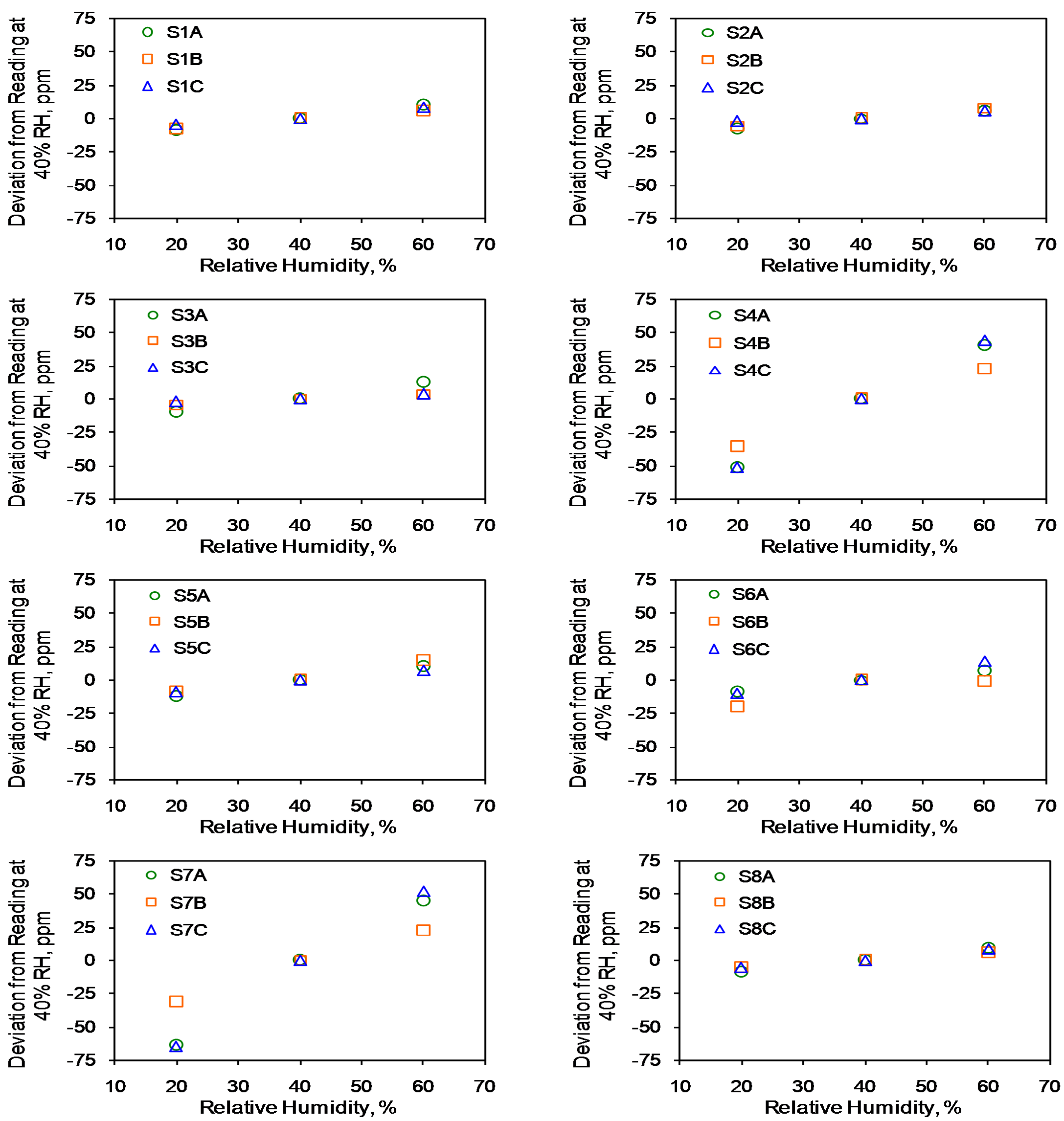

Figure 1. Humidity sensitivity test results of single-lamp, single-wavelength sensors.

The humidity sensitivity of each CO_2 sensor was calculated using a linear regression of the test results. The slope of the regression line represents the sensitivity of the sensor in terms of deviation in ppm reading per % change in relative humidity. The numerical results of the sensor readings at each of the test conditions along with the calculated sensitivity are also tabulated. Tables 2, 3, and 4 provide the values for the three sensor configurations. Positive values of humidity sensitivity indicate an increase in sensor reading as RH increases, and vice versa.

The majority of the sensors show little to no sensitivity to humidity. However, three sensor models were particularly sensitive to humidity. Specifically, all of the sensors from models S4 and S7 exhibit positive relative humidity sensitivity. Sensitivity values for these sensor range from 1.4 to 2.9 ppm/%RH. One sensor from model S14 (sensor A) has a sensitivity of -3 ppm/%RH.

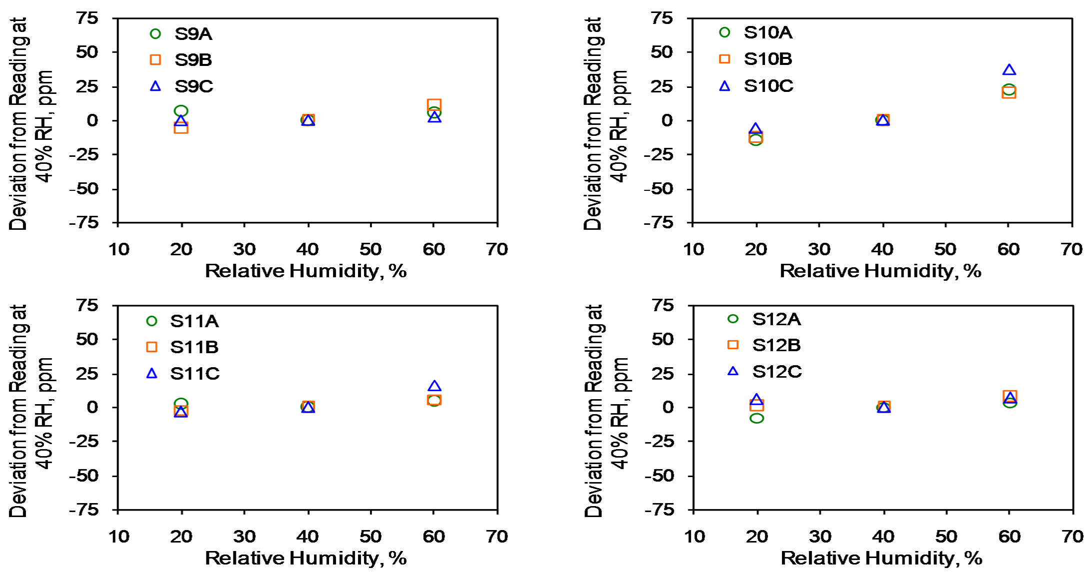

Figure 2. Humidity sensitivity test results of dual-lamp, single-wavelength sensors.

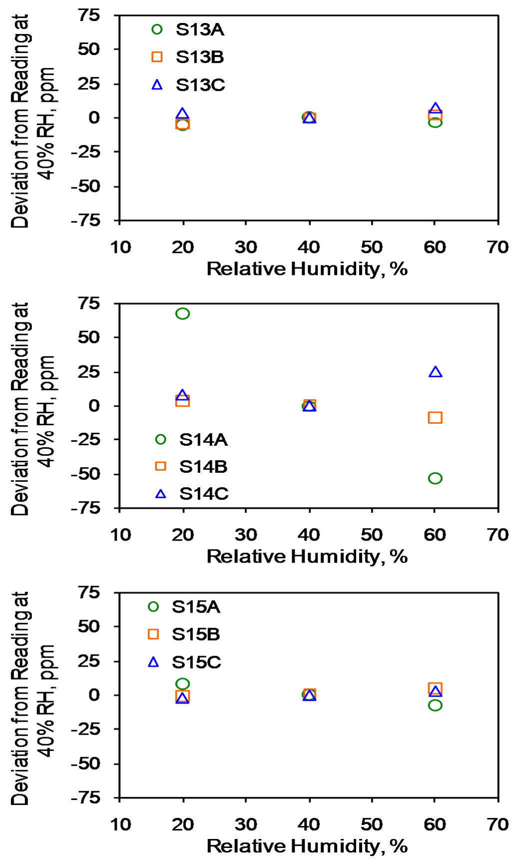

Figure 3. Humidity sensitivity test results of single-lamp, dual-wavelength sensors.

Table 2. Humidity Sensitivity Test Results of Single-Lamp, Single-Wavelength Sensors

Sensor Model	Sensor	Reading at			Sensitivity, ppm / %RH
		20% RH, ppm	40% RH, ppm	60% RH, ppm	
S1	A	1192	1201	1212	0.5
	B	1195	1203	1209	0.3
	C	1212	1217	1225	0.3
S2	A	1222	1229	1236	0.3
	B	1271	1277	1284	0.3
	C	1177	1179	1185	0.2
S3	A	1273	1283	1295	0.6
	B	1176	1181	1184	0.2
	C	1125	1127	1130	0.1
S4	A	1282	1333	1373	2.3
	B	1300	1335	1358	1.5
	C	1363	1414	1458	2.4
S5	A	1296	1309	1319	0.6
	B	1178	1187	1202	0.6
	C	1211	1219	1226	0.4
S6	A	1255	1263	1271	0.4
	B	1262	1282	1281	0.5
	C	1303	1314	1328	0.6
S7	A	1448	1513	1557	2.7
	B	1420	1451	1474	1.4
	C	1422	1487	1539	2.9
S8	A	1275	1283	1293	0.4
	B	1200	1205	1211	0.3
	C	1222	1227	1236	0.3

Table 3. Humidity Sensitivity Test Results of Dual-Lamp, Single-Wavelength Sensors

Sensor Model	Sensor	Reading at			Sensitivity, ppm / %RH
		20% RH, ppm	40% RH, ppm	60% RH, ppm	
S9	A	1174	1167	1172	0.0
	B	870	876	887	0.4
	C	942	943	945	0.1
S10	A	1209	1223	1246	0.9
	B	1218	1230	1250	0.8
	C	1285	1291	1329	1.1
S11	A	1163	1161	1165	0.1
	B	1261	1264	1269	0.2
	C	1073	1077	1092	0.5
S12	A	1239	1247	1251	0.3
	B	1258	1257	1264	0.2
	C	1301	1295	1302	0.0

Table 4. Humidity Sensitivity Test Results of Single-Lamp, Dual-Wavelength Sensors

Sensor Model	Sensor	Reading at			Sensitivity, ppm / %RH
		20% RH, ppm	40% RH, ppm	60% RH, ppm	
S13	A	1185	1191	1187	0.1
	B	1386	1391	1393	0.2
	C	1316	1313	1320	0.1
S14	A	1368	1300	1246	-3.0
	B	1172	1169	1160	-0.3
	C	1177	1169	1195	0.4
S15	A	1096	1088	1080	-0.4
	B	1174	1175	1180	0.2
	C	1213	1215	1218	0.1

TEMPERATURE SENSITIVITY TEST RESULTS

The effect of temperature on a CO_2 sensor's output is determined by comparing the sensor readings at 66°F (18.9°C) and 80°F (26.7°C) to the sensor reading at 73ºF (22.8ºC). The temperature sensitivity test results are presented graphically in terms of the deviation of the sensor readings at 66°F (18.9°C) and 80°F (26.7°C) from the reading at 73ºF (22.8ºC) (i.e., deviation from readings at 73ºF (22.8ºC) = measured CO_2 concentration at a particular temperature – measured CO_2 concentration at 73ºF (22.8ºC)). Figures 4, 5, and 6 illustrate the temperature sensitivity test results for the single-lamp single-wavelength, dual-lamp single-wavelength, and single-lamp dual-wavelength configurations, respectively.

The temperature sensitivity of each CO_2 sensor was calculated using a linear regression of the test results. The slope of the regression line represents the sensitivity of the sensor in terms of deviation in ppm reading per degree change in temperature. The numerical results of the sensor readings at each of the test conditions along with the calculated sensitivity are also tabulated. Tables 5, 6, and 7 provide the values for the three sensor configurations. Positive values of temperature sensitivity indicate an increase in sensor reading as temperature increases, and vice versa.

Temperature sensitivity is not consistent between sensor models. For many sensors, the temperature sensitivity is negligibly small. Nine sensor models showed temperature sensitivity within 5 ppm/1.8ºF (5 ppm/ºC). Sensor S12B showed the highest temperature sensitivity of 10 ppm increase in sensor reading per 1.8°F (1°C) decrease in temperature.

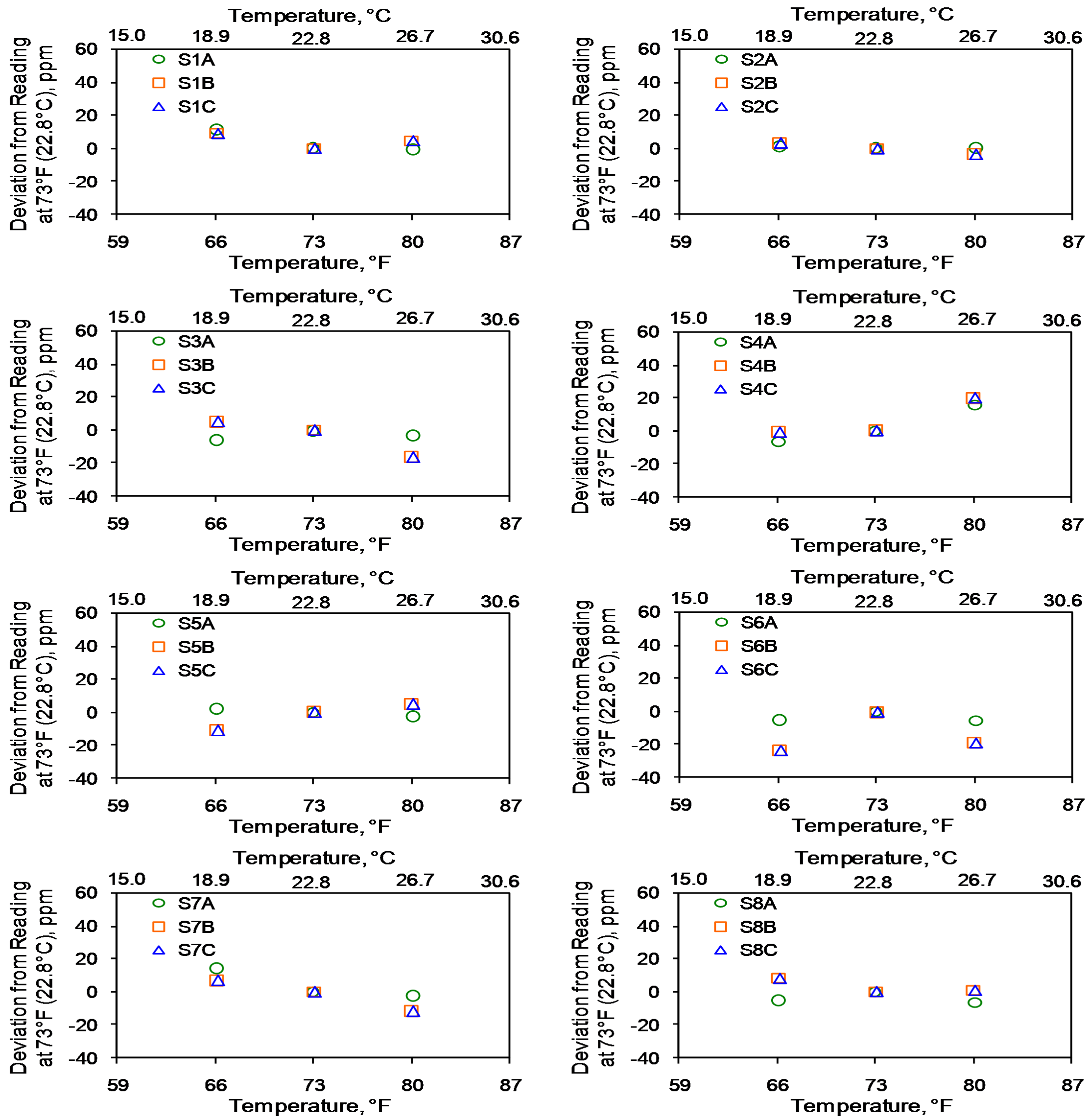

Figure 4. Temperature sensitivity test results of single-lamp, single-wavelength sensors.

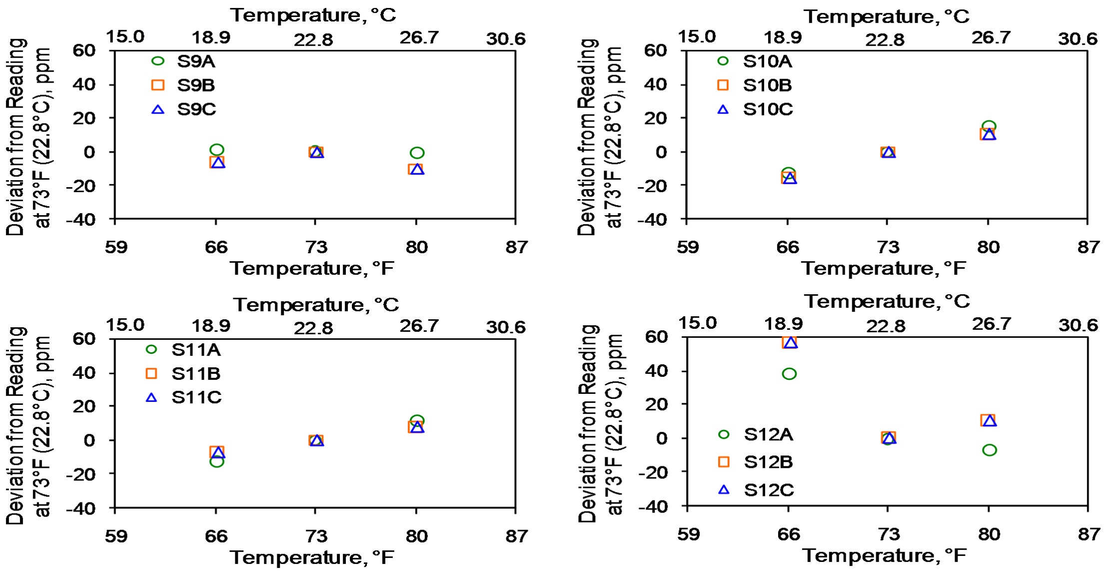

Figure 5. Temperature sensitivity test results of dual-lamp, single-wavelength sensors.

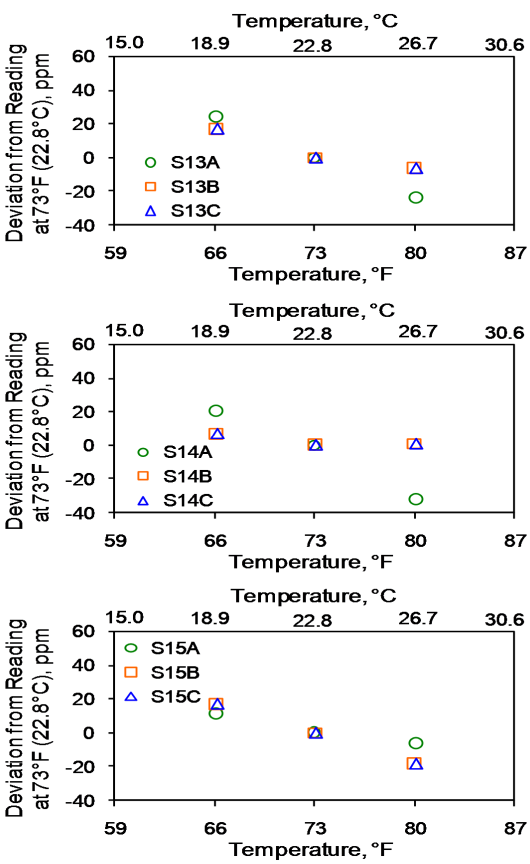

Figure 6. Temperature sensitivity test results of single-lamp, dual-wavelength sensors.

Table 5. Temperature Sensitivity Test Results of Single-Lamp, Single-Wavelength Sensors

Sensor Model	Sensor	Reading at 66°F (18.9°C), ppm	Reading at 73°F (22.8°C), ppm	Reading at 80°F (26.7°C), ppm	Temperature Sensitivity, ppm / 1.8°F (ppm / °C) Calculated	Temperature Sensitivity, ppm / 1.8°F (ppm / °C) Manufacturer Specified
S1	A	1194	1183	1182	-2	5
	B	1156	1150	1153	0	
	C	1187	1177	1182	-1	
S2	A	1230	1229	1229	0	NA
	B	1265	1268	1270	1	
	C	1184	1180	1177	-1	
S3	A	1271	1277	1274	0	3
	B	1163	1171	1178	2	
	C	1120	1115	1099	-3	
S4	A	1331	1337	1353	3	NA
	B	1316	1346	1382	9	
	C	1438	1439	1459	3	
S5	A	1314	1312	1309	-1	4
	B	1219	1206	1199	-3	
	C	1204	1215	1220	2	
S6	A	1238	1243	1238	0	NA
	B	1202	1214	1203	0	
	C	1228	1252	1233	1	
S7	A	1551	1537	1534	-2	NA
	B	1432	1462	1491	8	
	C	1499	1492	1481	-2	
S8	A	1265	1270	1264	0	NA
	B	1135	1134	1139	1	
	C	1190	1182	1183	-1	

Table 6. Temperature Sensitivity Test Results of Dual-Lamp, Single-Wavelength Sensors

Sensor Model	Sensor	Reading at 66°F (18.9°C), ppm	Reading at 73°F (22.8°C), ppm	Reading at 80°F (26.7°C), ppm	Temperature Sensitivity, ppm / 1.8°F (ppm / °C) Calculated	Temperature Sensitivity, ppm / 1.8°F (ppm / °C) Manufacturer Specified
S9	A	1165	1164	1162	0	5
	B	867	877	873	1	
	C	935	941	931	-1	
S10	A	1223	1236	1251	4	± 2
	B	1194	1209	1223	4	
	C	1285	1300	1311	3	
S11	A	1140	1153	1164	3	NA
	B	1274	1268	1266	-1	
	C	1121	1128	1136	2	
S12	A	1298	1259	1252	-6	NA
	B	1295	1231	1219	-10	
	C	1305	1248	1259	-6	

Table 7. Temperature Sensitivity Test Results of Single-Lamp, Dual-Wavelength Sensors

Sensor Model	Sensor	Reading at 66°F (18.9°C), ppm	Reading at 73°F (22.8°C), ppm	Reading at 80°F (26.7°C), ppm	Temperature Sensitivity, ppm / 1.8°F (ppm / °C): Calculated	Temperature Sensitivity, ppm / 1.8°F (ppm / °C): Manufacturer Specified
S13	A	1210	1185	1161	-6	2
	B	1402	1397	1385	-2	
	C	1330	1313	1307	-3	
S14	A	1239	1218	1185	-7	NA
	B	1121	1151	1164	6	
	C	1205	1198	1199	-1	
S15	A	1096	1085	1079	-2	3
	B	1202	1179	1153	-6	
	C	1230	1212	1194	-5	

PRESSURE SENSITIVITY TEST RESULTS

The effect of pressure on a CO_2 sensor's output is determined by comparing the sensor readings at 13.25 psia (91.36 kPa) and 11.80 psia (81.36 kPa) to the sensor reading at 14.70 psia (101.35 kPa). The pressure sensitivity test results are presented graphically in terms of the deviation of the sensor readings at 13.25 psia (91.36 kPa) and 11.80 psia (81.36 kPa) from the reading at 14.70 psia (101.35 kPa) (i.e., deviation from reading at 14.70 psia (101.35 kPa) = measured CO_2 concentration at a particular pressure – measured CO_2 concentration at 14.70 psia (101.35 kPa)). Figures 7, 8, and 9 illustrate the pressure sensitivity test results for the single-lamp single-wavelength, dual-lamp single-wavelength, and single-lamp dual-wavelength configurations, respectively.

The pressure sensitivity of each CO_2 sensor was calculated using a linear regression of the test results. The slope of the regression line represents the sensitivity of the sensor in terms of deviation in percent reading per unit change in pressure. The numerical results of the sensor readings at each of the test conditions along with the calculated sensitivity are also tabulated. Tables 8, 9, and 10 provide the values for the three sensor configurations. Positive values of pressure sensitivity indicate an increase in sensor reading as pressure increases, and vice versa. All sensors showed similar response to pressure change. The maximum and minimum pressure sensitivity were observed as 10.7% and 7.6% reading/psi (6.89 kPa), respectively.

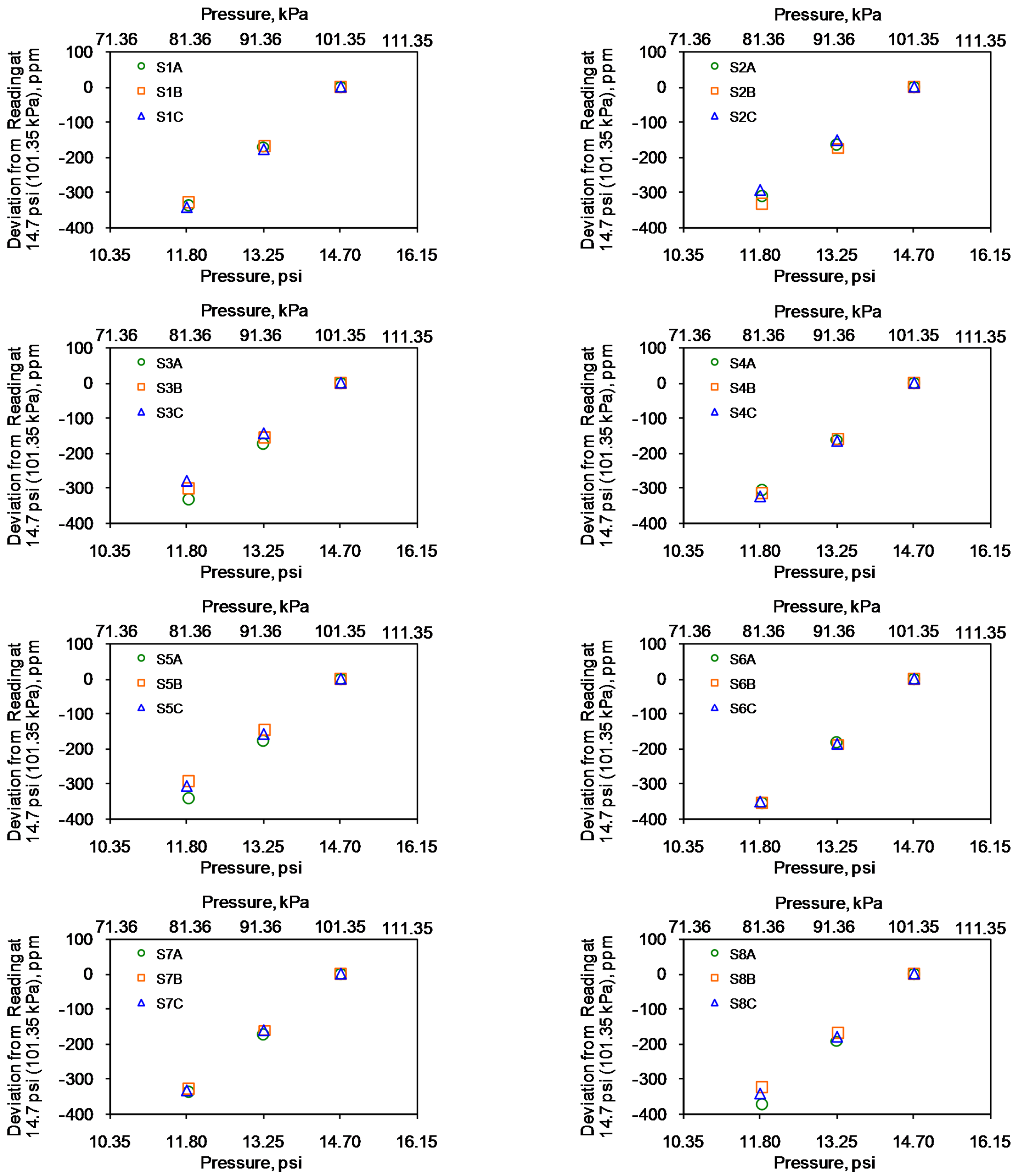

Figure 7. Pressure sensitivity test results of single-lamp, single-wavelength sensors.

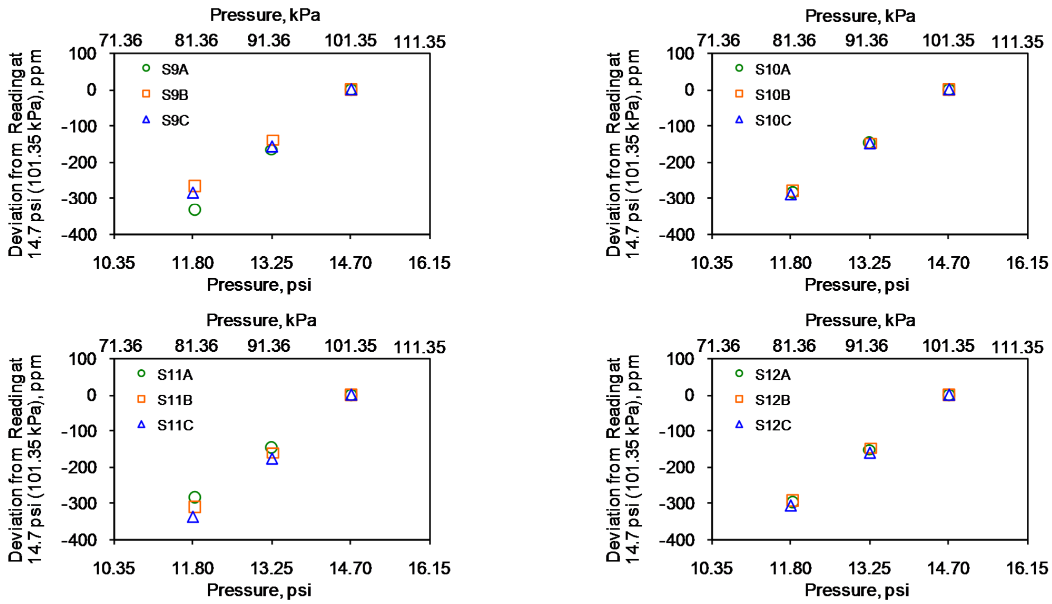

Figure 8. Pressure sensitivity test results of dual-lamp, single-wavelength sensors.

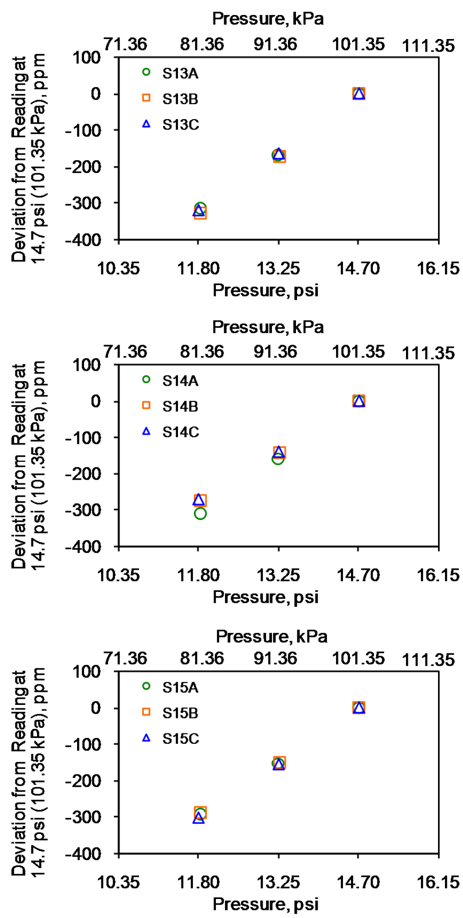

Figure 9. Pressure sensitivity test results of single-lamp, dual-wavelength sensors.

Table 8. Pressure Sensitivity Test Results of Single-Lamp, Single-Wavelength Sensors

Sensor Model	Sensor	Reading at			Pressure Sensitivity, % Reading / psi (6.89 kPa)	
		14.70 psia (101.35 kPa), ppm	13.25 psia (91.36 kPa), ppm	11.80 psia (81.36 kPa), ppm	Calculated	Manufacturer Specified
S1	A	1189	1018	853	9.8	NA
	B	1149	980	980	9.9	
	C	1184	1007	842	9.9	
S2	A	1233	1070	921	8.8	6.7
	B	1267	1093	1093	9.1	
	C	1180	1029	888	8.5	
S3	A	1275	1102	944	9.0	6.7
	B	1171	1017	1017	8.9	
	C	1114	971	835	8.6	
S4	A	1330	1167	1024	8.0	NA
	B	1343	1182	1182	8.2	
	C	1438	1274	1116	7.7	
S5	A	1315	1137	975	9.0	6.7
	B	1210	1063	1063	8.4	
	C	1214	1056	909	8.6	
S6	A	1240	1057	884	9.9	9.6
	B	1204	1016	1016	10.2	
	C	1237	1050	885	9.8	
S7	A	1539	1365	1203	7.6	7.2
	B	1457	1296	1296	7.8	
	C	1485	1325	1154	7.7	
S8	A	1260	1067	886	10.3	NA
	B	1132	962	962	10.0	
	C	1187	1007	845	9.9	

Table 9. Pressure Sensitivity Test Results of Dual-Lamp, Single-Wavelength Sensors

Sensor Model	Sensor	Reading at			Pressure Sensitivity, % Reading / psi (6.89 kPa)	
		14.70 psia (101.35 kPa), ppm	13.25 psia (91.36 kPa), ppm	11.80 psia (81.36 kPa), ppm	Calculated	Manufacturer Specified
S9	A	1161	995	829	9.9	9.8
	B	862	722	722	10.7	
	C	914	757	630	10.7	
S10	A	1238	1090	952	8.0	NA
	B	1206	1056	1056	8.1	
	C	1293	1143	1002	7.7	
S11	A	1150	1004	867	8.5	NA
	B	1263	1100	1100	8.6	
	C	1143	965	805	10.2	
S12	A	1275	1121	976	8.1	NA
	B	1246	1097	1097	8.2	
	C	1277	1117	972	8.2	

Table 10. Pressure Sensitivity Test Results of Single-Lamp, Dual-Wavelength Sensors

Sensor Model	Sensor	Reading at			Pressure Sensitivity, % Reading / psi (6.89 kPa)	
		14.70 psia (101.35 kPa), ppm	13.25 psia (91.36 kPa), ppm	11.80 psia (81.36 kPa), ppm	Calculated	Manufacturer Specified
S13	A	1185	1016	870	9.2	10.2
	B	1388	1216	1216	8.2	
	C	1313	1148	992	8.4	
S14	A	1212	1051	900	8.9	6.7
	B	1143	1002	1002	8.3	
	C	1202	1063	931	7.8	
S15	A	1087	935	795	9.3	NA
	B	1175	1025	1025	8.6	
	C	1219	1062	915	8.6	

Given the sensitivity of a NDIR CO_2 sensor reading to pressure, it is of interest to estimate the expected change in a sensor's reading due to the natural variation in barometric pressure for a given location. Using TMY2 weather data, the maximum change in barometric pressure was determined for nine US cities. From the CO_2 sensor sensitivity test results, the average pressure sensitivity is 8.9% reading/psi (6.89 kPa). Applying this sensitivity to the barometric pressure variation for each of the nine cities, the expected variation in CO_2 sensor reading were calculated. Table 11 summarizes the results. For the nine cites considered, Boston, Chicago and New York have the largest variation in barometric pressure. For these locations, the expected variation in a CO_2 sensor reading is 84 ppm for actual CO_2 concentration at 1100 ppm. The significance of these results is important when considering sensor calibration. Even for a "perfectly" calibrated sensor, the reading could be in error by several ppm depending on the barometric pressure at the time the sensor was calibrated compared to the barometric pressure at other times of the year.

Table 11. Expected Variation in CO_2 Sensor Output due to Variation in Local Barometric Pressure (at 1100 ppm CO_2 Concentration)

Location	Variation in Barometric Pressure, psi (kPa)	Variation in CO_2 Reading, ppm
Atlanta	0.508 (3.502)	50
Boston	0.860 (5.930)	84
Chicago	0.855 (5.895)	84
Denver	0.590 (4.068)	58
Los Angeles	0.566 (3.902)	55
Miami	0.377 (2.599)	37
New York	0.855 (5.895)	84
Sacramento	0.435 (2.999)	43
San Francisco	0.493 (3.399)	48

CONCLUSIONS

The result from the tests conducted under accurate and repeatable condition showed a wide variation in humidity and temperature sensitivity among the NDIR CO_2 sensor models. In some cases, significant variations in sensor performance exist between sensors of the same model while in other cases, all sensors of the same model showed almost identical behavior.

None of the sensor manufacturors specified humidity dependence of their CO_2 sensors. While majority of the sensors show little to no sensitivity to humidity, the test results revealed that three sensor models are highly sensitive to humidity. The maximum humidity sensitivity was observed as -3 ppm/% RH. It is suspected that the sensors with high humidity sensitivity use hygroscopic material as an optical filter.

Theoretically, increase in temperature at a fixed gas composition and pressure should decrease the number of molecules in optical path of a NDIR CO_2 sensor and hence decrease the sensor reading. Some sensors showed an opposite phenomenon. Nine sensor models showed temperature sensitivity within 5 ppm/1.8ºF (5 ppm/ºC). The maximum temperature sensitivity was observed as 10 ppm increase in sensor reading per 1.8°F (1°C) decrease in temperature for actual CO_2 concentration at 1100 ppm.

As was expected, the decrease in pressure decreased readings of all sensors. The maximum and minimum pressure sensitivity were observed as 129 and 92 ppm/psi (ppm/6.89 kPa), respectively at actual CO_2

concentration of 1100 ppm. Even for a best performing sensor, the natural barometric pressure variation results in significant change in NDIR CO_2 sensor reading.

The test results showed that the effects of temperature and pressure variation on NDIR CO_2 sensors are unavoidable. For the range of temperature and pressure variation in an air-conditioned space, the effect of pressure variation is more significant compared to the effect of temperature variation. An important consequence of the sensitivity of NDIR CO_2 sensor readings to pressure and temperature is field calibration. Some controls contactors field calibrate the sensors at the time the sensors are installed. In addition, many sensor models require calibration every 3 to 5 years. Field calibration typically involves flowing a calibration gas with a know concentration of CO_2 through the sensor's optical sensing element. Accurate calibration requires knowing the temperature and the pressure of the gas in the optical sensing element. Of these two, pressure is more important. If the calibration gas flow rate is low enough, then the pressure in the optical element would not be significantly different from atmospheric conditions. However, if the gas flow rate were too high, the gas pressure in the optical element would have an effect on the sensor reading.

ACKNOWLEDGEMENTS

This work is performed for National Building Controls Information Program (NBCIP), which is sponsored by the Iowa Energy Center, NSTAR Electric & Gas Corporation and the California Energy Commission.

REFERENCES

Fahlen, P., H. Andersson, and S. Ruud. 1992. Demand Controlled Ventilating Systems - Sensor Tests. Swedish National Testing and Research Institute, Boras, Sweden, SP Report 1992:13.

Fisk, W.J., D. Faulkner, and D.P. Sullivan. 2006. Accuracy of CO_2 sensors in commercial buildings: a pilot study. LBNL-61962, Lawrence Berkeley National Laboratory, Berkeley, CA.

Pandey, S.K., K. Kim, and S. Lee. 2007. Use of a dynamic enclosure approach to test the accuracy of the NDIR sensor: evaluation based on the CO2 equilibration pattern. Molecular Diversity Preservation International, Matthaeusstrasse, Switzerland, ISSN: 1424-8220.

Shrestha, S.S., and G.M. Maxwell. 2009. An experimental evaluation of HVAC-grade carbon-dioxide sensors: part 1, test and evaluation procedure. *ASHRAE Transactions* 115(2).

Chapter 5: An Experimental Evaluation of HVAC-Grade Carbon-Dioxide Sensors: Part 4, Effects of Ageing on Sensor Performance

A paper to be submitted to the ASHRAE Transactions

Som S. Shrestha
Student Member ASHRAE

Gregory M. Maxwell, PhD
Member ASHRAE

ABSTRACT

This is the fourth paper in a four-part series reporting on the test and evaluation of typical wall-mounted carbon-dioxide sensors used in building HVAC applications. Fifteen models of NDIR HVAC-grade wall-mounted CO_2 sensors were tested and evaluated to determine the effect of ageing on the sensors' performance. In all, 45 sensors were evaluated: three from each of the 15 models. Among the 15 models tested, eight models have a single-lamp, single-wavelength configuration, four models have a dual-lamp, single-wavelength configuration, and three models have a single-lamp, dual-wavelength configuration. All single-lamp, single-wavelength sensors and one single-lamp, dual-wavelength sensor incorporate an "automatic baseline adjustment" algorithm in the sensor's electronics package.

Each sensor was tested under "as received" conditions, and then, over the course of one year, performance tests were conducted at four-month intervals. All tests were conducted at 40% relative humidity, 73°F (22.8°C) temperature, 14.70 psia (101.35 kPa) pressure, and 1100 ppm CO_2 concentration. For each sensor, the readings from the four tests were compared in order to evaluate the effect of continuous operation on the sensor's performance. The test results showed a wide variation in sensor performance among the various manufacturers. The maximum deviation in a sensor's reading was observed to be 420 ppm (38%) while the minimum deviation in a sensor's reading was observed to be 0 ppm.

INTRODUCTION

This is part four of a four-part series of papers reporting on the test and evaluation of typical CO_2 sensors used in building HVAC systems. In this study, fifteen models of NDIR (non-dispersive infrared) HVAC-grade CO_2 sensors were tested and evaluated to examine the affects of ageing on sensor performance. To compensate for sensor ageing, some sensors automatically reset the baseline value (normally 400 ppm) according to minimum CO_2 concentration observed over a time period. This technique relies on the fact that many buildings experience unoccupied periods during which CO_2 levels drop to outdoor levels. Other techniques used to compensate for the sensor ageing include dual-lamp, single-wavelength and single-lamp, dual-wavelength configurations. The working principles, physical construction, advantages and disadvantages of NDIR CO_2 sensors are well documented in the literature (Raatschen (1990), Emmerich and Persily (2001), Schell and Int-House (2001), Fahlen et al. (1992)).

Among the 15 models tested, eight models have a single-lamp, single-wavelength configuration, four models have a dual-lamp, single-wavelength configuration, and three models have a single-lamp, dual-wavelength configuration. In all, 45 sensors (three from each model) were evaluated. The tests were designed to assess the performance of the sensors while they operated under typical building conditions for a one-year period.

PREVIOUS STUDIES

In the past, limited studies have been done to investigate the performance of HVAC-grade CO_2 sensors using a controlled environment. No published information is available that shows systematic study to quantify effect of ageing on NDIR CO_2 sensors.

Fahlen et al. (1992) evaluated the performance of two CO_2 sensors, one photo-acoustic type and one infrared spectroscopy type, in lab tests and long term field tests. The lab tests included performance and environmental tests. The authors conclude that the deviation between actual concentration and the sensors' reading are normally well within ± 50 ppm at a concentration level of 1000 ppm. However, at a concentration of 2000 ppm the test results showed a deviation of up to -300 ppm. The output of one sensor increased dramatically during environmental testing. This sensor failed to return to its normal value.

Fisk et al. (2006) conducted a pilot study that evaluated the in-situ accuracy of 44 NDIR CO_2 sensors located in nine commercial buildings. The evaluation was performed either by multi-point calibration using CO_2 calibration gas or by a single-point calibration check using a co-located and calibrated reference CO_2 sensor. Their results indicated that the accuracy of CO_2 sensors is frequently less than what is needed to measure peak indoor-outdoor CO_2 concentration differences with an error that is less than 20%. Thus, the authors conclude that there is a need for more accurate CO_2 sensors and/or better maintenance and calibration.

Pandey et al. (2007) evaluated the accuracy of two NDIR CO_2 sensor models. They tested three sensors of each model. The tests were performed in an enclosure where all six sensors were exposed to CO_2 concentration of 0 ppm, 500 ppm, and 1000 ppm (other environmental conditions, such as humidity, temperature, and pressure were not specified.) The maximum deviation was observed as -73 ppm at a CO_2 concentration of 500 ppm.

A study conducted at the Iowa Energy Center showed that, among the three new, co-located sensors, one sensor read about 105 ppm higher, compared to the two other sensors, at about 400 ppm (House 2006). Nine months later, the sensor that read 105 ppm higher at the beginning, read 265 ppm higher compared to the two other sensors.

This paper describes a series of tests conducted in four months interval for one year to evaluate effect of ageing on performance of NDIR CO_2 sensors. In addition, the paper presents test and evaluation results, including the sensors behavior during initial power-up and conditioning period. The benefit of the present work is that it provides repeated assessment of the performance of each sensor under repeatable conditions.

CO_2 SENSOR SPECIFICATIONS

CO_2 sensor manufacturers provide detailed specifications for their products. This information is available from the company's website and/or literature packaged with the product. Table 1 summarizes some of the product information for the models evaluated in this study. (Specific product names are not used in this paper, rather the sensors are referred to as S1 through S15 with the letters A, B and C used to differentiate between sensors of the same model.) The table indicates the sensor configuration, manufacturer-specified long-term stability, calibration time interval, and calibration procedure. As can be seen from the table, the models range from sensors that require no calibration during their fifteen-year lifespan, to sensors that require calibration every three to five years. Many sensors where calibration is suggested (or mandatory) require special calibration software and the use of calibration gas. In some cases, a single-point calibration is all that is required.

Table 1. Manufacturer-Specified Long-Term Stability, Calibration Time Interval, and Calibration Procedure

Sensor Model	Configuration	Manufacturer-Specified Long-Term Stability	Manufacturer-Recommended Calibration Time Interval	Manufacturer-Recommended Calibration Procedure
S1	Single-lamp, single-wavelength	NA	Automatic baseline correction for self calibration (15 years) lifetime self calibration	No calibration required for life of the sensor.
S2	Single-lamp, single-wavelength	NA	Automatic self calibration	Requires Calibration Kit.
S3	Single-lamp, single-wavelength	NA	Self calibration for life of the sensor	No calibration required for life of the sensor.
S4	Single-lamp, single-wavelength	NA	5 years	One point calibration with 2000 ppm CO_2.
S5	Single-lamp, single-wavelength	< 2% FS over life of sensor (15 years typical)	5 years	0 ppm and 2000 ppm CO_2.
S6	Single-lamp, single-wavelength	NA	5 years	Typically calibration is unnecessary. However, the sensor can be rezored.
S7	Single-lamp, single-wavelength	± 75 PPM per year at 1200 PPM	3 to 5 Years	Calibration gas of known CO_2 concentration (0 to 2000 ppm). One point calibration.
S8	Single-lamp, single-wavelength	NA	5 Years	One point calibration with 0 ppm CO_2.
S9	Dual-lamp, single-wavelength	NA	3 Years	0 ppm and 2000 ppm CO_2.
S10	Dual-lamp, single-wavelength	< 20 ppm / year	Not required	No provision for calibration.
S11	Dual-lamp, single-wavelength	NA	NA	0 ppm and 2000 ppm CO_2.
S12	Dual-lamp, single-wavelength	20 ppm / year	15 Years	No provision for calibration.
S13	Single-lamp, dual-wavelength	< ± 5.0% FS / 5 Years	5 Years	Requires calibration software.
S14	Single-lamp, dual-wavelength	NA	5 Years	Requires Calibration Kit.
S15	Single-lamp, dual-wavelength	< 5.0% FS / 5 years	5 years	Requires calibration software.

Notes: NA indicates that the information was not available in the manufacturer's product literature. Full scale (FS) is 2000 ppm for all sensors.

Sensors S1 through S8 are single-lamp, single-wavelength sensor, sensors S9 through S12 are dual-lamp, single-wavelength sensors, and sensors S13 through S15 are single-lamp, dual-wavelength sensors. All single-lamp, single-wavelength sensors incorporate an "automatic baseline adjustment" algorithm in the sensor's electronics package. One single-lamp, dual-wavelength sensor (S14) also incorporates an "automatic baseline adjustment" algorithm in it, with an option to turn on or off. The manufacturer's default selection was "on", and no adjustment was made to change the setting. The details of the "automatic baseline adjustment" algorithm are described in part 2 of this paper.

EXPERIMENTAL TEST PROCEDURE

The CO_2 sensors were tested using two experimental apparatus specifically designed and fabricated for the performance evaluation. Performance testing under controlled environmental conditions was conducted in the test chamber shown in Figure 1 while continuous operation of the sensors in the laboratory environment was conducted in the lab station shown in Figure 2. Technical details of these apparats and instrumentation are described in Part 1 (Shrestha and Maxwell 2009) of this paper.

The performance of each sensor was evaluated under "as received" conditions, and then, over the course of one year, performance tests were conducted every four months. All performance tests were conducted at 40% relative humidity, 73^{o}F (22.8^{o}C) temperature, 14.70 psia (101.35 kPa) pressure, and 1100 ppm CO_2 concentration.

Before the first test was conducted, all sensors were placed in the lab station and powered up and allowed to operate in the laboratory environment for at least a three weeks period. This time period was sufficient for all sensor models to stabilize, and for sensors that make "automatic baseline adjustment" to complete their "self-calibration process". The environmental conditions in the laboratory are typical of air-conditioned, part-time occupied space. Daily variations in space humidity, barometric pressure, temperature and levels of CO_2 concentration were observed and recorded. Figure 3 shows the CO_2 concentration in the laboratory for two weeks prior to performance testing. Figure 4 shows the temperature and pressure in the laboratory for two weeks prior to performance testing.

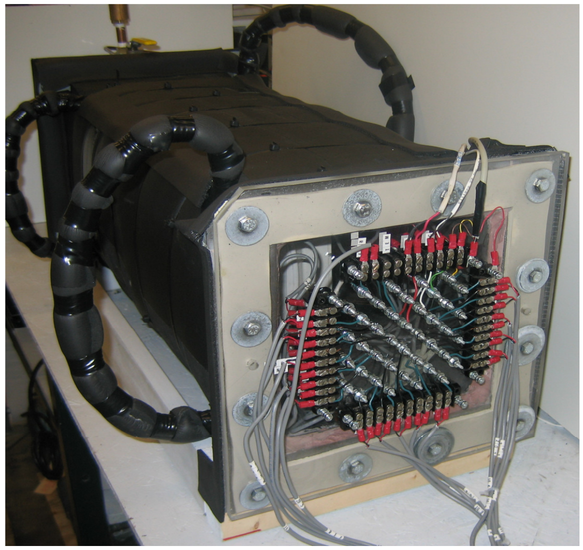

Figure 1. Test chamber.

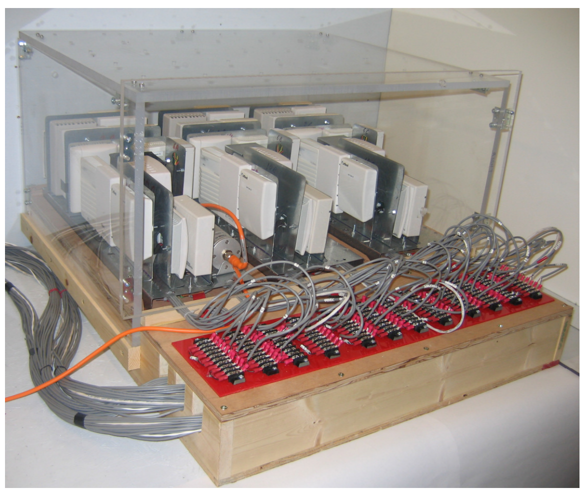

Figure 2. Lab station.

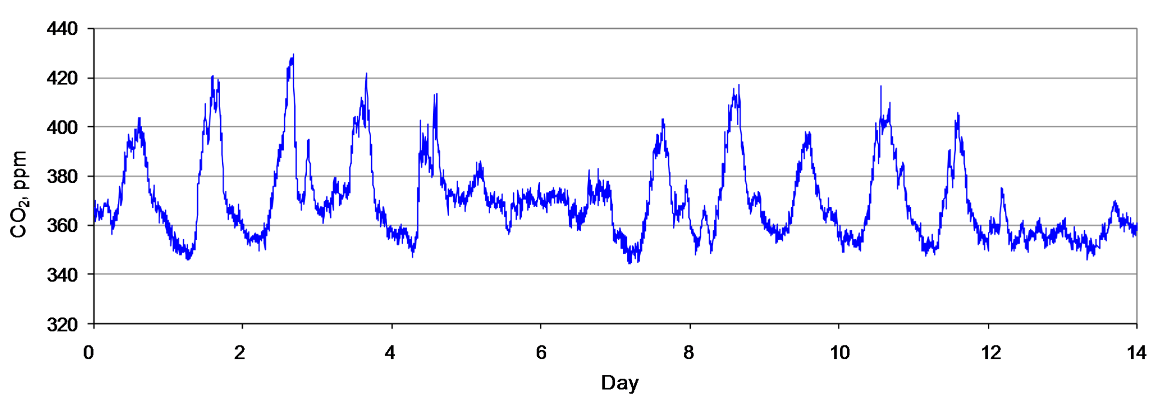

Figure 3. CO_2 concentration in the laboratory.

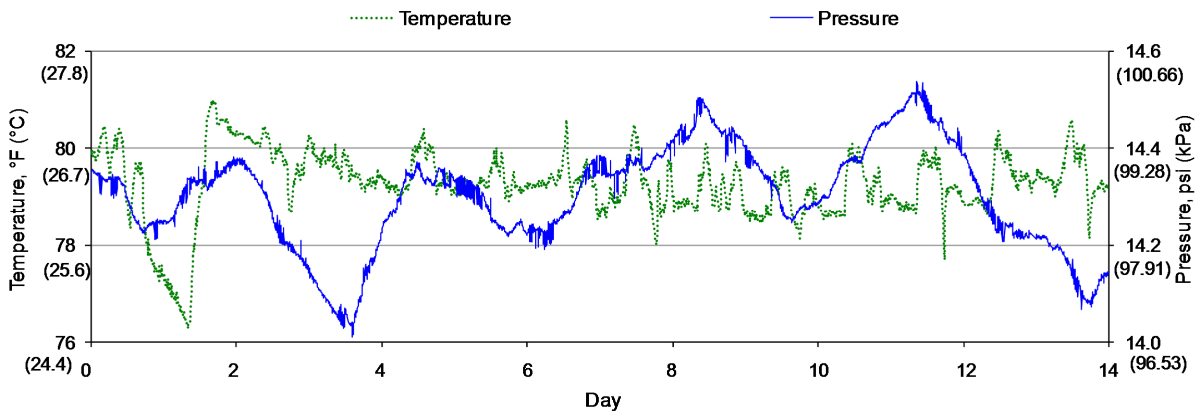

Figure 4. Temperature and pressure in the laboratory.

Figure 5 shows the readings for sensor models S1 through S8 all of which use "automatic baseline adjustment" algorithms. Baseline adjustments are seen for many of the sensors in the figure. In some cases, the adjustments appear as sudden, large-scale changes in the sensor reading, while in other cases, the changes are more gradual. The overall trend is that while sensors of a given model may have different readings early on, they tend to read the same after the conditioning period.

Figure 6 shows the readings for sensor models S9 through S12. These sensors have a dual-lamp, single-wavelength configuration and do not use automatic baseline correction algorythms. The sensors are seen to stabalize during the period. It is interesting to note that the three sensors of model S12 agree more closely with each other at the beginning of the period, but then have different readings at the end of the period.

Figure 7 shows the reading for sensor models S13 through S15. These sensor use a single-lamp, dual-wavelength configuration. Sensor model S14 incorporates an "automatic baseline adjustment" algorithm as is evident by the abrupt changes in the sensors' readings. Sensors from models S13 and S15 show very stable operation throughout the entire period.

After the initial power up and conditioning phase, the sensors were placed in the test chamber for a series of performance tests. The detailed test procedures are described in Part 1 (Shrestha and Maxwell 2009). Specific to effects of ageing, the sensor readings were recorded while the test chamber conditions were maintained at 40% RH, 73ºF (22.8ºC), 14.70 psia (101.35 kPa), and 1100 ppm CO_2 concentration. These tests were repeated every four months during the one-year period.

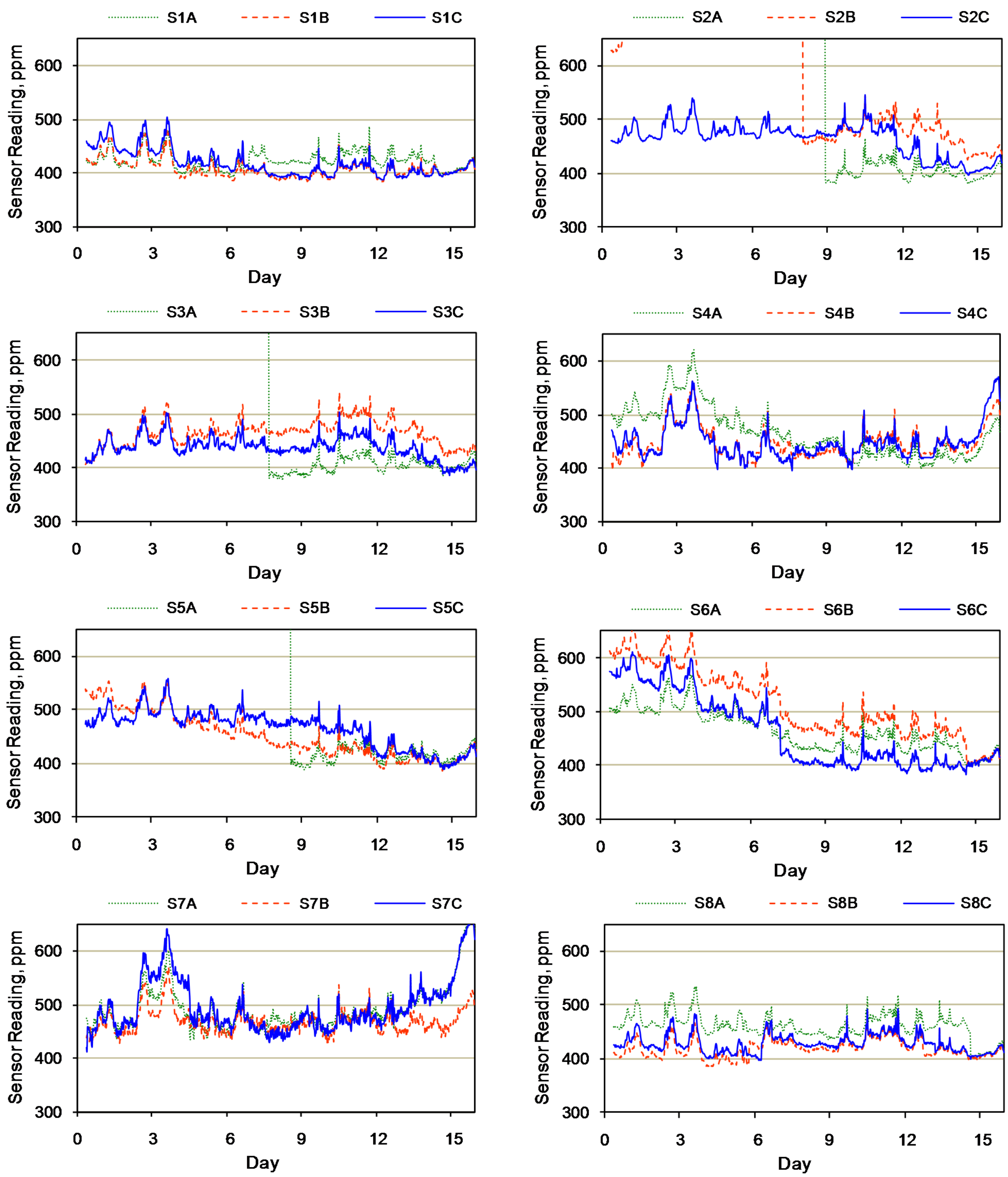

Figure 5. Power-up and conditioning of single-lamp, single-wavelength sensors.

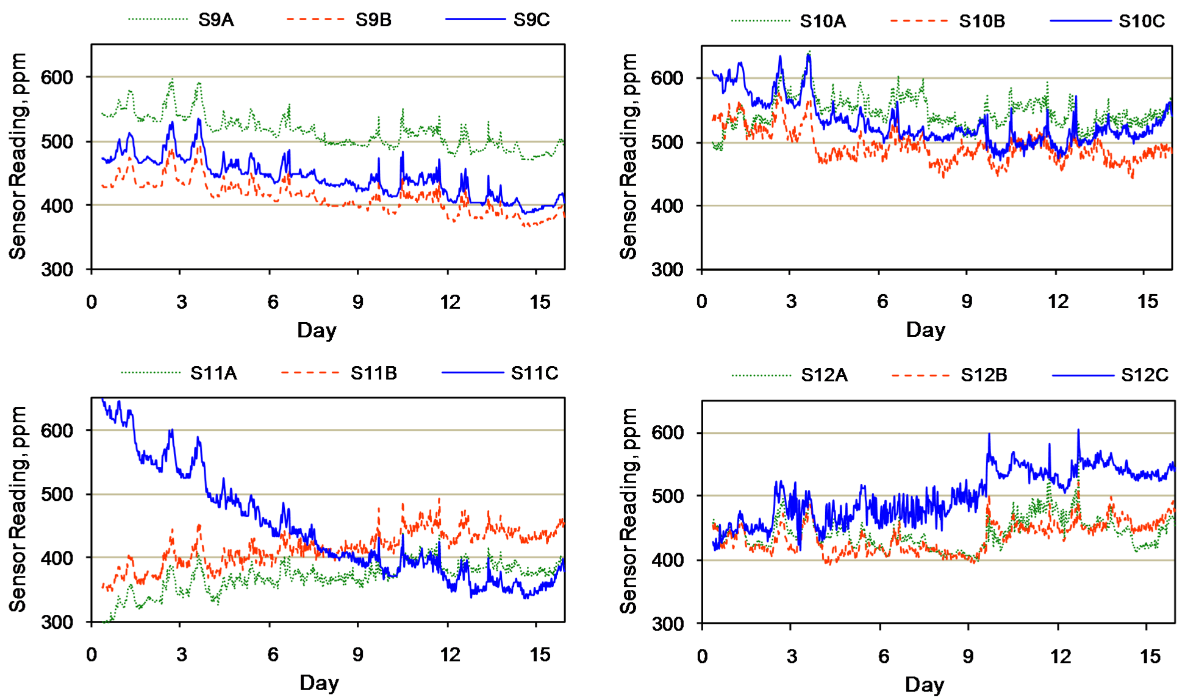

Figure 6. Power-up and conditioning of dual-lamp, single-wavelength sensors.

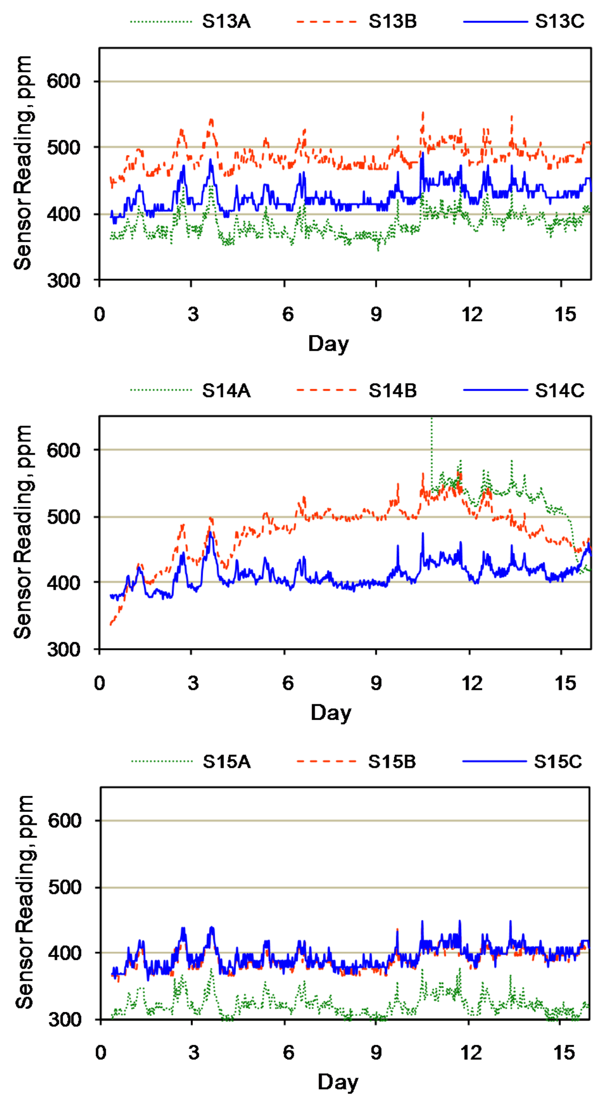

Figure 7. Power-up and conditioning of single-lamp dual-wavelength sensors.

On average, sensors would spend approximately two days in the test chamber during performance testing. During the rest of the time, the sensors were located in the lab station where they would periodically be exposed to higher levels of CO_2. For three days per week, the CO_2 concentration was increased to approximately 1100 ppm for a period of 8 to 12 hours. The specific days of the week and number of hours per day were chosen at random. Figure 8 illustrates typicall CO_2 concentrations during the “exercise period” At all other times, the sensors experienced ambient laboratory conditions.

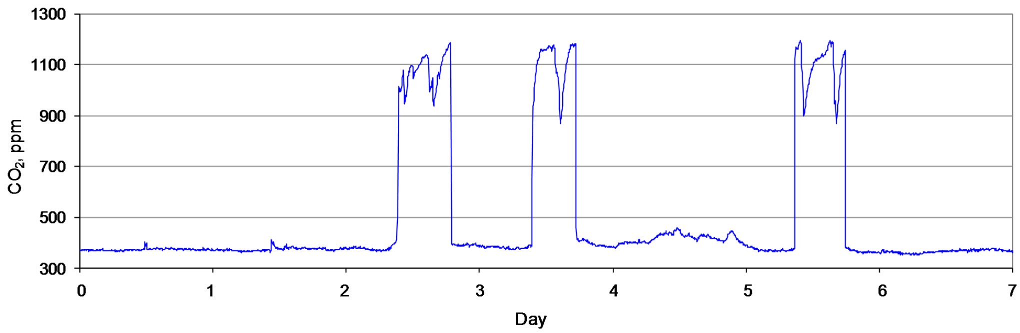

Figure 8. Lab Station CO_2 concentration during exercise period.

AGEING TEST RESULTS

The effects of ageing on the sensors' performance is presented in terms of the deviation of measured CO_2 concentration by a sensor in a given test from the measured CO_2 concentration by the sensor in the first test (beginning of life) (i.e., deviation = measured CO_2 concentration in a subsequent test – measured CO_2 concentration in the first test). The deviation is calculated for each sensor reading at 1100 ppm CO_2 concentration in the test chamber. As mentioned earlier, three sensors from each of fifteen models were tested. The letters A, B and C are used to distinguish between each sensor of a given model. Data plots are used to illustrate the effects of ageing on the CO_2 sensors' performance while numerical results are provided in tables.

Single-lamp, single-wavelength sensors: The test results for sensor models S1 through S8 are shown graphically in Figure 9 and are presented numerically in Table 2. Recall that the tests were conducted with CO_2 concentration of 1100 ppm; therefore, a deviation of 11 ppm corresponds to 1% change in the sensor performance. The accuracy of the CO_2 gas mixture in the test apparatus is 1% of the concentration which also corresponds to 11 ppm. Thus, within the uncertainty of the experimental apparatus, sensor with deviations of 1% or less can be considered as stable with no affect of ageing.

From Table 1, sensor model S5 is expected to have a deviation less than 40 ppm over 15 years and sensor model S7 is expected to have a deviation of ± 75 PPM per year at 1200 PPM. Upon examination of the performance of these sensors as shown in Table 2, at the end of one year, these sensors are within the specified limits.

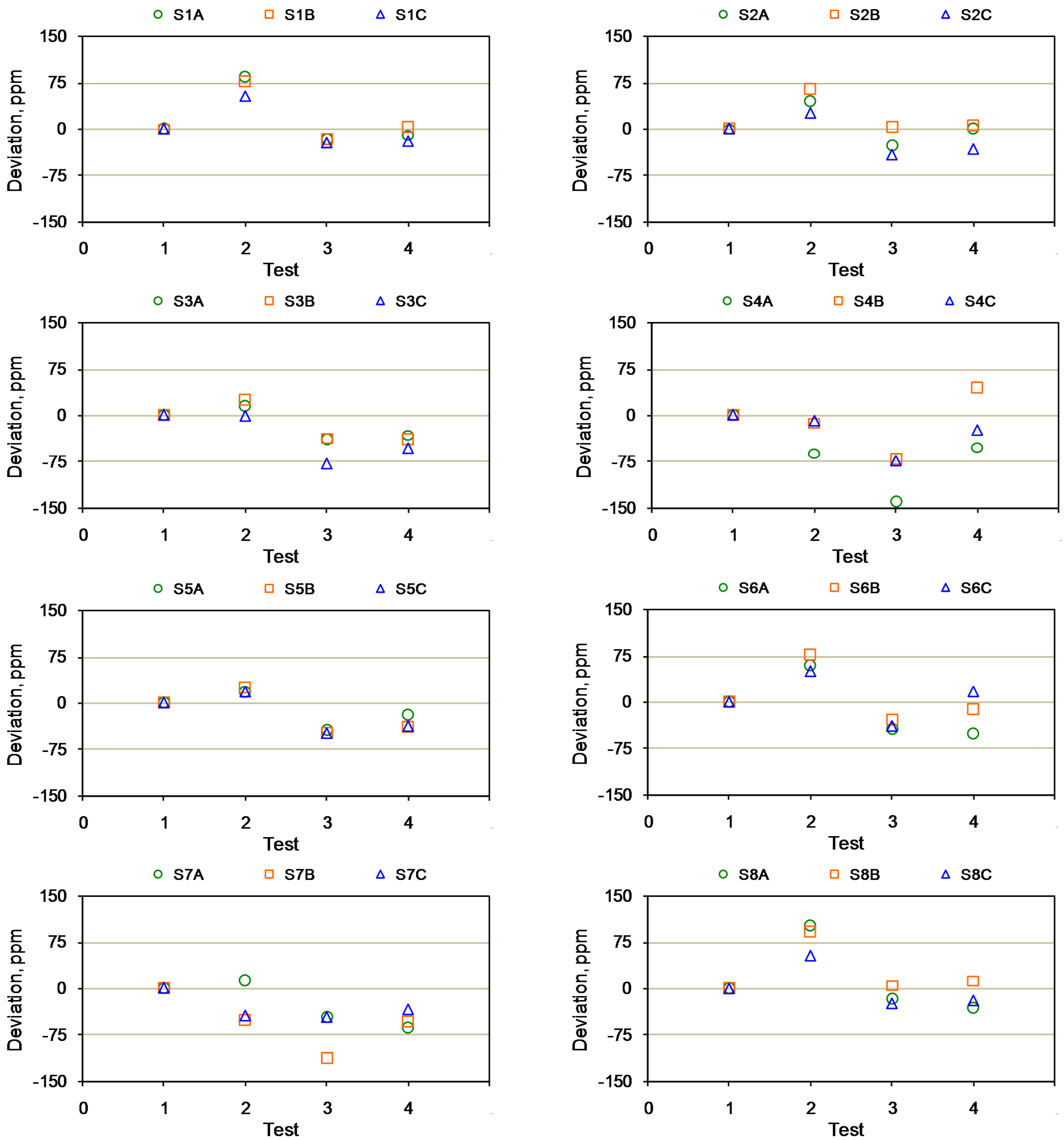

Figure 9. Deviation from the reading from the first test for single-lamp, single-wavelength sensors.

Table 2. Ageing Test Result of Single-Lamp, Single-Wavelength Sensors

Sensor Model	Sensor	Deviation from Reading at First Test, ppm		
		Second Test	Third Test	Fourth Test
S1	A	83	-17	-11
	B	77	-17	3
	C	53	-22	-20
S2	A	45	-26	0
	B	65	4	6
	C	25	-42	-33
S3	A	15	-39	-33
	B	25	-38	-40
	C	-2	-78	-53
S4	A	-63	-141	-53
	B	-13	-72	46
	C	-10	-74	-25
S5	A	19	-45	-19
	B	25	-50	-40
	C	17	-49	-38
S6	A	60	-44	-52
	B	76	-30	-12
	C	49	-38	17
S7	A	14	-47	-65
	B	-52	-113	-55
	C	-44	-47	-34
S8	A	101	-18	-33
	B	92	4	11
	C	52	-24	-19

Dual-lamp single-wavelength sensors: The test results for sensor models S9 through S12 are shown graphically in Figure 10 and are presented numerically in Table 3. From Table 1, sensor models S10 and S12 are expected to have a deviation of 20 ppm per year. When compared to the results in Table 3, these sensor models closely follow the specified deviation. Sensor model S9 shows the largest deviations for all three sensors of this model.

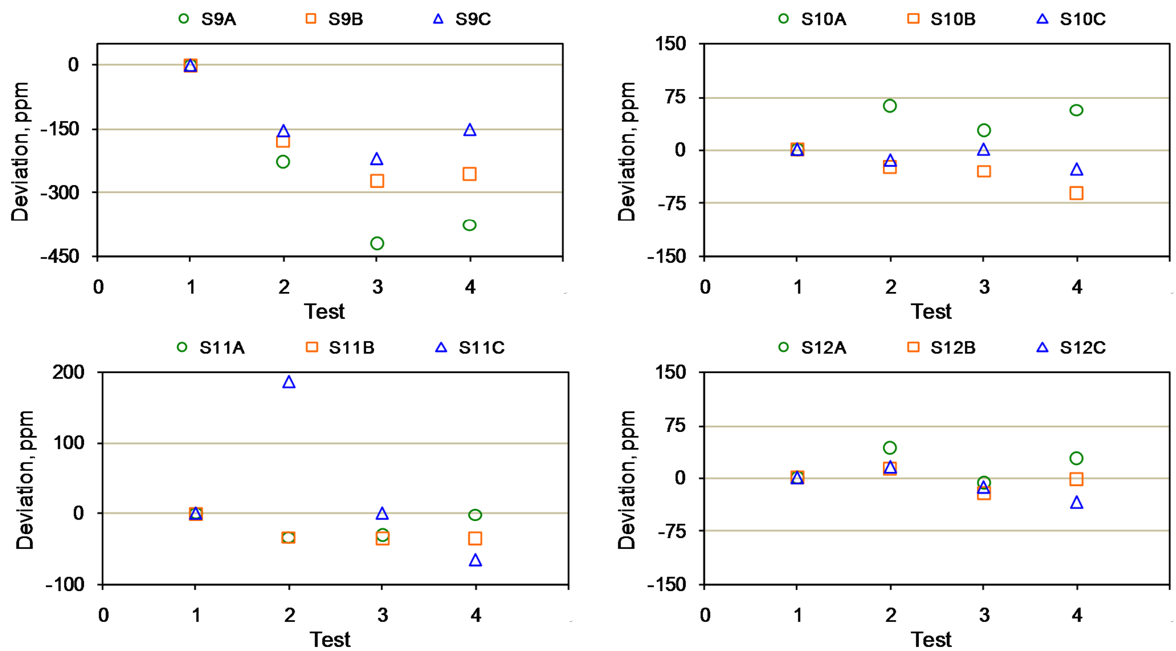

Figure 10. Deviation from the reading from the first test for dual-lamp, single-wavelength sensors.

Table 3. Ageing Test Result of Dual-Lamp, Single-Wavelength Sensors

Sensor Model	Sensor	Deviation from Reading at First Test, ppm		
		Second Test	Third Test	Fourth Test
S9	A	-226	-420	-376
	B	-181	-274	-256
	C	-155	-221	-152
S10	A	63	28	56
	B	-24	-30	-61
	C	-15	0	-28
S11	A	-34	-32	-2
	B	-34	-37	-36
	C	186	0	-66
S12	A	42	-8	26
	B	13	-21	-3
	C	15	-13	-34

Single-lamp dual-wavelength sensors: The test results for sensor models S13 through S15 are shown graphically in Figure 11 and are presented numerically in Table 4. From Table 1, sensor models S13 and S15 have deviation less than 100 ppm in 5 years (< 5.0% FS / 5 years). When compared to the values in Table 4, except for the "A" sensor of model S13, these sensors are within the specified deviation.

Sensor model S14 uses an “automatic baseline adjustment” algorithm. There is not specified value for the deviation of this sensor (refer to Table 1); however, the deviations for this sensor model presented in Table 4 are consistent with the other sensors that employ an “automatic background adjustment” scheme.

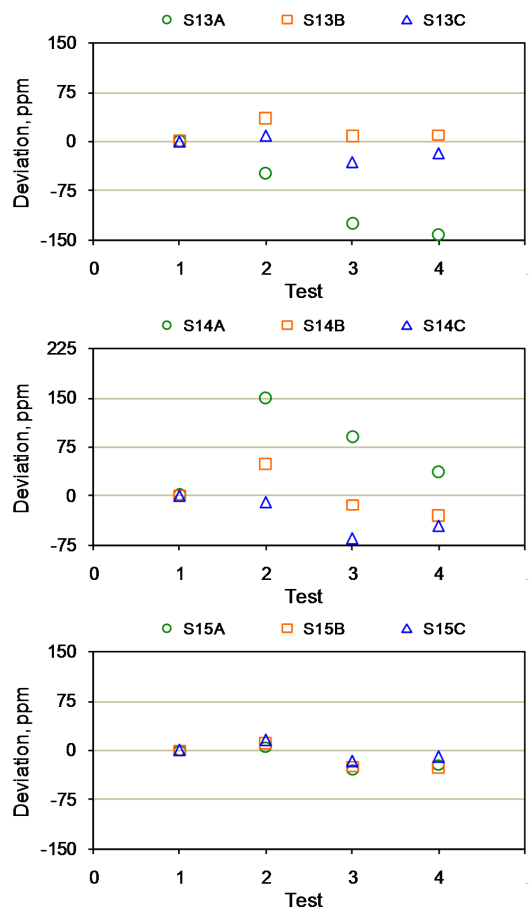

Figure 11. Deviation from the reading from the first test for single-lamp, dual-wavelength sensors.

Table 4. Ageing Test Result of Single-Lamp, Dual-Wavelength Sensors

Sensor Model	Sensor	Deviation from Reading at First Test, ppm		
		Second Test	Third Test	Fourth Test
S13	A	-49	-125	-142
	B	36	8	9
	C	9	-32	-18
S14	A	150	90	35
	B	48	-15	-31
	C	-10	-64	-45
S15	A	4	-30	-24
	B	11	-25	-27
	C	15	-16	-10

CONCLUSIONS

The result from the tests conducted under accurate and repeatable condition showed a wide variation in ageing effect among manufacturers. Some sensor models showed nominal ageing effect of less than 30 ppm deviation, whereas all three sensors of one model that use dual-lamp, single-wavelength configuration showed significant ageing effect, up to -376 ppm deviation, in one year at 1100 ppm CO_2 concentration.

Sensor manufacturers use one of three configurations (single-lamp single-wavelength, dual-lamp single-wavelength, or single-lamp dual-wavelength) to compensate for the long-term effects of operational and environmental conditions. However there is no clear indication to conclude that any one configuration is better than the rest, at least for one year of operation.

ACKNOWLEDGEMENTS

This work is performed for National Building Controls Information Program (NBCIP), which is sponsored by the Iowa Energy Center, NSTAR Electric & Gas Corporation and the California Energy Commission.

REFERENCES

Emmerich, S.J., and A.K. Persily. 2001. *State-of-the-art review of CO_2 demand controlled ventilation technology and application, Report NISTIR 6729, National Institute of Science and Technology (NIST), USA.*

Fahlen, P., H. Andersson, and S. Ruud. 1992. Demand Controlled Ventilating Systems - Sensor Tests. Swedish National Testing and Research Institute, Boras, Sweden, SP Report 1992:13.

House, J. 2006. Personal communication.

Fisk, W.J., D. Faulkner, and D.P. Sullivan. 2006. Accuracy of CO_2 sensors in commercial buildings: a pilot study. LBNL-61962, Lawrence Berkeley National Laboratory, Berkeley, CA.

Pandey, S.K., K. Kim, and S. Lee. 2007. Use of a dynamic enclosure approach to test the accuracy of the NDIR sensor: evaluation based on the CO_2 equilibration pattern. Molecular Diversity Preservation International, Matthaeusstrasse, Switzerland, ISSN: 1424-8220.

Raatschen, W., ed. 1990. Demand Controlled Ventilating System. State of the Art Review. Stockholm, Sweden: Swedish Council for Building Research, Stockholm, Sweden, D9:1990.

Schell, M., and D. Int-Hout. 2001. Demand control ventilation using CO_2. *ASHRAE Journal* Vol. 43, No. 2: 18-24.

Shrestha, S.S., and G.M. Maxwell. 2009. An experimental evaluation of HVAC-grade carbon-dioxide sensors: part 1, test and evaluation procedure. *ASHRAE Transactions* 115(2).

Chapter 6: General Conclusions

GENERAL DISCUSSION

The effectiveness of CO_2-based demand controlled ventilation (DCV) relies upon the performance of CO_2 sensors. However, studies on accuracy of CO_2 sensors and the effects of humidity, temperature, and pressure variations on sensor output are limited, despite the importance of sensor performance. Moreover, the findings of some studies are contradictory.

Further review of the literature reveled that there is no present standard method of test (MOT) available by which CO_2 sensors are evaluated. Therefore, an experimental procedure for testing and evaluating the sensors was developed for this research.

This study presents systematic procedures to test and evaluate the accuracy, linearity, repeatability, hysteresis, humidity sensitivity, temperature sensitivity, and pressure sensitivity of NDIR CO_2 sensors used in DCV applications. Further, it describes the experimental apparatus, instrumentation, and data acquisition system along with test conditions, used to test the sensors. Additionally, a procedure for procurement and handling of sensors is also described.

The results from testing forty-five HVAC-grade NDIR CO_2 sensors from fifteen models under accurate and repeatable conditions have shown a wider variation in sensor performance among manufacturers. In some cases, significant variations in sensor performance exist between sensors of the same model while in other cases, all sensors of the same model showed almost identical behavior. None of the sensor models meet their manufacturer specified accuracy statement for all three sensors of a given model over the full range of test conditions. For some models, none of the three sensors of the model meet the accuracy specifications at any test condition.

Given the test results and that the sensors were tested under "as received" conditions, it might appear that sensor calibration should be performed before putting sensors into service. However, for sensors with automatic baseline adjustment algorithm, it is impossible to predict the sensor's performance over a prolonged time period during which the sensor baseline might make multiple adjustments. In fact, the literatures for several sensor models that incorporate automatic baseline adjustment algorithm claim that the sensors do not require calibration. Given the sensor is “self adjusting” using an arbitrary background reading of 400 ppm, it is unclear how the sensor manufacturer can claim an absolute accuracy for their sensor. However, some of the models that utilize automatic baseline adjustment algorithm do appear to be “accurate” if one accounts for the bias created by the baseline adjustment. Some sensors have provision for only one point calibration. For sensors that show increasingly larger values of deviation as the CO_2 concentration increases (see Figure 4g), a simple bias adjustment would not make the sensors reading accurate over the full range of CO_2 concentrations.

The test results for sensors that use dual-lamp, single-wavelength or single-lamp, dual-wavelength configuration generally show a constant value of deviation as the CO_2 concentration increases. Two of the dual-lamp, single-wavelength sensors have no provision for on-site calibration.

Nonlinearity, repeatability and hysteresis do not appear to be significant for most of the sensors tested. Only three sensors models specified their nonlinearity as less than 1% full scale (20 ppm), and all three sensor models meet their linearity specification. While the largest nonlinearity was observed as 27 ppm, many sensors' nonlinearity is less than 5 ppm.

Five sensor models specified their repeatability and all five sensor models meet their repeatability specification. One sensor registered the maximum repeatability error as 25 ppm. All other sensors have repeatability within 14 ppm.

None of the sensor manufacturers specified hysteresis for their sensors. The maximum hysteresis of a sensor was 31 ppm. Most of the sensors have hysteresis within 13 ppm.

The result from the tests conducted under accurate and repeatable condition showed a wide variation in humidity and temperature sensitivity among the NDIR CO_2 sensor models. In some cases, significant variations in sensor performance exist between sensors of the same model while in other cases, all sensors of the same model showed almost identical behavior.

None of the sensor manufacturors specified humidity dependence of their CO_2 sensors. While majority of the sensors show little to no sensitivity to humidity, the test results revealed that three sensor models are highly sensitive to humidity. The maximum humidity sensitivity was observed as -3 ppm/% RH. It is suspected that the sensors with high humidity sensitivity use hygroscopic material as an optical filter.

Theoretically, increase in temperature at a fixed gas composition and pressure should decrease the number of molecules in optical path of a NDIR CO_2 sensor and hence decrease the sensor reading. Some sensors showed an opposite phenomenon. Nine sensor models showed temperature sensitivity within 5 ppm/1.8ºF (5 ppm/ºC). The maximum temperature sensitivity was observed as 10 ppm increase in sensor reading per 1.8°F (1°C) decrease in temperature for actual CO_2 concentration at 1100 ppm.

As was expected, the decrease in pressure decreased readings of all sensors. The maximum and minimum pressure sensitivity were observed as 129 and 92 ppm/psi (ppm/6.89 kPa), respectively at actual CO_2 concentration of 1100 ppm. Even for a best performing sensor, the natural barometric pressure variation results in significant change in NDIR CO_2 sensor reading.

The test results showed that the effects of temperature and pressure variation on NDIR CO_2 sensors are unavoidable. For the range of temperature and pressure variation in an air-conditioned space, the effect of pressure variation is more significant compared to the effect of temperature variation. An important consequence of the sensitivity of NDIR CO_2 sensor readings to pressure and temperature is field calibration. Some controls contactors field calibrate the sensors at the time the sensors are installed. In addition, many sensor models require calibration every 3 to 5 years. Field calibration typically involves flowing a calibration gas with a know concentration of CO_2 through the sensor's optical sensing element. Accurate calibration requires knowing the temperature and the pressure of the gas in the optical sensing element. Of these two, pressure is more important. If the calibration gas flow rate is low enough, then the pressure in the optical element would not be significantly different from atmospheric conditions. However, if the gas flow rate were high, the gas pressure in the optical element would have an effect on the sensor reading.

Some sensor models showed nominal ageing effect of less than 30 ppm deviation, whereas all three sensors of one model that use dual-lamp, single-wavelength configuration showed significant ageing effect, up to -376 ppm deviation, in one year at 1100 ppm CO_2 concentration.

Sensor manufacturers use one of three configurations (single-lamp single-wavelength, dual-lamp single-wavelength, or single-lamp dual-wavelength) to compensate for the long-term ageing effects of operational and environmental conditions. However there is no clear indication to conclude that any one configuration is better than the rest, at least for one year of operation.

RECOMMENDATIONS FOR FUTURE RESEARCH

As discussed earlier, there is no present standard method of test (MOT) available by which NDIR CO_2 sensors are evaluated. It would be desirable to develop the MOT presented in this research to make it a standard method of test.

This research has a great potential to expanded to make CO_2-based DCV system more energy efficient. For a fixed composition of air, any change in temperature or pressure will change number of CO_2 molecules in the optical cavity of a NDIR CO_2 sensor. Thus, the effects of temperature and pressure variation on NDIR CO_2 sensors are unavoidable. Hence, an algorithm to account for the temperature, and more importantly the preessure variation is important, not only to insure energy savings, but also to assure adequate IAQ.

References

CEC, 2002, High Performance Commercial Building Systems, *California Energy Commission, Public Interest Energy Research Program*, HPCBS # E5P23T1b

CEC. 2006. *2005 Building Energy Efficiency Standards for Residential and Nonresidential Buildings*. CALIFORNIA ENERGY COMMISSION Title 24, Part 6, of the California Code of Regulations.

DOE. 2007. 2007 Building Energy Databook. http://buildingsdatabook.eere.energy.gov/ Washington, DC: U.S. Department of Energy, Energy Efficiency and Renewable Energy.

Dougan, D.S., and L. Damiano. 2004. CO_2-based demand control ventilation: do risk outweigh potential rewards?. *ASHRAE Journal* Vol. 46, No. 10: 47-53.

Emmerich, S.J., and A.K. Persily. 1997. Literature review on CO_2-based demand-controlled ventilation. *ASHRAE Transactions* 103 (2): 229-43.

Emmerich, S.J., and A.K. Persily. 2001. *State-of-the-art review of CO_2 demand controlled ventilation technology and application, Report NISTIR 6729, National Institute of Science and Technology (NIST), USA.*

Fahlen, P., H. Andersson, and S. Ruud. 1992. Demand Controlled Ventilating Systems - Sensor Tests. Swedish National Testing and Research Institute, Boras, Sweden, SP Report 1992:13.

Fisk, W.J., D. Faulkner, and D.P. Sullivan. 2006. Accuracy of CO_2 sensors in commercial buildings: a pilot study. LBNL-61962, Lawrence Berkeley National Laboratory, Berkeley, CA.

Hyland, R.W., and A. Wexler. 1983. Formulations for the thermodynamic properties of the saturated phases of H_2O from 173.15 K to 473.15 K. *ASHRAE Transactions* 89(2A):500-519.

House, J. 2006. Personal communication.

Pandey, S.K., K. Kim, and S. Lee. 2007. Use of a dynamic enclosure approach to test the accuracy of the NDIR sensor: evaluation based on the CO_2 equilibration pattern. Molecular Diversity Preservation International, Matthaeusstrasse, Switzerland, ISSN: 1424-8220.

Raatschen, W., ed. 1990. Demand Controlled Ventilating System. State of the Art Review. Stockholm, Sweden: Swedish Council for Building Research, Stodcholm, Sweden, D9:1990.

Roth, K.W., D. Westphalen, M.Y. Pheng, P. Llana, and L. Quartararo. 2005. Energy impact of commercial building controls and performance diagnostics: Market characterization, energy impact of building faults and energy saving potential. http://www.tiaxllc.com/aboutus/pdfs/energy_imp_comm_bldg_cntrls_perf_diag_110105.pdf

Schell, M., and D. Int-Hout. 2001. Demand control ventilation using CO_2. *ASHRAE Journal* Vol. 43, No. 2: 18-24.

Shrestha, S.S., and G.M. Maxwell. 2009. An experimental evaluation of HVAC-grade carbon-dioxide sensors: part 1, test and evaluation procedure. *ASHRAE Transactions* 115(2):

Sun J., Reddy T.A, 2006, A new approach to developing building energy system simulation programs suitable for both design and optimal operation, *ASHRAE Transactions,* Volume 112, Part 1 CH-06-13-4.